(12)

CRDC-CR-85057

THE OPTICAL CONSTANTS OF SMOKE MATERIALS (NATURALLY OCCURRING MINERALS) PLUS IRON AND GRAPHITE IN THE MILLIMETER AND SUBMILLIMETER

by Robert J. Bell
Ralph W. Alexander, Jr.
Larry L. Long
Mark A. Ordal
Ray Paul
J. Peacher

PHYSICS DEPARTMENT
University of Missouri-Rolla
Rolla, Missouri 65401

September 1985

U.S. Army Armament, Munitions & Chemical Command
Aberdeen Proving Ground, Maryland 21010-5423

Disclaimer

The findings in this report are not to be construed as an official Department of the Army position unless so designated by other authorizing documents.

Destruction Notice

For classified documents, follow the procedures in DoD 5200.22-M Industrial Security Manual, Section II-19 or DoD 5200.1-R, Information Security Program Regulation, Chapter IX. For unclassified, limited documents, destroy by any method that will prevent disclosure of contents or reconstruction of document.

Distribution Statement

Approved for public release; distribution unlimited.

UNCLASSIFIED
SECURITY CLASSIFICATION OF THIS PAGE

REPORT DOCUMENTATION PAGE

AD-A160 614

1a REPORT SECURITY CLASSIFICATION: UNCLASSIFIED	1b RESTRICTIVE MARKINGS
2a SECURITY CLASSIFICATION AUTHORITY	3 DISTRIBUTION / AVAILABILITY OF REPORT: Approved for public release; distribution unlimited.
2b DECLASSIFICATION / DOWNGRADING SCHEDULE	
4 PERFORMING ORGANIZATION REPORT NUMBER(S): CRDC-CR-85057	5 MONITORING ORGANIZATION REPORT NUMBER(S)
6a NAME OF PERFORMING ORGANIZATION: Physics Department, University of Missouri-Rolla; 6b OFFICE SYMBOL (If applicable)	7a NAME OF MONITORING ORGANIZATION
6c ADDRESS (City, State, and ZIP Code): Rolla, MO 65401	7b ADDRESS (City, State, and ZIP Code)
8a NAME OF FUNDING / SPONSORING ORGANIZATION: CRDC; 8b OFFICE SYMBOL (If applicable): SMCCR-RSP-B	9 PROCUREMENT INSTRUMENT IDENTIFICATION NUMBER: DAAK-11-82-C-0052
8c ADDRESS (City, State, and ZIP Code): Aberdeen Proving Ground, MD 21010-5423	10 SOURCE OF FUNDING NUMBERS: PROGRAM ELEMENT NO. / PROJECT NO. / TASK NO. / WORK UNIT ACCESSION NO.

11 TITLE (Include Security Classification)
The Optical Constants of Smoke Materials (Naturally Occurring Minerals), Plus Iron and Graphite in the Millimeter and Submillimeter

12 PERSONAL AUTHOR(S) Bell, Robert J., Alexander, Jr., Ralph W., Long, Larry L., Ordal, Mark A., Paul, Ray, and Peacher, J.

13a TYPE OF REPORT	13b TIME COVERED	14 DATE OF REPORT (Year, Month, Day)	15 PAGE COUNT
Contractor	FROM 82-5 TO 84-5	1985 September	104

16 SUPPLEMENTARY NOTATION
COR: Merrill Milham, SMCCR-RSP-B, (301) 671-3854

17 COSATI CODES		
FIELD	GROUP	SUB-GROUP
15	02	

18 SUBJECT TERMS (Continue on reverse if necessary and identify by block number)
Optical constants; Metallic chaffs and powders; Soil aerosols; Iron; Obscurants; Aluminum (Continued on reverse)

19 ABSTRACT (Continue on reverse if necessary and identify by block number)

Optical constants were measured for seven minerals from 20-400 cm^{-1}. These data were combined with those of Dr. Querry from the University of Missouri-Kansas City to cover the 20-4000 cm^{-1} range. Such optical constants are needed to calculate the transmission in the millimeter and submillimeter of soil aerosols in the atmosphere and to assess the value of soil aerosols as obscurants. These optical constants were obtained by Kramers-Kronig analysis of reflectance spectra of pressed powder pellets.

The optical constants of iron, aluminum and graphite were obtained from reflectance spectra measured in our laboratory and that of Dr. Querry to cover the region from 20 cm^{-1} to 20,000 cm^{-1}. Literature values were tabulated for 10 additional metals. These optical constants are needed for evaluation of metallic chaffs and powders as obscurants. Other techniques for measuring optical constants of metals in the millimeter and submillimeter were evaluated.

20 DISTRIBUTION / AVAILABILITY OF ABSTRACT	21 ABSTRACT SECURITY CLASSIFICATION
☒ UNCLASSIFIED/UNLIMITED ☐ SAME AS RPT ☐ DTIC USERS	UNCLASSIFIED
22a NAME OF RESPONSIBLE INDIVIDUAL: BRENDA C. ECKSTEIN	22b TELEPHONE (Include Area Code): (301) 671-2914; 22c. OFFICE SYMBOL: SMCCR-SPS-IR

DD FORM 1473, 84 MAR — 83 APR edition may be used until exhausted. All other editions are obsolete.

SECURITY CLASSIFICATION OF THIS PAGE
UNCLASSIFIED

18. Subject Terms (Continued)

Graphite
Reflectance spectra

PREFACE

The work described in this report was authorized under Project No. DAAK-11-82-C-0052, The Optical Constants of Smoke Materials in the Submillimeter and Millimeter. This work was started in May 1982 and completed in May 1984.

The use of trade names or manufacturers' names in this report does not constitute endorsement of any commercial products. This report may not be cited for purposes of advertisement.

CONTENTS

THE OPTICAL CONSTANTS OF SMOKE MATERIALS (NATURALLY OCCURRING MINERALS) PLUS IRON AND GRAPHITE IN THE MILLIMETER AND SUBMILLIMETER

1. INTRODUCTION

The goal of this work was to measure the optical constants of a number of naturally occurring minerals in the submillimeter and millimeter wavelength range. In addition, graphite was included as a result of later discussions with the contract monitor.

There are four very important features of this work. First, we have obtained optical constants by means of Kramers-Kronig transformation of reflectance data using data from this laboratory and the laboratory of Dr. Marvin Querry of the Optical Science Laboratory of the Physics Department, University of Missouri-Kansas City. This means that a very large spectral range is available, which is critically important for accurate results from the Kramers-Kronig transformation. In the case of the natural minerals, having data sets from both laboratories is especially crucial because the reflectance spectra have many features in the region where the two data sets overlap. This means that the so-called wing corrections are difficult to make satisfactorily using only one or the other of the two data sets. Second, measurements have been made on iron and graphite in the submillimeter and millimeter where very little previous data for metals exists. Third, the available literature for the optical constants of metals has been searched, evaluated, and tabulated for the spectral region from the submillimeter to the visible. Part of this compilation was published and is attached as Appendix A. Fourth, the optical constants of a graphite sample were found to be considerably different from the published values in the millimeter and submillimeter. This again demonstrates the value of having measurements made in both Rolla and Kansas City on the same sample from the millimeter to the visible.

The reflectance of a number of natural minerals was measured in the 20-400 cm^{-1} spectral range. These data were combined with that supplied by Dr. Querry (when available) to obtain optical constants for the spectral range from 20 to 4000 cm^{-1} by use of the Kramers-Kronig transformation. Reflectance measurements were made on graphite and combined with Dr. Querry's data to obtain optical constants from the millimeter to the ultraviolet. Iron was measured using the waveguide technique (discussed below) in the submillimeter range. The optical constants obtained were then combined with Querry's to cover the region from 20 cm^{-1} to 50,000 cm^{-1}. We have improved the data analysis for both the cavity and the plane parallel waveguide methods and have corrected some errors in the published methods[1] of analyzing the data. We explored other methods of obtaining the optical constants of metals in the millimeter and submillimeter. Measurement of reflectance as a function of angle of incidence to high angles of incidence was analyzed and determined to be impractical for this spectral region. Preliminary

results indicate that the measurement of the propagation distances of surface electromagnetic waves on a metal-air interface may be a good way to measure optical constants if some experimental difficulties can be resolved. A number of other methods for estimating the optical constants of metals at long wavelengths using non-optical measurements were considered and found unsatisfactory. These are discussed later. Our work, along with that of Querry suggests that gypsum made anhydrous (e.g., by exposure to vacuum) would make a good standard sample for pressed pellet powder studies undertaken by various laboratories.

The optical constants obtained in this project are important for the calculation of atmospheric transmission in the presence of aerosols derived from soils. These aerosols may be present from a deliberate attempt to screen by using the available soil as an obscurant or due to explosions. Recently, Milham has compared the observed transmission in a smoke chamber with the calculated transmission using measured optical constants and scattering theory.[2] Reasonable agreement was obtained as is shown in Fig. 1 taken from his paper.

For a long time it has been known that metallic chaff in long thin strips makes a good obscurant at radar wavelengths. The same is true at shorter wavelengths if one can produce long thin objects with much smaller dimensions. In the event that attempts to do so are successful, the optical constants of metals over a wide spectral range will be needed. For this reason, we have measured the optical constants of iron and graphite.

Because the measurement techniques are different for the natural minerals and the metals, the body of this report is broken into two sections, the first (section 2) is devoted to the natural minerals, and the second (section 3) is devoted to the metals and graphite. This is followed by a summary section (section 4). Supplementary materials, including a summary of the data available in the literature for metals, and the program used for the Kramers-Kronig transformation, appears in the appendices.

We acknowledge the support and cooperation of Dr. Marvin Querry of the University of Missouri-Kansas City. Dr. Querry supplied us with his infrared and visible data on a number of samples prior to publication and provided us with most of his sample materials. We emphasize that having data from both his and our spectral range greatly improved the accuracy of the Kramers-Kronig analysis necessary to obtain the optical constants from the reflectance data. Availability of his samples allowed comparison of the data from both laboratories in the region of spectral overlap. All frequencies in this report are in wavenumbers.

2. NATURAL MINERALS

This section begins with some definitions. Optical constants were measured, and are presented in two forms. They may be expressed as a complex index of refraction, $n_c = n + ik$, or as a complex dielectric constant, $\varepsilon = \varepsilon_1 + \varepsilon_2$. The ways of expressing the optical constants are related by

$$\varepsilon_1 = n^2 - k^2 \quad (1)$$

and

$$\varepsilon_2 = 2nk. \quad (2)$$

Table 1 lists the natural minerals whose optical constants were measured as part of this project. Most of them are not available as single crystals. This is particularly true for clay minerals, which, of course, are major constituents of many soils. Because most of these minerals are available only as powders, measurement techniques appropriate to powders had to be used.

A number of techniques have been used for powder samples in the past such as transmission measurements through samples mixed with KBr and pressed into pellets. A variation of this method suited to long wavelengths uses a low loss polymer such as polyethylene in place of Kbr. This method is sensitive to absorption, i.e., k, but not to the real part of the refractive index, n. This method is also bothered by the scattering by the small sample particles embedded in the KBr or polyethylene matrix. The scattering is very difficult to account for in any satisfactory way and leads to overestimates of k. Because of these difficulties, this method was not used except for preliminary measurements and to check the reflection measurements described below. Figure 2 shows the transmission for a polyethylene pellet containing kaolin and illustrates the difficulties with the method. A background which increases approximately quadratically with increasing wavenumber (decreasing wavelength) can be seen. Discussions with Dr. Querry indicate that his experiences in the infrared also indicate that the pressed pellet transmission technique is not satisfactory, except perhaps as a supplement to the reflection method in regions were the absorption is very small. Other problems with the technique are discussed by Volz.[3]

Another technique which has been used on powders is the attenuated total reflection technique (ATR). This technique has been used by, for example, Dr. Moeller of Fairleigh Dickenson University,[4] and by Herrick who discusses the technique in his well-known book.[5] It suffers from the problem of obtaining a powder sample of bulk, or nearly bulk density in optical contact with the prism used for ATR. As a result the method is useful for locating strong absorptions, but not for obtaining the optical constants from the measured attenuated total reflectance.

A third technique is to press the powder sample with no binder or matrix into a pellet using relatively high pressure. For many minerals, this results in a pellet with a mirror-like or near mirror-like finish at visible wavelengths. Such surfaces are more than sufficiently smooth for infrared and submillimeter reflectance measurements. Dr. Marvin Querry was the first to fully develop this method and show that it gave good results.[6] Because of the excellent results obtained by Querry using pressed pellets, we adopted this method for most of our measurements upon the naturally occurring minerals.

Before discussing the measurements, it is necessary to discuss some of the drawbacks of the pressed pellet technique. A major problem results from the anisotropy of most of the minerals studied. When a pressed pellet is made, the orientation of the crystallites making up the

sample is random or, as we shall see later, partially oriented. This means that the measured reflectance from the pressed pellet is an average of some kind over all the possible orientations of the crystal axes. This drawback is suffered by all methods which use powdered samples, but must be accepted for materials for which single crystals are unavailable. It may be less of a drawback than first appears because any scattering calculation of an aerosol transmission must average over particle orientation and the average obtained from the pressed pellet measurements is probably as good as any. In any case, regions of strong absorptic- are clearly identified.

Another drawback of the pressed pellet is not all materials are sufficiently soft to make pellets which stick together. For the minerals of this study, pellets could be made from all of them. However, the surface finish varied. Softer materials made pellets with smoother surfaces.

Our conclusion in agreement with Querry is that of the available techniques, the pressed pellet reflectance method is the best for those materials from which pellets can be pressed.

TABLE 1. Natural Minerals Studied

Sample	Spectral Range[a]	Comments	Cards[b]
Gypsum	70-400 cm^{-1}	Naturally occurring rock	yes
Gypsum	20-400 cm^{-1}	Chemically pure powder	no
Gypsum	20-4000 cm^{-1}	Naturally occurring powder	yes
Gypsum	20-400 cm^{-1}	Made anhydrous by exposure to vacuum	yes
Kaolin	20-4000 cm^{-1}	Naturally occurring powder	yes
Limonite	20-4000 cm^{-1}	Naturally occurring powder	yes
Limonite	70-400 cm^{-1}	Naturally occurring rock	no
Illite	20-4000 cm^{-1}	Naturally occurring powder	yes
Montmorillonite	20-400 cm^{-1}	Naturally occurring powder	yes
Hematite	70-400 cm^{-1}	Limonite made anhydrous by heating	yes
Gypsum	70-400 cm^{-1}	surface roughened by 1 micrometer grit	no
Gypsum	70-400 cm^{-1}	surface roughened by 3 micrometer grit	no
Gypsum	70-400 cm^{-1}	surface roughened by 8 micrometer grit	no
Gypsum	70-400 cm^{-1}	surface roughened by #600 grit	no
Gypsum	70-400 cm^{-1}	surface roughened by #400 grit	no
Montmorillonite	70-400 cm^{-1}	surface roughened by 1 micrometer grit	no
Montmorillonite	70-400 cm^{-1}	surface roughened by 3 micrometer grit	no
Montmorillonite	70-400 cm^{-1}	surface roughened by 8 micrometer grit	no
Montmorillonite	70-400 cm^{-1}	surface roughened by #600 grit	no
Montmorillonite	70-400 cm^{-1}	surface roughened by #800 grit	no

a. Includes reflectance data for Dr. Marvin Querry, Optical Science Laboratory, Physics Department, University of Missouri-Kansas City when available for 400 cm^{-1} to 4000 cm^{-1}.

b. Yes means that punched cards were sent under separate cover for the Chemical Research and Development Command data base. No means that the spectra either differed insignificantly from a similiar sample for which cards were submitted, or data was better presented in the form of a graph in this report.

2.1 The Pressed Powder Pellet Reflectance Technique.

Before pressing into pellets, powders were ground as finely as possible with a mortar and pestle. This powder was then pressed with a commercial infrared pellet die to make one-half inch diameter pellets. Forces on the die ram ranged up to 25 thousand pounds. This process usually produced pellets with a good surface finish and a density ranging from 75 to 90 percent of the bulk density. Evidence is discussed below that a surface layer exists on the pellet which has a density considerably higher than the average density of the pellet. This means that the reflection measurements are made on a surface layer having a density near the bulk value.

The reflection measurements were made with a commercial RIIC FS-720 Fourier transform spectrometer. A laboratory-built reflection attachment was used to obtain reflection spectra of several samples without the need to break the instrument vacuum when changing samples. A gold or aluminum mirror was used as the reference. In the 20-400 cm^{-1} region, no correction needs to be made for the reflectivity of these reference mirrors.

The spectrometer was controlled by an IBM PC which acquired the interferogram and then computed the Fourier transform. Several interferograms could be co-added (averaged) if needed to improve the signal to noise ratio. The resulting reflectance spectra were then Kramers-Kronig transformed to obtain ε_1 and ε_2, or n and k. When reflectance data from Querry were available they were added on to our data set before the Kramers-Kronig transform was performed. Since some features of the Kramers-Kronig transform are non-trivial, it is discussed in the next section.

2.2 The Kramers-Kronig Transform.

When an electromagentic wave is reflected, the reflectance and phase shift are not independent. The complex reflection coefficient r for normal incidence is given by[7]

$$r = \frac{N-1}{N+1} = |r| \exp(i\theta) \tag{3}$$

where $N = n + ik$ and Θ is the phase angle. The reflectance R is given by the square of the reflection coefficient.

$$R = |r|^2 = \left| \frac{n + ik - 1}{n + ik + 1} \right|^2 \tag{4}$$

Separating into real and imaginary parts

$$R = \left| \frac{n^2 + k^2 - 1}{(n+1)^2 + k^2} + i \frac{2k}{(n+1)^2 + k^2} \right|^2 \tag{5}$$

and completing the square, the reflectance can be expressed in terms of the real and imaginary parts of the index of refraction

$$R = |r|^2 = \frac{(n-1)^2 + k^2}{(n+1)^2 + k^2} \tag{6}$$

Expanding the first equation and solving for n and k a relationship between the phase shift and index of refraction can be developed.

$$n = \frac{1 - |r|^2}{1 - 2|r|\cos(\theta) + |r|^2} \tag{7}$$

$$k = \frac{2|r|\sin(\theta)}{1 - 2|r|\cos(\theta) + |r|^2} \tag{8}$$

From the above expressions it is clear that if the phase angle in addition to the reflectance is known then the optical properties are easily determined.

To determine the phase a Kramers-Kronig analysis is done. This analysis is based upon complex variable theory and its only physical assumptions is that the response of the material to the incident radiation be causal (i.e., no light is reflected until the light strikes the material) and linear.

To derive the Kramers-Kronig relations one starts with the Cauchy Integral Formula

$$f(Zo) = \frac{1}{2\pi i} \int_c \frac{f(Zo)\, dz}{Z - Zo} \tag{9}$$

where f is analytic everywhere within and on a simple closed contour, taken in the positive sense and z_o is any point interior to the contour[8]

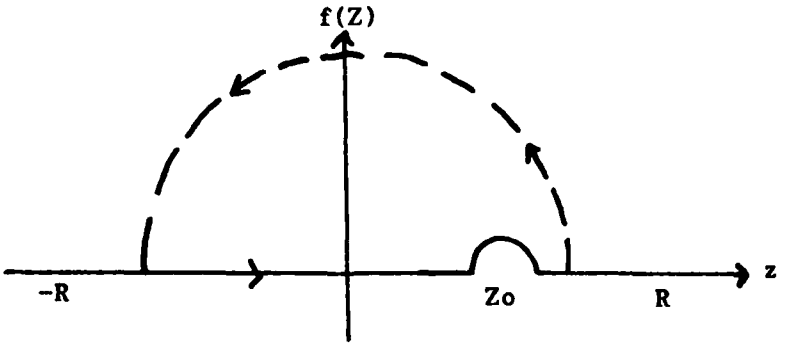

Using the above contour the value of the integer is zero since there are no enclosed poles. Writing the integral over each section of the contour'

$$\lim_{R\to\infty}\left[\int_{-R}^{R}\frac{f(z)}{z-z_0}\,dz+\int\frac{f(z)}{z-z_0}\,dz+\int\frac{f(z)}{z-z_0}\,dz\right]=0 \tag{10}$$

and allowing R to go to infinity the second integeral vanishes. Applying the Residue Theorem to the third integral one obtains

$$\text{P.V.}\int_{-\infty}^{\infty}\frac{f(Z)\,dZ}{Z-Z_0}=i\pi f(Z) \tag{11}$$

where P.V. denotes the Cauchy principal value. Seperating into real and imaginary parts

$$Re\left[f(z)\right]=\frac{1}{\pi}\,P.V.\int_{-\infty}^{\infty}\frac{Im\left[f(z)\right]}{z-z_0}\,dz \tag{12}$$

$$Im\left[f(z)\right]=-\frac{1}{\pi}\,P.V.\int_{-\infty}^{\infty}\frac{Re\left[f(z)\right]}{z-z_0}\,dz \tag{13}$$

Since the system is time-independent and causal, the crossing relation can be applied $f(Z) = f^{*}(-Z)$

$$Re\left[f(z)\right]=\frac{2}{\pi}\,P.V.\int_{0}^{\infty}\frac{z\,Im\left[f(z)\right]}{z^2-z_0^2}\,dz \tag{14}$$

$$Im\left[f(z)\right]=\frac{2z_0}{\pi}\,P.V.\int_{0}^{\infty}\frac{Re\left[f(z)\right]}{z^2-z_0^2}\,dz \tag{15}$$

To determine the Kramers-Kronig relations the reflection coeficient is identified with f(Z), (i.e., f(Z) is replaced by $\ln(r(\omega))$ where $\ln(r(\omega)) = \ln|r(\omega)| + i\,\theta$ substituting into the previous equation the phase is then expressed as an integeral dependent upon the reflectance.

$$\theta(\omega_o)=-\frac{2\omega_o}{\pi}\,\text{P.V.}\int_{-\infty}^{\infty}\frac{\ln|r(\omega)|}{\omega^2-\omega_o^2}\,d\omega \tag{16}$$

Clearly, if the reflectance is known for all frequencies, then the complex index of refraction can be determined from the equations

expressing n and k in terms of r and θ. These equations represent exact relationships, as long as the reflectance is known for the complete range of frequencies. Since the reflectance cannot be determined for all frequencies and in fact the reflectance is usually known for only a very limited range, approximations must be made for the reflectance outside of the experimental values. These are referred to as wing corrections. This leads to the basic problem of how to obtain the optical constants over a limited frequency range from the experimental data. The most common method is to evaluate the integral analytically from zero to the lowest experimental point and from the highest experimental point to infinity using a constant reflectance. Another common method is to extend the reflectance data by fitting a model to it, usually a Lorentz type model. The model then is used to calculate reflectance points outside of the experimental range. There are many additional methods used to perform the wing corrections, but none can replace having actually data over a very large range. If a large enough range is available, such that the denominator of the previous equation is small, then the wing correction will only effect the edge of the actual data.

Specializing to the far infrared (i.e., frequencies smaller than 500 cm^{-1}, wavelengths greater than 20 microns) there usually exists a strong resonance located outside of the experimental data which makes a linear wing correction doubtful at best unless some information is known about the resonance. Therefore, the preferred method for narrow range mineral data is to do a single Lorentz type oscillator fit to extend the high wave number end of the data and then do a constant reflectance wing for both ends. The best method is to use a near infrared data made available by Dr. Querry of U.M.K.C.. Figure 3 presents the optical constants n and k for gypsum in the 0 - 400 cm^{-1} spectral range in three forms: first U.M.R., second U.M.K.C. and finally the combined set. As stated earlier the main differences will be located at the edge of the data set. Notice that the effect of the U.M.R. data is to basically extend the U.M.K.C. data set and improve the resolution below 400 cm^{-1}.

The program used to compute the optical constants is in appendix B of this report. The program is written in IBM Basic but must be compiled by the IBM Basic compiler, since unnecessary line numbers have been removed to improve the efficiency of the compiler. Eventually this program will be rewritten in a version of Pascal that will be compatible with the IBM-PC and the larger main frame computer.

2.3 Discussion of the Data for Natural Minerals.

In this section we discuss the measurements for the natural minerals listed in Table 1. Some measurements of the effect of surface roughness upon the reflectance measurements were made to insure that this was not an important problem. Surface roughness is discussed in section 2.4.

2.3.1 Gypsum.

Gypsum is a soft material which presses into pellets with a mirror-like surface. It has an hexagonal crystal structure and hence is not isotropic. Electron micrographs of the surface of the pressed gypsum pellets showed that the pressing operation tended to align the crystallites of the powder such that the hexagonal axis was perpendicular to the pellet surface. The pressing also seemed to fracture larger crystallites so that the surface layer was made up of crystallites of very nearly the same size. Evidence discussed below indicates that the surface layer of a pellet has a higher density than the bulk of the pellet. After pressing with 12 tons of force on a one-half inch diameter pellet, the bulk density of the pellet was 2.0 gm/cm^3. Measurements by Querry[10] and by Volz,[3] indicate that the pressure we used is not quite sufficient to produce the maximum reflectance possible, but comes very close.

Figure 4 shows the measured reflectance of a pressed pellet of gypsum powder. As discussed above, this spectrum was combined with the spectrum supplied by Querry for 400-4000 cm^{-1} and the Kramers-Kronig transformation used to obtain n and k plotted in Fig. 5. This of course is an average over the various orientations of the gypsum crystallites at the pellet surface. Gypsum is available as a single crystal and Querry has made comparisons between the spectra of a single crystal and the powder sample in the infrared in his talk at the CSL Conference on Aerosols and Obscurants in 1983.[11]

Pellets were prepared from powder from several different sources, including chemically pure gypsum (calcium sulfate). No significant differences were seen between these samples, so only the one set of optical constants is included here.

2.3.2 Anhydrous Gypsum.

Naturally occurring gypsum contains waters of hydration. Heating gypsum or exposing it to vacuum causes the loss of this water. The resulting anhydrous gypsum is called anhydrite. We studied the effect of this loss of water upon the optical constants. The pellet sample was prepared from gypsum as described in the previous section. It was then exposed to vacuum for a number of days which produced a surface anydrite layer which retained most of the surface finish quality of the original gypsum pellet. The reflectance of this pellet is shown as Fig. 6. Data from Querry were not available for this sample so the optical constants were obtained by Kramers-Kronig transform of our reflectance spectrum from 20 to 400 cm^{-1}. The real and imaginary parts of the dielectric function are shown in Fig. 7. Note the considerable differences between the spectra of the hydrated and anhydrous gypsum. The ease with which gypsum loses its water of hydration suggests that an aerosol formed in a low humidity atmosphere would probably consist of a mixture of hydrated gypsum particles and particles of gypsum that had lost various amounts of water.

2.3.3 Kaolin.

Kaolin is also a soft material which presses into pellets with a good surface finish. Our reflectance measurements from 20 to 400 cm^{-1} are shown in Fig. 8. When combined with the Kansas City reflectance measurements and Kramers-Kronig transformed, the index of refraction shown in Fig. 9 is obtained. Chemically pure kaolin was also measured, but showed no significant differences from the naturally occurring material. X-ray diffraction and x-ray fluorescence indicated that the naturally occurring sample was 90% kaolinite, 5% muscovite, and 5% quartz.

2.3.4 Limonite.

Limonite is harder than the two previous materials, but pellets with good surface finish could be pressed. The measured reflectance spectrum is shown in Fig. 10. The resulting index of refraction is plotted in Fig. 11.

In addition to the powder sample, a solid piece of limonite was ground and polished. The reflectance of this sample is shown in Fig. 12. Because other data was not available, the Kramers-Kronig transformation was limited to the range 20 to 400 cm^{-1}. The index of refraction for this region is shown in Fig. 13. Note there are some differences between the powder sample and the rock sample. This is probably due to partial orientation of the crystallites in the rock during its formation.

2.3.5 Illite.

Illite is yet another naturally occurring clay material. The reflectance of a pressed pellet is shown in Fig. 14 and the index of refraction is shown in Fig. 15.

2.3.6 Montmorillonite.

The reflectance of a pressed pellet of montmorillonite is shown in Fig. 16. The index of refraction for our spectral range (below 400 cm^{-1}) obtained using Querry's measurements for an upper wing correction is shown in Fig. 17. X-ray fluorescence and x-ray diffraction measurements gave the following composition for this sample:

Montmorillonite	80%
Quartz	20%

2.3.7 Hematite.

Hematite is the anhydrous form of limonite. Our samples were produced by heating the light orange limonite until it turned dark red. Pellets were pressed from this red powder. The measured reflectance is shown as Fig. 18. As no infrared data were available, only the region from 20 to 400 cm^{-1} is shown for the index of refraction in Fig. 18. Once again appreciable changes in the spectra are seen upon loss of the water of hydration.

2.3.8 Surface Roughness.

The effect of surface roughness was studied to make sure that the surfaces of the pressed pellets were sufficiently smooth not to influence the reflectance measurements. That this is indeed true can be seen from Fig. 20. Plotted there is the reflectance as a function of wavenumber for pellets 'polished' with abrasive papers of various grit sizes from 1 micrometer to #400 grit. There are at least two important observations to be made. Note that roughening with 1 micrometer grit and 8 micrometer grit lead to identical spectra. We interpret this as meaning roughness at the level of 8 micrometers does not influence the IR measured reflectance. Second, the fact that polishing with 1 micrometer grit reduces the reflectance of the as pressed pellet indicates that the polishing operation is removing a thin layer of density greater than the average density of the pellet. It is this evidence that convinces us that the measured reflectance (and hence the derived optical constants) corresponds more closely to material of nearly the density of single crystals than the measured average density of the pellets would indicate.

The effects of surface roughness upon reflectance has been studied in the near infrared and visible by a number of workers. For example, see the paper by H. E. Bennett and J. O. Porteus.[12] Their analysis suggests that the reflectance should depend upon the wavelength, λ, and the RMS surface roughness, s, in the form:

$$R = Ro \exp [-(As/\lambda)^2] \qquad (17)$$

where Ro is the reflectance of the smooth surface and A is a constant. Figure 21 shows a fit to the montmorillonite reflectance data for surfaces polished with 8 micrometer, #600 and #400 grits. The fit with Eq. (17) is also shown where s is chosen to give a good fit and is considerably smaller than the grit size. The significance of this fit should not be over emphasized because the model is being pushed rather hard to use it for our wavelength region and roughness. If the data is plotted as a function of wavenumber, instead of wavelength, a linear fit as a function of wavelength works quite well, as shown in Fig. 22. The significance of this is not obvious.

A gypsum pellet was also polished with several grit sizes, this time starting with the course #400 grit and then with sucessively finer grits. Gypsum was chosen because it has several strong absorptions between 100-400 cm^{-1}. The results are shown in Fig. 23. Once again the results suggest the removal of a thin surface layer of density higher than the average for the pellet.

3. IRON AND GRAPHITE

Like all metals, iron has a very high reflectance, nearly unity, in the millimeter and submillimeter. This extremely high reflectance makes the usual reflectance measurements very difficult. For this reason, we looked at other methods of measuring the absorption for iron. Both methods in effect make use of multiple reflections to enhance the absorption. Table C-1 lists the iron, steel and graphite samples studied.

Table 2. Iron, Steel and Graphite Samples Studied

I. Iron

(A) From the literature:

(1) single crystal, $\rho_{dc} = 8.9 \times 10^{-6}$ ohm-cm, $\rho_{Opt} = 14 \times 10^{-6}$. Ref. 13.

(2) bulk, polycrystaline, ρ_{dc} not measured, from handbooks $\rho_{dc} = 10 \times 10^{-6}$ ohm-cm, $\rho_{Opt} = 14 \times 10^{-6}$ ohm-cm, Ref. 14.

(B) Private communications U.M.K.C. data from (M. Querry), solid, polycrystalline rod, $\rho_{Opt} = 8.4 \times 10^{-6}$ ohm-cm ρ_{dc} not measured.

(C) UMR measured, 200 nm thick evaporated Fe film on teflon FEP, $\rho_{dc} = 86 \times 10^{-6}$ ohm-cm = ρ_{Opt}.

II. Steel

(A) UMR studied, steel shim stock (See Table 3 presented later). measured $\rho_{dc} = 12 \times 10^{-6}$ ohm-cm, $\rho_{Opt} = 16 \times 10^{-6}$ ohm-cm.

(B) Data from J. D. McMuller from surface electromagnetic wave experiments on type 304 stainless steel. $\rho_{dc} = 72 \times 10^{-6}$ ohm-cm, $\rho_{sew} = 67 \times 10^{-6}$ ohm-cm. Ref. 15 and 16.

III. Graphite

(A) Dixon 200-10, ρ_{dc} not known, $\rho_{Opt} = 1.3 \times 10^{-3}$ ohm-cm.

(B) POCO HPD-1, $\rho_{dc} = 1.7 \times 10^{-3}$ ohm-cm.

(C) Reactor grade: measured $\rho_{dc} = 0.85 \times 10^{-3}$ ohm-cm.

(D) Single Crystal data, ρ_{dc} and ρ_{Opt} unknown. Ref. 17.

3.1 The Plane Parallel Waveguide.

A waveguide consisting of two infinite plane parallel metal sheets does not have a low frequency cut-off as do ordinary rectangular or cylindrical waveguides.[18] When a plane parallel waveguide is operated at wavelengths longer than twice the plane separation, only one mode propagates. By measuring the attenuation coefficient, α, at submillimeter and lower frequencies of this mode, one can then determine the imaginary part of the dielectric constant:

$$\varepsilon_2 = 2\left[\frac{n}{\alpha d}\right]^2 \frac{1}{1 + \omega/\omega_\tau} \quad . \tag{18}$$

The index of refraction of the spacer is n, d is its thickness, and ω_τ is the estimated scattering frequency. We used teflon for the spacer. In order to eliminate the effects of reflection at the ends of the waveguide and any absorption in the dielectrice spacer filling the waveguide, one measures the ratio of the intensity I_1 and I_2 of two different lengths of waveguide. From this one finds α from

$$\alpha = [\ln(I_2/I_1)]/(x_2-x_1)] - \alpha_{Teflon} \tag{19}$$

where α_{Teflon} is the absorption coefficient of teflon as a function of wavenumber, (x_2-x_1) is the difference in length of the two waveguides. The absorption coefficient of teflon has to be measured separately. We have done this for the Dupont teflon FEP which we used as a spacer for the waveguide. The measured absorption coefficients are shown in Fig. 24.

In practice, one does not use a single waveguide since the required width across the guide is only of order 25 micrometers. Instead, a stack of such waveguides is used as shown schematically in Fig. 25.

3.2 Iron.

A stacked waveguide sample of iron was prepared by evaporating high purity iron on Dupont FEP teflon sheet one mil (25 micrometers) thick. The evaporation was done on both sides of the teflon so that when the teflon sheet was stacked to make the waveguide sample, the unavoidable oxide layer was sandwiched between two iron layers. Ion sputtering, combined with ESCA showed that the iron layer was about 2000 Angstroms thick, and the only detectable impurities were oxygen and carbon at the surface of the iron.

The ratio of the transmission of a long iron waveguide sample to a short one was used to obtain ε_2 for the evaporated iron film. The long sample was 3.70 mm long and the short sample was 1.95 mm long. Using Eq. (18) along with the absorption coefficient for teflon shown in Fig. 24, the imaginary part of the dielectric function, $\varepsilon_2(\omega)$, was calculated. This is plotted as a function of frequency in Fig 26. At long wavelengths, the Drude model relates ε_2 to ρ_{dc}, the DC resistivity by

$$\varepsilon_2 = 60/(\omega\ \rho_{dc}) \tag{20}$$

The DC resistivity for our evaporated iron samples was measured to be 86 x 10^{-6} ohm-cm. With this value of ρ_{dc}, Eq. (20) is plotted in Fig. 26. This value of the resistivity is a factor of nine higher than the value for bulk iron. The high value for the evaporated film is due to imperfections in the thin film and probably due to cracking when the film is flexed in handling. This result shows that attempts to make 'chaff' using a plastic base with a metallic coating may face problems with the

metal coating having a higher than expected resistivity. This would enhance absorption, but reduce scattering.

To avoid the problems of the thin film, such as the high resistivity, a waveguide sample was made using 1 mil fully-hardened steel shim stock with teflon FEP spacers. With such samples, an oxide coating, much thinner than the wavelength is present on the steel. Because its thickness is so much less than the wavelength, the oxide does not affect our results. Chemical analysis of the steel shim stock shows that it is 99% iron with less one per cent impurities. The major impurity is manganese, present at about 0.5%. The detailed analysis is shown in Table 3.

Table 3. Characterization of the Steel Shim Stock

Constituents by percent:	Iron	99+%
	Manganese	0.3% to 0.60%
	Carbon	0.08% to 0.13%
	Sulphur	0.050% maximum
	Phosphorus	0.040% maximum
Traces:	Cobalt, Chromium, Copper, Magnesium, Molybdenum, Niobium, Nickel, Silicon, Tin, and Vanadium	
Physical characteristics:	Hardened, Temper 1 Rockwell 890 minimum Full-hard $\rho_{dc} = 12.1 \times 10^{-6}$ ohm-cm	
Supplier information:	Precision Brand 2252 Curtiss Street Downes Grove, IL, 60515 (312)-969-7200 Spec. # QQ S 698 AISI 1010 Code A-1 NIDA/SIDA # 16130 Manufacture's code # 698158	

The dielectric function derived from the waveguide transmission measurements on steel shimstock [again using Eq. (18)] is shown in Fig. 27. Note that these measurements extend down to 30 GHz (1.1 cm^{-1}). The measurements at 33 GHz and 95 GHz (3.2 cm^{-1}) were obtained using GaAs IMPATT diode sources. The DC resistivity of the steel shim stock was measured, and the Drude model prediction from Eq. (20) is also plotted in Fig 27. Note the reasonable agreement between the measurements and the estimated values for ε_2 (solid line). This DC resistivity of 12 x 10^{-6} ohm-cm is slightly higher than the handbook value for iron, 10 x 10^{-6}, which in turn is slighlty higher than the value of $\rho_{Optical}$, 8.4 x 10^{-6} ohm-cm calculated from our Drude model fit to Querry's Kramers-Kronig analysis of data for pure iron. Our best estimate for the steel shim stock is $\rho_{Optical} \simeq 16 \times 10^{-6}$ ohm-cm.

Figure 28 shows the real and imaginary parts of the dielectric function of iron, and Figure 29 the real and imaginary parts of the complex index of refraction, n and k, derived from a Kramers-Kronig analysis of Querry's data for iron. Also plotted in this figure is our Drude model fit to Querry's results. The fit at any frequency ω is facilitated by using

$$\omega_\tau = \omega\varepsilon_2/(1 - \varepsilon_1) \tag{21}$$

and

$$\omega_p^2 = (1 - \varepsilon_1)(\omega^2 + \omega_\tau^2) \tag{22}$$

Figure 30 shows the literature values for iron. Prior to our and Querry's measurements, measurements had been made only for wavelengths shorter that 25 micrometers as shown. A comparison of this figure with Fig. 29 of Querry's data indicates that the inferred value of the DC resistivity is lower for Querry's sample. $\rho_{Optical}$ is 8.4 x 10^{-6} for Querry's sample and $\rho_{Optical}$ is 14 x 10^{-6} for the best fit to the literature data. The literature data are referenced in the figure caption.

3.3 Nonresonant Cavity.

Non-resonant cavities have been used by several workers for qualitative measurements in the far infrared on moderately highly reflecting materials. Pinkerton and Sievers[1] improved the necessary calculations for data reduction to allow quantitative measurements. The basic idea of this method is to use a cavity with dimensions large compared to the wavelengths being investigated. This means that the cavity has many modes per unit wavelength and an averaging procedure can be used to calculate losses in the cavity. The radiation of interest is coupled into the cavity from a light cone through a small coupling hole. After many reflections inside the cavity, the unabsorbed radiation leaks out the exit hole. Then the cavity provides a means of obtaining many reflections and is thus useful for studying highly reflecting materials such as metals. A schematic diagram of the cylindrical cavity we used is shown in Fig 31.

In practice, one measures the 'transmission' of the cavity, i.e., the intensity of the light leaking out the exit hole. The ratio of two such measurements is the quantity of interest — one measurement is the intensity when part of the cavity is made partly of a sample metal — the other measurement the intensity when the cavity is composed entirely of one type of reference metal. The optical properties of the reference metal (e.g.,brass, or aluminum alloy) must be known before one can obtain results on the samples of interest. Pinkerton and Sievers[1] used the waveguide transmission technique to measure ε_2 for a sample of brass foil presumed to be similar in optical properties to the so-called 'cartridge' brass used to fabricate their nonresonant cavities. We have noted that the cavity method itself can be used to measure ε_2 of the actual cavity walls by using a sample with well characterized optical constants (in this case a gold foil). In our analysis of the nonresonant cavity we solve for the optical properties of the reference metal (e.g., Al alloy)

instead of the sample metal (gold) in order to 'calibrate' the cavity. Knowing the geometrical parameters of the cavity and the optical constants of the reference metal, one can derive the optical constants of the sample from the ratio of the reference transmission to the sample transmission. We chose gold as the calibration standard because its optical constants are well known and have been measured at very long wavelengths by Brandli and Sievers[18] using the waveguide technique (see reference Ref. 19 and references therein).

For metals at millimeter wavelengths the cavity analysis is fairly simple because the approximation that n and k are equal (equivalently $\varepsilon_2 \gg \varepsilon_1$) is valid. This is the approximation originally made by Lamb for microwave cavities.[20] Pinkerton and Sievers[1] made a higher order approximation at the expense of considerable complication in computation. Unfortunately for S-polarization their approximation is too weak. We evaluated the exact integrals for both polarizations instead of approximating the integrand function and expanding the approximate integrand in a power series. We used the exact integrals to introduce the reference material. Unfortunately the exact solution is extremely difficult to invert for data analysis. Using the two approximations $(1/n^2) \ll 1$ and $(1/k^2) \ll 1$ before integrating, we found at submillimeter and longer wavelengths that

$$r = \frac{n}{n^2 + k^2} \simeq \frac{3P_s}{16}\,(1 + P_s/4) \qquad (23)$$

where

$$P_s = \frac{1}{S_4}\left(\frac{I_r}{I_s}\right)\left[2S_1 + (S_2 + S_3 + S_4)P_r\right] - \frac{1}{S_4}\left[2S_1 + (S_2 + S_3)P_r\right] \qquad (24)$$

involving signal strengths I_r and I_s, areas S_1= area of each of the input or output holes; S_2= area of sidewalls excluding the input and output holes; S_3= area of endplate made of the reference material; and S_4= area of endplate made of the sample material; and P_r for the reference material given exactly by

$$P_r = 4n\left\{\left[1 + \frac{1}{n^2+k^2}\right] - n\left[1 + \frac{1}{(n^2+k^2)^2}\right]\ln\left(n^2+k^2+2n+1\right)\right.$$
$$\left. + \left(\frac{n^2-k^2}{k}\right)\left[\frac{1}{(n^2+k^2)^2}\tan^{-1}\left(\frac{k}{n+1}\right) + \tan^{-1}\left(\frac{k}{n^2+k^2+n}\right)\right] + n\ln\left(n^2+k^2\right)\right\} \qquad (25)$$

Analysis of the nonresonant cavity results is nontrivial. The equations obtained both by Pinkerton and Sievers and by us involve four initially unknown quantities — ε_1 and ε_2 (or n and k) for both the reference metal (brass or Al alloy) and the sample (e.g, iron, graphite). Naturally, the dielectric function of the reference metal only needs to be determined once -- as a calibration of the cavity for a particular wavelength region. As mentioned earlier, ε_2 for the reference metal can be measured by the parallel waveguide method. Alternatively, we can use our so-called calibration technique to extract the optical properties of

the reference metal from nonresonant cavity measurements. In principle, the nonresonant cavity method yields both ε_1 and ε_2 (or n and k). In practice the extraction of both parameters may prove to be numerically intractable due to the relative insensitvity of the equations to ε_1. For the reference metal Pinkerton and Sievers assumed that $\varepsilon_1=0$ (i.e., $n=k$) and solve the resulting one parameter transcendental equation numerically for each experimental point. We have instead tried a Drude model behavior for ε_1 as well as numerical solution of the two parameter transcendental equation that results if both ε_1 and ε_2 of the other metal are known.

To make the analysis more tractable we assume the Drude model works at the long wavelengths in question. With this assumption, one can obtain approximations for the equations arising in the analysis of the nonresonant cavity which are better than the simpler approximation made by Lamb but at the same time much less troublesome computationally than the other more exact approaches tried by Pinkerton and Sievers and by us. After much experience trying these methods, we feel that our approximations given above are the most satisfactory. Compared to the Pinkerton and Sievers method, our simplest method is much simpler computationally and conceptually, and is at least as good an approximation.

Using a cavity with one planar side that is replaceable, we have made measurements on iron, graphite, aluminum, copper using gold as the reference metal. The signal to noise ratio is very poor in this data and much time has been devoted to trying various data reduction methods as discussed in the preceeding paragraphs. Our tentative conclusion is that this method is inferior to the use of the waveguide method. Of course, some materials such as graphite may not be suitable for preparation of waveguides because they cannot be obtained in thin (of order 1 mil thick) sheets.

3.4 Graphite.

Graphite is a material intermediate between metals and insulators in terms of its long wavelength reflectance. Its reflectance is probably too low to measure using the cavity method discussed above, but is sufficiently high as to be difficult to measure using a single reflection. However, the usual near normal incidence reflectance measurement has proven to be the best method tried so far. As was done for the minerals, samples were pressed from graphite powder. Near mirror like surfaces were produced when Dixon 200-10 graphite powder was pressed. The reflectance of this sample is shown in Fig 32. Measurements were made from 15 to 365 cm^{-1} using our commercial RIIC FS-720 Fourier transform interferometer and at 3.2 cm^{-1} using a GaAs IMPATT diode and our asymmetric Fourier transform interferometer. Reflectance data from 180 cm^{-1} to the ultraviolet was available from Querry for this sample and was combined with our data. After Kramers-Kronig analysis, the dielectric function plotted in Fig 33 was obtained. Figure 34 shows the complex index of refraction, n and k, for this sample.

Various graphite samples have been measured by other workers. H. R. Philip measured a sample of pyrolytic graphite to very long wavelengths. As shown in one of our quarterly reports, the reflectance measured by H. R. Philipp is similar to the reflectance measured by us and Querry on the Dixon 200-10 pressed powder sample, but our reflectance is slightly lower, particularly at long wavelengths. This slightly lower reflectance manifests itself as a leveling off of ε_1 and ε_2 at long wavelengths. Alternatively, the lower reflectance causes k to decrease at long wavelengths, producing the peak in k at about 17 cm^{-1} or near $\varepsilon_{2,max} \simeq 29$ cm^{-1}. This behavior is consistent with a low free carrier concentration. The Drude model fit of the reflectance data may be fortuitous. In an article just published, Woolf, et al. (Ref. 21) find from DC measurements that pyrolytic graphite has a free carrier concentration of 9.7×10^{18} per cm^3. This is consistent with our data. We need to make measurements upon oriented polycrystalline pyrolytic graphite samples in order to decide if the differences between our and Querry's data and that of H. R. Philip is due to differences in orientation, or differences in the oriented polycrystalline graphite used by H. R. Philip and our Dixon 200-10 powder sample. One thing clear from the literature is the wide variance among samples. We hope to pin down the origin of this variance in future work.

3.5 Slopes.

There are experiments which give either ε_1 or ε_2 but not both. With the Drude model ε_1 and ε_2 are given by

$$\varepsilon_1 = 1 - \frac{\omega_p^2/\omega_\tau^2}{1 + \omega^2/\omega_\tau^2} \tag{26}$$

and

$$\varepsilon_2 = \frac{\omega_p^2/(\omega_\tau \omega)}{1 + \omega^2/\omega_\tau^2} \tag{27}$$

where ω_τ is the scattering frequency and ω_p is the plasma frequency. Taking a derivative yields

$$D = -\omega \, d(\ln(\varepsilon_2))/d\omega \tag{28}$$

which gives

$$\omega_\tau = \omega \left[(3-D)/(D-1) \right]^{1/2} \tag{29}$$

and

$$\omega_p = \left[\varepsilon_2 \omega_\tau \omega \left(1 + \omega^2/\omega_\tau^2 \right) \right]^{1/2}. \tag{30}$$

Note the limits

$$\begin{aligned} \omega^2 &\ll \omega_\tau^2 \;\Rightarrow\; D=1 \\ \omega &= \omega_\tau \;\Rightarrow\; D=2 \\ \omega^2 &\gg \omega_\tau^2 \;\Rightarrow\; D=3. \end{aligned} \tag{31}$$

If one only has ε_1 he can obtain ε_2 using the derivative

$$E = -\omega \, d \, [\, \ln(1 - \varepsilon_1) \,]/d\omega \tag{32}$$

from which

$$\omega_\tau = \omega \, [\, (2-E)/E \,]^{1/2} \tag{33}$$

and

$$\omega_p = \{ \, (1-\varepsilon_1)\omega_\tau^2 \, [\, 1+\omega^2/\omega_\tau^2 \,] \, \}^{1/2} \tag{34}$$

with limits

$$\begin{aligned} \omega^2 &<< \omega_\tau^2 \quad => \quad E=0 \\ \omega &= \omega_\tau \quad => \quad E=1 \\ \omega^2 &>> \omega_\tau^2 \quad => \quad E=2 \end{aligned} \tag{35}$$

The magnitude of D and/or E indicates whether or not the ε_1 or ε_2 data is above or below the crossover frequency, ω_τ, for $-\varepsilon_1$ equal ε_2. This is the boundary between the classical and relaxation regions. If D and E are outside their ranges of $1 \leq D \leq 3$ or $0 \leq E \leq 2$, they are not Drude-like at that frequency. We usually smooth the data before taking derivatives.

3.6 Casimir-Wooten Diagrams.

The boundries between, A, classical; B, relaxation; C, transmission; D, anomalous skin effect; and E, anomalous reflection are determined by ω and ω_p (Refs. 22-24). The Fermi velocity can be expressed in terms of ω_p:

$$\chi \equiv \left(\frac{v_F}{2\pi c} \right) \omega_p = \left(\frac{3^{1/3} \hbar}{2 c^{1/3} e^{2/3} m^{2/3}} \right) \omega_p^{5/3} = 4.25 \times 10^{-7} \omega_p^{5/3} \tag{36}$$

Recall that $\omega_p^2 = ne^2/(\pi c^2 m^*)$; so the plasma frequency mainly depends on the concentration of free carriers, n.

For Fe using Querry's data $\omega_p = 3.21 \times 10^4$ cm^{-1}, ($\omega_\tau = 144$ cm^{-1}) resulting in $\chi = 13.78$ cm^{-1}. See Fig. 35. Note that Querry's data is free carrier-like in the range of the solid line and exhibits band structure at higher frequencies, dashed line. His ω_τ is 144 cm^{-1}.

These diagrams make it possible to see in which regimes the data for a particular conductor lies. The classical range is the simple Drude model (as stated in section 3.5) with $\omega < \omega_\tau$. The relaxation region is also the Drude range except $\omega > \omega_\tau$.

4. INSTRUMENTATION

4.1 Asymmetric Michelson Fourier Transform Spectrometer.

We have constructed an asymmetric interferometer for the submillimeter and millimeter wavelength regions.[25] The design is patterned after a design by the late E. F. Bell.[26] Our dry box enclosed instrument is for long wavelengths use.

An asymmetric interferometer (sometimes called a 'dispersive' interferometer) gives both the real and imaginary parts of the dielectric function of the sample without resort to a model or Kramers-Kronig analysis. The sample is put in the fixed mirror arm of the interferometer and the reference mirror is also, in turn, put there. As shown by E. F. Bell[26] the Fourier integrals yield the complex amplitude ($r_{os}\ \exp(-i\theta_s(\omega))$) when referenced to a known metal:

$$\left\{\frac{r_{os}(\omega)\, e^{-i\phi_s(\omega)}}{r_{or}(\omega)\, e^{-i\phi_r(\omega)}}\right\} = \left\{\frac{\int_{-\infty}^{\infty} e^{-i2\pi\omega\delta}\left[I_s(\delta)-I_s(\infty)\right]d\delta}{\int_{-\infty}^{\infty} e^{-i2\pi\omega\delta}\left[I_r(\delta)-I_r(\infty)\right]d\delta}\right\} \quad (37)$$

where $[\, I_s(\delta)-I_s(\infty)\,]$ is the interferogram of the sample and the subscript 's' refers to the reference metal.

We have used the interferometer with the diode sources to obtain data at mm wavelengths for graphite. However, we did not use the asymmetric feature. We have shown that the samples have to be flat to about ($\lambda/200$) which prevented using the instrument for the pressed natural minerals pellets since the surface of the pellet is slightly concaved and it is difficult to polish the surface to the required degree of flatness. For the iron studies the reflectance is so near unity that direct reflection studies are not possible in the submillimeter and millimeter wavelength regions.

However we'll continue improving our technology so as to use the asymmetric interferometer more fully.

4.2 InSb Detectors.

Our biggest experimental problem has been poor detectors for the submillimeter and millimeter wavelength regions. We have made InSb detectors, borrowed some from NRL, purchased one, and have been lent one (by K. D. Moeller) with an extremely thin absorbing Bi film evaporated on a dielectric substrate with the detector. For their use we have modified a LHe dewar, and have made some 'shake-down' efforts. However running out of funds in May 1984 has held us up. We must have better signal to noise ratios in our parallel plate and non-resonant cavity experiments. These detectors become sensitive around 200 cm^{-1} down to 10 to 1 cm^{-1}.

REFERENCES

1. F. E. Pinkerton and A. J. Sievers, Infrared Phys. 22, 377 (1982).

2. M. E. Milham and R. H. Frickel, JOSA. 1, 526, (1983).

3. F. E. Volz, Applied Optics 22, 1842, (1093).

4. V. P. Tomaselli and D. Moeller, Proceedings of the 1983 CSL Scientific Conference on Obscuration and Aerosol Research, 159 Edited by J. Farmer and R. H. Kohl.

5. N. J. Harrick, Internal Reflection Spectroscopy, (Wiley, NY, 1967).

6. M. R. Querry, Proceedings of the 1983 CSL Scientific Conference on Obscuration and Aerosol Research, Edited by J. Farmer and R. H. Kohl, 147 (1983).

7. G. Andermann, A. Caron, and David A. Dows, JOSA, 55, 10, (1965).

8. R. V. Churchill, J. W. Brown, and R. F. Verhey, Complex Variables and Applications (McGraw-Hill, NY, 1976).

9. R. H. Good Jr. and T. J. Nelson, Classical Theory of Electric and Magnetic Fields (Academic Press, NY, 1971).

10. Dr. Marvin Querry, private communication.

11. M. R. Querry, Proceedings of the 1983 CSL Scientific Conference on Obscuration and Aerosol Research, Edited by J. Farmer and R. H. Kohl, 147 (1983).

12. H. E. Bennett and J. O. Porteus, JOSA. 51, 2, 123 (1961).

13. A. S. Siddiqui and D. M. Treherne, Infrared Phys. 17, 33 (1977).

14. J. H. Weaver, E. Colavita, D. W. Lynch, and R. Rosei, Phys. Rev. B 19, 3850 (1979).

15. J. D. McMullen, Solid State Comm. 17, 331 (1975).

16. C. A. Ward, R. J. Bell, R. W. Alexander, G. S. Kovener, and I. Tyler, Appl. Opt. 13, 2378 (1974).

17. E. A. Taft and H. R. Philip, Phys. Rev. 138, A197 (1965).

18. G. Brandli and A. J. Sievers, Phys. Rev. B 5, 3550 (1972).

19. M. A. Ordal, L. L. Long, R. J. Bell, S. E. Bell, R. R. Bell, R. W. Alexander, Jr., and C. A. Ward, Appl. Opt. 22, 1099 (1983).

20. W. E. Lamb, Jr., Phys. Rev. 70, 308 (1946).

21. L. D. Woolf, J. Chin, Y. R. Lin-Liu, and H. Ikezi, Phys. Rev. B 30, 861 (15 July 1984).

22. H. B. G. Casimir and J. Ubbink, Philips Technical Review, 28, 366 (1967).

23. F. Wooten, Optical Properties of Solids (Academic Press, NY, 1972).

24. B. Donovan, Elementary Theory of Metals, Vol. 2 of the International Encyclopedia of Physical Chemistry and Chemical Physics, Ed. M. Blackman (Pergamon Press, Oxford, 1967).

25. R. J. Bell (with Ralph Alexander), Introductory Fourier Transform Spectroscopy (Academic Press, NY, 1972).

26. E. E. Bell, Infrared Phys. 6, 57 (1966) and E. E. Russell and E. E. Bell, Infrared Phys. 6, 75 (1966).

APPENDIX A

OPTICAL PROPERTIES OF THE METALS Al, Co, Cu, Au, Fe, Pb, Ni, Pd, Pt, Ag, Ti, AND W IN THE INFRARED AND FAR INFRARED

M. A. ORDAL, L. L. LONG, R. J. BELL, S. E. BELL,
R. R. BELL, R. W. ALEXANDER, JR., AND C. A. WARD

PHYSICS DEPARTMENT
UNIVERSITY OF MISSOURI-ROLLA
ROLLA, MISSOURI 65401

Reprinted from APPLIED OPTICS 22, 1099, 1983

Reprinted from **Applied Optics**, Vol. 22, page 1099, April 1, 1983

Optical properties of the metals Al, Co, Cu, Au, Fe, Pb, Ni, Pd, Pt, Ag, Ti, and W in the infrared and far infrared

M. A. Ordal, L. L. Long, R. J. Bell, S. E. Bell, R. R. Bell, R. W. Alexander, Jr., and C. A. Ward

Infrared optical constants collected from the literature are tabulated. The data for the noble metals and Al, Pb, and W can be reasonably fit using the Drude model. It is shown that $-\epsilon_1(\omega) = \epsilon_2(\omega) \simeq \omega_p^2/(2\omega_\tau^2)$ at the damping frequency $\omega = \omega_\tau$. Also $-\epsilon_1(\omega_\tau) \simeq -(1/2)\,\epsilon_1(0)$, where the plasma frequency is ω_p.

I. Introduction

Many measurements of the optical constants of metals have been made, primarily at near IR, visible, and UV wavelengths. Brandli and Sievers[1] have measured Au and Pb in the far IR. For the near and far IR we have compiled these data and have tabulated the real and imaginary parts of the dielectric function, ϵ_1 and ϵ_2, respectively, the index of refraction n and the extinction index k for each metal. Drude model[2] parameters giving a reasonable fit to the data are given for Au, Ag, Cu, Al, Pb, and W. In general, the Drude model is not expected to be appropriate for transition metals in the near and middle IR, but a good fit can be obtained for W with a Drude model dielectric function.

Weaver *et al.*[3] have compiled extensive tables or optical properties of metals which have been recently published. Most of their tables do not extend beyond 12-μm wavelength, while our compilation extends to the longest wavelength for which data are available. Another standard compilation is that of Haas and Hadley in the *AMERICAN INSTITUTE OF PHYSICS HANDBOOK*.[4] However, this includes data only up to 1967. Except for a few cases, the data presented here are more recent.

Bennett and Bennett[5] have shown that the Drude model fits the measured reflectance of gold, silver, and aluminum in the 3–30-μm wavelength range with one adjustable parameter; i.e., the Drude model parameters were obtained from the dc resistivity and fitted with one free electron per atom for gold and silver and 2.6 free electrons per atom for aluminum. Brandli and Sievers have shown that the Drude model is an excellent fit to their far IR measurements on lead and provides a good fit for gold with no adjustable parameters.

II. Definitions and Equations

In keeping with IR spectroscopic notation, all frequencies will be expressed in cm^{-1}. The complex dielectric function ϵ_c and the complex index of refraction n_c are defined as

$$\epsilon_c \equiv \epsilon_1 + i\epsilon_2 \equiv n_c^2 \equiv (n + ik)^2 \tag{1}$$

The Drude model dielectric function is

$$\epsilon_c = \epsilon_\infty - \frac{\omega_p^2}{\omega^2 + i\omega\omega_\tau}, \tag{2}$$

where ω, ω_p, and ω_τ have units of cm^{-1}. Separating the real and imaginary parts yields

$$\epsilon_1 = \epsilon_\infty - \frac{\omega_p^2}{\omega^2 + \omega_\tau^2}, \tag{3}$$

$$\epsilon_2 = \frac{\omega_p^2\,\omega_\tau}{\omega^3 + \omega\omega_\tau^2}. \tag{4}$$

In these equations, the plasma frequency[6] is

$$\omega_p(\mathrm{cm}^{-1}) = \frac{1}{2\pi c}\left(\frac{4\pi N e^2}{m^*\epsilon_\infty}\right)^{1/2}, \tag{5}$$

where N is the free electron density, e is the electron charge, m^* is the effective mass of the electrons, and ϵ_∞ is the high frequency dielectric constant. The damping frequency ω_τ expressed in cm^{-1} is

$$\omega_\tau(\mathrm{cm}^{-1}) = \frac{1}{2\pi c\tau}, \tag{6}$$

where τ is the electron lifetime in seconds and c is the velocity of light. Note that for low frequencies

When this work was done all authors were with University of Missouri Rolla, Physics Department, Rolla, Missouri 65401; C. A. W. Krebs is now with McDonnell Douglas Astronautics Company, Electrooptic Technology, P.O. Box 516, St. Louis Missouri 63166; S. E. Bell and R. R. Bell are now at Route 4, Box 124, Rolla, Missouri 65401.

Received 12 October 1982.
0003-6935/83/071099-21$01.00/0.

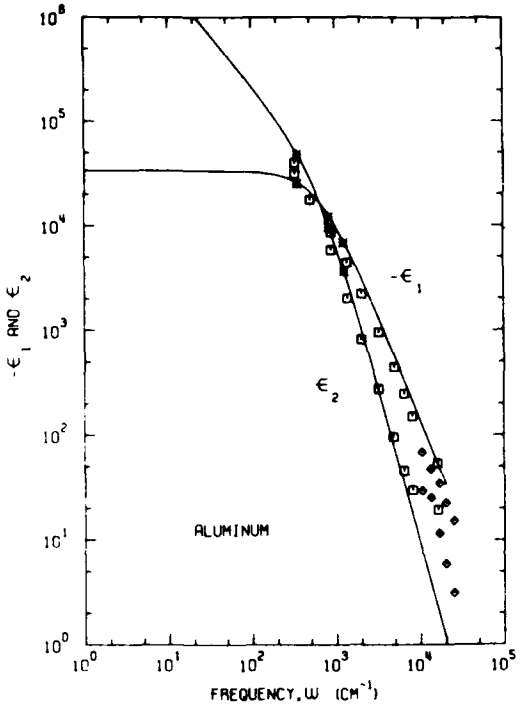

Fig. 1. Aluminum: $-\epsilon_1(\omega)$ and $\epsilon_2(\omega)$ vs frequency. The solid line is the Drude model. The data from Ref. 7 are: Shiles *et al.*, □ for both $-\epsilon_1$ and ϵ_2; Bennett and Bennett * for $-\epsilon_1$ and ϵ_2; Schulz, ◇ for $-\epsilon_1$ and ϵ_2.

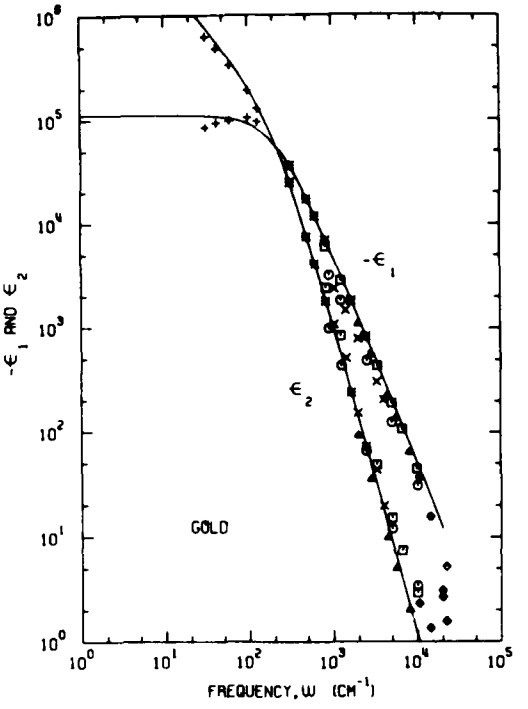

Fig. 3. Gold: $-\epsilon_1(\omega)$ and $\epsilon_2(\omega)$ vs frequency. The solid line is the Drude model. The data from Ref. 9 are: Bennett and Bennett, ✱ for both $-\epsilon_1$ and ϵ_2; Schulz, ◇ for both; Motulevich and Shubin, □ for both; Padalka and Shklyarevskii, ○ for both; Bolotin *et al.*, × for both; Brandli and Sievers, + for both; Weaver *et al.*, △ for both.

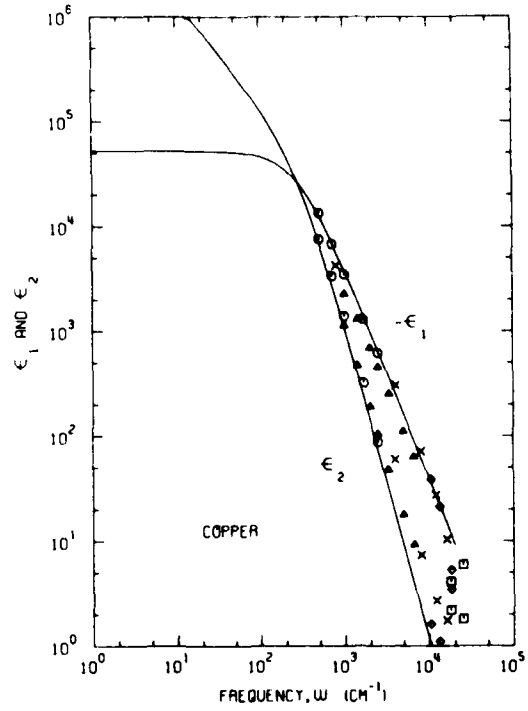

Fig. 2. Copper: $-\epsilon_1(\omega)$ and $\epsilon_2(\omega)$ vs frequency. The solid line is the Drude model. The data from Ref. 8 are: Schulz, ◇ for both $-\epsilon_1$ and ϵ_2; Lenham and Treherne, ✱ for $-\epsilon_1$ and ϵ_2; Robusto and Braunstein, □ for both; Hageman *et al.*, × for both; and Dold and Mecke, △ for both.

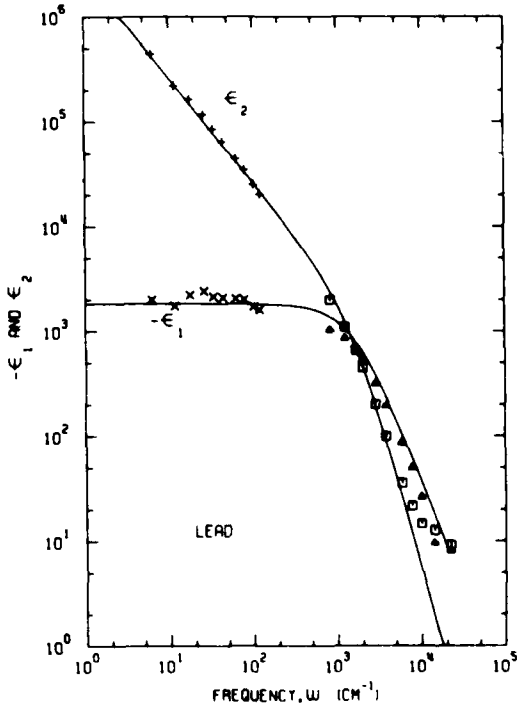

Fig. 4. Lead: $-\epsilon_1(\omega)$ and $\epsilon_2(\omega)$ vs frequency. The solid line represents the Drude model. The data from Ref. 10 are: Brandli and Sievers, × for $-\epsilon_1$ and + for ϵ_2; and Golovashkin and Motulevich, △ for $-\epsilon_1$ and □ for ϵ_2.

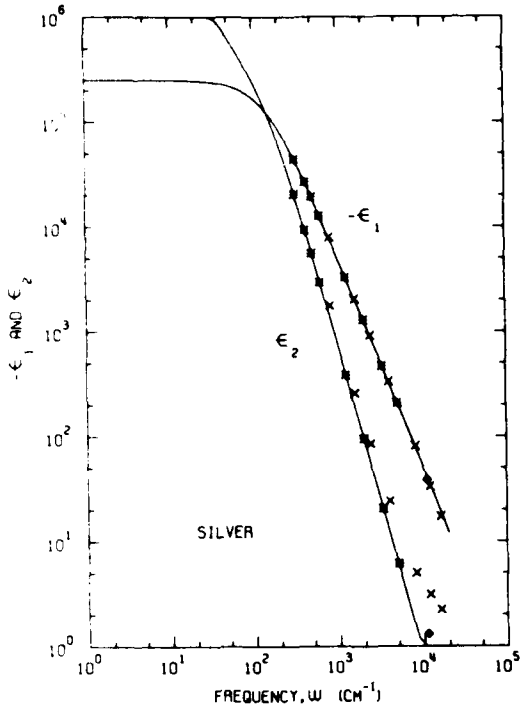

Fig. 5. Silver: $-\epsilon_1(\omega)$ and $\epsilon_2(\omega)$ vs frequency. The solid line is the Drude model. The data from Ref. 11 are: Bennett and Bennett, ✱ for both $-\epsilon_1$ and ϵ_2; Schulz, ◊ for both; and Hagemann *et al.*, × for both.

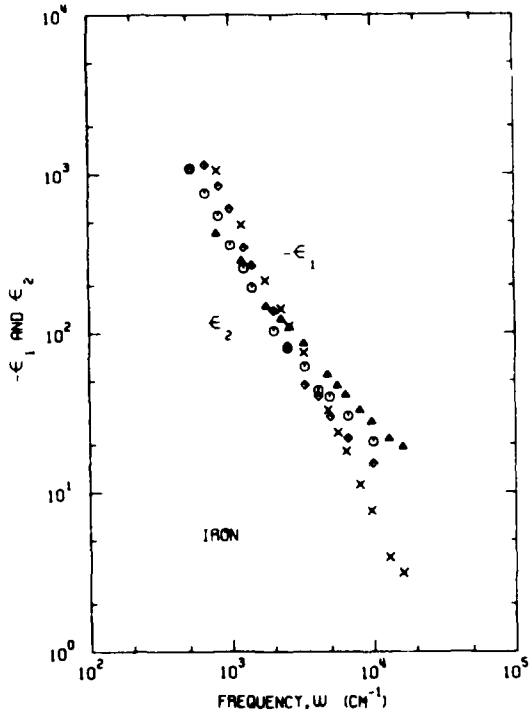

Fig. 7. Iron: $-\epsilon_1(\omega)$ and $\epsilon_2(\omega)$ vs frequency. The data from Ref. 13 are: Weaver *et al.*, × for $-\epsilon_1$ and △ for ϵ_2; Bolotin et al., ◊ for $-\epsilon_1$ and ○ for ϵ_2.

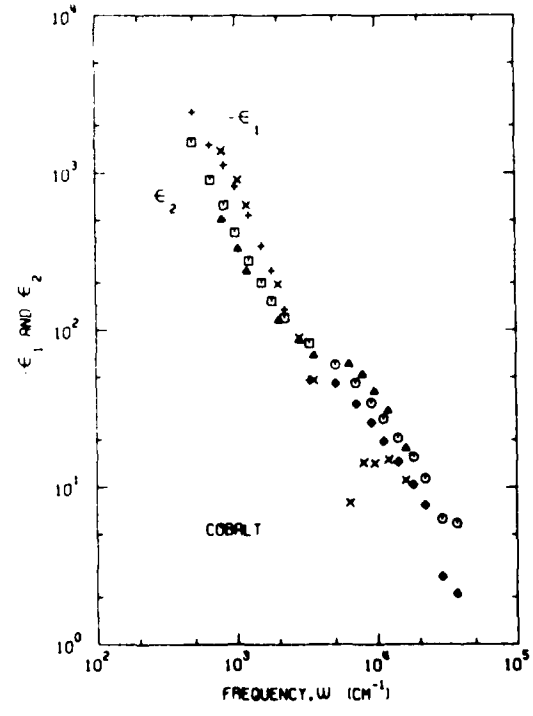

Fig. 6. Cobalt: $-\epsilon_1(\omega)$ and $\epsilon_2(\omega)$ vs frequency. The data from Ref. 12 are: Kirillova and Charikov, + for $-\epsilon_1$ and □ for ϵ_2; Johnson and Christy, ◊ for $-\epsilon_1$ and ○ for ϵ_2; and Weaver *et al.*, × for $-\epsilon_1$ and △ for ϵ_2.

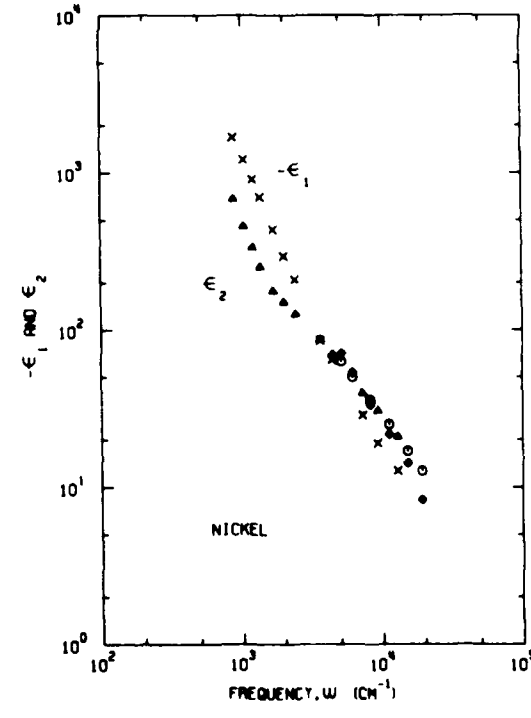

Fig. 8. Nickel: $-\epsilon_1(\omega)$ and $\epsilon_2(\omega)$ vs frequency. The data from Ref. 14 are: Lynch *et al.*, × for $-\epsilon_1$ and △ for ϵ_2; Johnson and Christy, ◊ for $-\epsilon_1$ and ○ for ϵ_2.

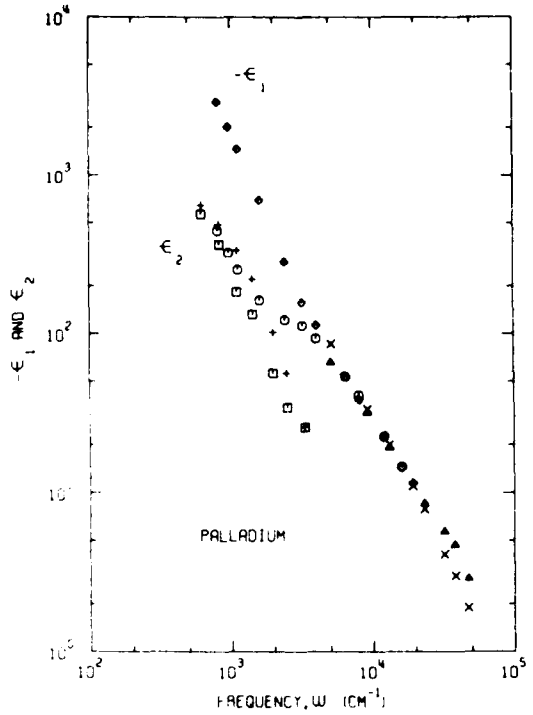

Fig. 9. Palladium: $-\epsilon_1(\omega)$ and $\epsilon_2(\omega)$ vs frequency. The data from Ref. 15 are: Weaver and Benbow, ◇ for $-\epsilon_1$ and ○ for ϵ_2; Bolotin *et al.*, + for $-\epsilon_1$ and □ for ϵ_2; Johnson and Christy, × for $-\epsilon_1$ and △ for ϵ_2.

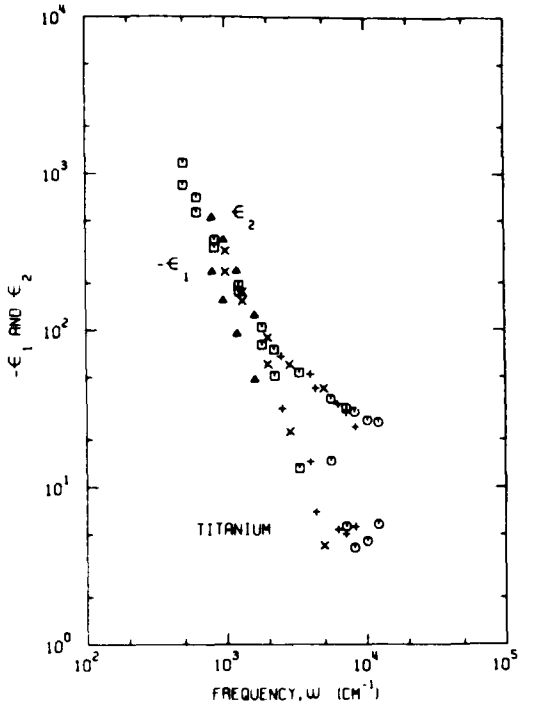

Fig. 11. Titanium: $-\epsilon_1(\omega)$ and $\epsilon_2(\omega)$ vs frequency. The data from Ref. 17 are: Kirillova and Charikov, □ for both $-\epsilon_1$ and ϵ_2; Lynch *et al.*, △ for both; Johnson and Christy, ○ for both; Kirillova and Charikov, + for both; Bolotin *et al.*, × for both.

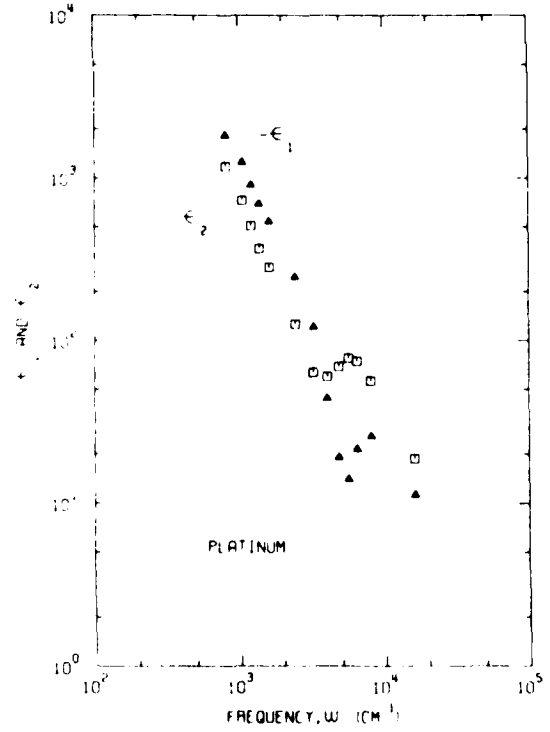

Fig. 10. Platinum: $-\epsilon_1(\omega)$ and $\epsilon_2(\omega)$ vs frequency. The data from Ref. 16 are Weaver *et al.*, △ for $-\epsilon_1$ and □ for ϵ_2.

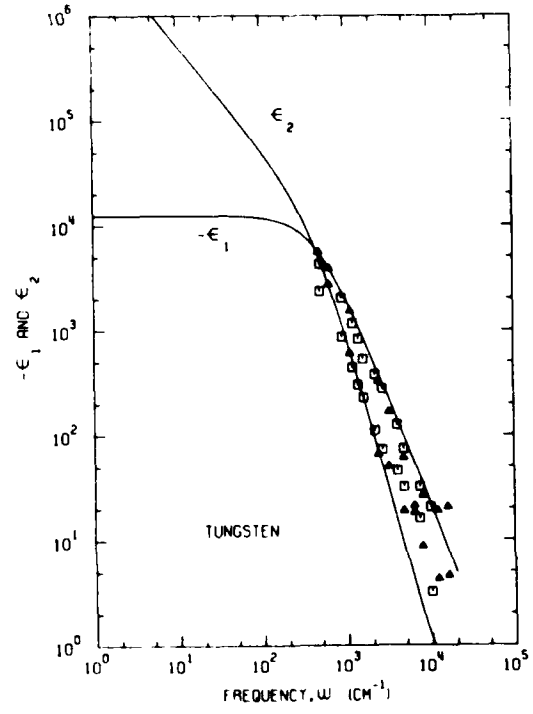

Fig. 12. Tungsten: $-\epsilon_1(\omega)$ and $\epsilon_2(\omega)$ vs frequency. The solid line is the Drude model. The data from Ref. 18 are: Nomerovannaya *et al.*, □ for both $-\epsilon_1$ and ϵ_2; Weaver *et al.*, △ for both.

TABLE 1. Al, ALUMINUM
E. Shiles, T. Sasaki, M. Inokuti, and D. Y. Smith, Phys. Rev. B 22, 1612 (1980)

ω(cm⁻¹)	λ(μm)	-ε1	ε2	n	k
3.23E+02	3.10E+01	3.18E+04	4.02E+04	9.86E+01	2.04E+02
3.39E+02	2.95E+01	3.01E+04	3.62E+04	9.22E+01	1.96E+02
3.71E+02	2.70E+01	2.68E+04	3.03E+04	8.26E+01	1.83E+02
4.03E+02	2.48E+01	2.43E+04	2.59E+04	7.50E+01	1.73E+02
4.36E+02	2.30E+01	2.14E+04	2.24E+04	6.93E+01	1.62E+02
4.68E+02	2.14E+01	1.95E+04	2.01E+04	6.52E+01	1.54E+02
5.00E+02	2.00E+01	1.80E+04	1.79E+04	6.07E+01	1.47E+02
5.32E+02	1.88E+01	1.66E+04	1.60E+04	5.67E+01	1.41E+02
5.81E+02	1.72E+01	1.50E+04	1.38E+04	5.20E+01	1.33E+02
6.45E+02	1.55E+01	1.32E+04	1.13E+04	4.58E+01	1.24E+02
7.10E+02	1.41E+01	1.18E+04	9.49E+03	4.09E+01	1.16E+02
7.74E+02	1.29E+01	1.05E+04	7.89E+03	3.62E+01	1.09E+02
8.87E+02	1.13E+01	8.77E+03	5.94E+03	3.02E+01	9.84E+01
1.05E+03	9.54E+00	6.93E+03	4.07E+03	2.35E+01	8.65E+01
1.21E+03	8.27E+00	5.58E+03	2.86E+03	1.86E+01	7.70E+01
1.37E+03	7.29E+00	4.51E+03	2.05E+03	1.49E+01	6.88E+01
1.61E+03	6.20E+00	3.39E+03	1.39E+03	1.17E+01	5.94E+01
2.02E+03	4.96E+00	2.25E+03	8.28E+02	8.59E+00	4.82E+01
2.42E+03	4.13E+00	1.63E+03	5.54E+02	6.76E+00	4.10E+01
2.82E+03	3.54E+00	1.24E+03	3.87E+02	5.44E+00	3.56E+01
3.23E+03	3.10E+00	9.71E+02	2.80E+02	4.45E+00	3.15E+01
4.84E+03	2.07E+00	4.53E+02	9.73E+01	2.27E+00	2.14E+01
6.45E+03	1.55E+00	2.52E+02	4.61E+01	1.44E+00	1.60E+01
8.07E+03	1.24E+00	1.54E+02	3.02E+01	1.21E+00	1.25E+01
1.21E+04	8.27E-01	6.15E+01	4.56E+01	2.75E+00	8.31E+00
1.61E+04	6.20E-01	5.42E+01	1.95E+01	1.30E+00	7.48E+00

TABLE 1. Al, ALUMINUM (Continued)
H. E. Bennett and J. M. Bennett, Optical Properties and Electronics Structure of Metals and Alloys, ed. F. Abeles (North-Holland, 1966), p. 175.

ω(cm⁻¹)	λ(μm)	-ε1	ε2	n	k
3.13E+02	3.20E+01	2.60E+04	5.56E+04	1.33E+02	2.09E+02
3.23E+02	3.10E+01	2.58E+04	5.31E+04	1.29E+02	2.06E+02
3.33E+02	3.00E+01	2.56E+04	5.08E+04	1.25E+02	2.03E+02
3.45E+02	2.90E+01	2.54E+04	4.84E+04	1.21E+02	2.00E+02
3.57E+02	2.80E+01	2.47E+04	4.59E+04	1.17E+02	1.96E+02
3.70E+02	2.70E+01	2.45E+04	4.36E+04	1.13E+02	1.93E+02
3.85E+02	2.60E+01	2.38E+04	4.12E+04	1.09E+02	1.89E+02
4.00E+02	2.50E+01	2.36E+04	3.91E+04	1.05E+02	1.86E+02
4.17E+02	2.40E+01	2.31E+04	3.64E+04	1.00E+02	1.82E+02
4.35E+02	2.30E+01	2.25E+04	3.42E+04	9.60E+01	1.78E+02
4.55E+02	2.20E+01	2.19E+04	3.18E+04	9.15E+01	1.74E+02
4.76E+02	2.10E+01	2.10E+04	2.93E+04	8.68E+01	1.69E+02
5.00E+02	2.00E+01	2.05E+04	2.71E+04	8.21E+01	1.65E+02
5.26E+02	1.90E+01	1.96E+04	2.47E+04	7.73E+01	1.60E+02
5.56E+02	1.80E+01	1.88E+04	2.24E+04	7.24E+01	1.55E+02
5.88E+02	1.70E+01	1.80E+04	2.02E+04	6.74E+01	1.50E+02
6.25E+02	1.60E+01	1.69E+04	1.79E+04	6.23E+01	1.44E+02
6.67E+02	1.50E+01	1.58E+04	1.58E+04	5.71E+01	1.38E+02
7.14E+02	1.40E+01	1.47E+04	1.37E+04	5.19E+01	1.32E+02
7.69E+02	1.30E+01	1.37E+04	1.18E+04	4.67E+01	1.26E+02
8.33E+02	1.20E+01	1.24E+04	9.88E+03	4.15E+01	1.19E+02
9.09E+02	1.10E+01	1.10E+04	8.06E+03	3.63E+01	1.11E+02
1.00E+03	1.00E+01	9.84E+03	6.49E+03	3.12E+01	1.04E+02
1.11E+03	9.00E+00	8.41E+03	5.02E+03	2.63E+01	9.54E+01
1.25E+03	8.00E+00	7.02E+03	3.72E+03	2.15E+01	8.65E+01

TABLE 1. Al, ALUMINUM (Continued)
L. G. Schulz, J. Opt. Soc. Am. 44, 357 (1954) and 362 (1954).

ω(cm⁻¹)	λ(μm)	-ε1	ε2	n	k
1.05E+04	9.50E-01	6.92E+01	2.98E+01	1.75E+00	8.50E+00
1.11E+04	9.00E-01	5.54E+01	3.02E+01	1.96E+00	7.70E+00
1.18E+04	8.50E-01	4.68E+01	2.97E+01	2.08E+00	7.15E+00
1.25E+04	8.00E-01	4.57E+01	2.81E+01	1.99E+00	7.05E+00
1.33E+04	7.50E-01	4.75E+01	2.56E+01	1.80E+00	7.12E+00
1.43E+04	7.00E-01	4.66E+01	2.17E+01	1.55E+00	7.00E+00
1.54E+04	6.50E-01	4.20E+01	1.64E+01	1.24E+00	6.60E+00
1.67E+04	6.00E-01	3.51E+01	1.16E+01	9.70E-01	6.00E+00
1.82E+04	5.50E-01	2.77E+01	8.09E+00	7.60E-01	5.32E+00
2.00E+04	5.00E-01	2.27E+01	5.95E+00	6.20E-01	4.80E+00
2.22E+04	4.50E-01	1.84E+01	4.23E+00	4.90E-01	4.32E+00
2.50E+04	4.00E-01	1.52E+01	3.14E+00	4.00E-01	3.92E+00

TABLE 2. Cu, COPPER
L. G. Schulz, J. Opt. Am. 44, 357 and 362 (1954).

ω(cm⁻¹)	λ(μm)	-ε1	ε2	n	k
1.05E+04	9.50E-01	3.87E+01	1.62E+00	1.30E-01	6.22E+00
1.11E+04	9.00E-01	3.43E+01	1.52E+00	1.30E-01	5.86E+00
1.18E+04	8.50E-01	2.99E+01	1.31E+00	1.20E-01	5.47E+00
1.25E+04	8.00E-01	2.57E+01	1.22E+00	1.20E-01	5.07E+00
1.33E+04	7.50E-01	2.13E+01	1.11E+00	1.20E-01	4.62E+00
1.43E+04	7.00E-01	1.74E+01	1.00E+00	1.20E-01	4.17E+00
1.54E+04	6.50E-01	1.33E+01	9.49E-01	1.30E-01	3.65E+00
1.67E+04	6.00E-01	9.40E+00	1.04E+00	1.70E-01	3.07E+00
1.82E+04	5.50E-01	5.34E+00	3.48E+00	7.20E-01	2.42E+00
2.00E+04	5.00E-01	5.08E+00	4.26E+00	8.80E-01	2.42E+00
2.22E+04	4.50E-01	4.08E+00	3.83E+00	8.70E-01	2.20E+00

TABLE 2. Cu, COPPER (Continued)
A. P. Lenham and D. M. Treherne, J. Opt. Soc. Am. 56, 683 (1966).

ω(cm⁻¹)	λ(μm)	-ε1	ε2	n	k
5.00E+02	2.00E+01	1.35E+04	7.61E+03	3.16E+01	1.20E+02
5.56E+02	1.80E+01	1.15E+04	6.11E+03	2.76E+01	1.11E+02
6.25E+02	1.60E+01	9.00E+03	4.64E+03	2.37E+01	9.78E+01
7.14E+02	1.40E+01	6.80E+03	3.36E+03	1.98E+01	8.48E+01
8.33E+02	1.20E+01	5.05E+03	2.29E+03	1.57E+01	7.28E+01
1.00E+03	1.00E+01	3.50E+03	1.40E+03	1.16E+01	6.03E+01
1.25E+03	8.00E+00	2.20E+03	7.28E+02	7.66E+00	4.75E+01
1.67E+03	6.00E+00	1.30E+03	3.24E+02	4.46E+00	3.63E+01
2.00E+03	5.00E+00	1.00E+03	1.40E+02	2.21E+00	3.17E+01
2.50E+03	4.00E+00	6.22E+02	8.80E+01	1.76E+00	2.50E+01

TABLE 2. Cu, Copper (Continued)
P. F. Robusto and Braunstein, Phys. Stat. Sol. (b) 107, 443 (1981).

ω(cm⁻¹)	λ(μm)	-ε1	ε2	n	k
1.56E+04	6.40E-01	7.69E+00	1.70E+00	3.04E-01	2.79E+00
1.67E+04	6.00E-01	5.98E+00	1.70E+00	3.44E-01	2.47E+00
1.79E+04	5.60E-01	4.09E+00	2.20E+00	5.26E-01	2.09E+00
1.92E+04	5.20E-01	3.71E+00	6.99E+00	1.45E+00	2.41E+00
2.08E+04	4.80E-01	3.10E+00	7.01E+00	1.51E+00	2.32E+00
2.27E+04	4.40E-01	2.39E+00	6.79E+00	1.55E+00	2.19E+00
2.50E+04	4.00E-01	1.81E+00	5.92E+00	1.48E+00	2.00E+00

TABLE 2. Cu, COPPER (Continued)
H. J. Hagemann, W. Gudat, and C. Kunz, J. Opt. Soc. Am. 65, 742 (1975).

ω(cm⁻¹)	λ(μm)	-ε1	ε2	n	k
8.07E+02	1.24E+01	4.24E+03	4.25E+03	2.97E+01	7.16E+01
4.03E+03	2.48E+00	3.08E+02	6.03E+01	1.71E+00	1.76E+01
8.07E+03	1.24E+00	7.17E+01	7.46E+00	4.40E-01	8.48E+00
1.21E+04	8.27E-01	2.76E+01	2.74E+00	2.60E-01	5.26E+00
1.37E+04	7.29E-01	1.96E+01	1.95E+00	2.20E-01	4.43E+00
1.41E+04	7.08E-01	1.80E+01	1.79E+00	2.10E-01	4.25E+00
1.45E+04	6.89E-01	1.63E+01	1.70E+00	2.10E-01	4.04E+00
1.49E+04	6.70E-01	1.48E+01	1.69E+00	2.20E-01	3.85E+00
1.53E+04	6.53E-01	1.34E+01	1.54E+00	2.10E-01	3.67E+00
1.61E+04	6.20E-01	1.04E+01	1.75E+00	2.70E-01	3.24E+00

TABLE 2. Cu, COPPER (Continued)
B. Dold and R. Mecke, Optik 22, 435 (1965).

ω(cm⁻¹)	λ(μm)	-ε1	ε2	n	k
1.00E+03	1.00E+01	2.27E+03	1.14E+03	1.16E+01	4.90E+01
1.11E+03	9.00E+00	1.99E+03	9.05E+02	9.90E+00	4.57E+01
1.25E+03	8.00E+00	1.66E+03	6.72E+02	8.10E+00	4.15E+01
1.43E+03	7.00E+00	1.31E+03	4.71E+02	6.40E+00	3.68E+01
1.67E+03	6.00E+00	9.99E+02	3.17E+02	4.95E+00	3.20E+01
2.00E+03	5.00E+00	6.95E+02	1.92E+02	3.60E+00	2.66E+01
2.50E+03	4.00E+00	4.56E+02	1.05E+02	2.45E+00	2.15E+01
3.33E+03	3.00E+00	2.54E+02	4.80E+01	1.50E+00	1.60E+01
5.00E+03	2.00E+00	1.12E+02	1.80E+01	8.50E-01	1.06E+01
6.67E+03	1.50E+00	6.37E+01	9.28E+00	5.80E-01	8.00E+00
8.00E+03	1.25E+00	4.46E+01	6.57E+00	4.90E-01	6.70E+00

TABLE 3. Au, GOLD
H. E. Bennett and J. M. Bennett, Optical Properties and Electronic Structure of Metals and Alloys edited by F. Abeles (North-Holland, Amsterdam, 1966), p. 175.

ω(cm⁻¹)	λ(μm)	-ε1	ε2	n	k
3.13E+02	3.20E+01	3.69E+04	2.54E+04	6.28E+01	2.02E+02
3.33E+02	3.00E+01	3.37E+04	2.17E+04	5.66E+01	1.92E+02
3.57E+02	2.80E+01	3.06E+04	1.84E+04	5.05E+01	1.82E+02
3.85E+02	2.60E+01	2.73E+04	1.53E+04	4.46E+01	1.71E+02
4.17E+02	2.40E+01	2.41E+04	1.24E+04	3.89E+01	1.60E+02
4.55E+02	2.20E+01	2.08E+04	9.89E+03	3.34E+01	1.48E+02
5.00E+02	2.00E+01	1.77E+04	7.67E+03	2.82E+01	1.36E+02
5.56E+02	1.80E+01	1.48E+04	5.78E+03	2.33E+01	1.24E+02
6.25E+02	1.60E+01	1.22E+04	4.19E+03	1.87E+01	1.12E+02
7.14E+02	1.40E+01	9.51E+03	2.86E+03	1.45E+01	9.86E+01
8.33E+02	1.20E+01	7.14E+03	1.84E+03	1.08E+01	8.52E+01
1.00E+03	1.00E+01	5.05E+03	1.09E+03	7.62E+00	7.15E+01
1.25E+03	8.00E+00	3.29E+03	5.68E+02	4.93E+00	5.76E+01
1.43E+03	7.00E+00	2.54E+03	3.83E+02	3.79E+00	5.05E+01
1.67E+03	6.00E+00	1.88E+03	2.42E+02	2.79E+00	4.34E+01
2.00E+03	5.00E+00	1.31E+03	1.41E+02	1.95E+00	3.62E+01
2.50E+03	4.00E+00	8.39E+02	7.25E+01	1.25E+00	2.90E+01
3.33E+03	3.00E+00	4.75E+02	3.07E+01	7.04E-01	2.18E+01

TABLE 3. Au, Gold (Continued)
L. G. Schulz, J. Opt. Soc. Am. 44, 357 and 362 (1954).

ω(cm⁻¹)	λ(μm)	-ε1	ε2	n	k
1.05E+04	9.50E-01	3.72E+01	2.32E+00	1.90E-01	6.10E+00
1.11E+04	9.00E-01	3.27E+01	2.06E+00	1.80E-01	5.72E+00
1.25E+04	8.00E-01	2.34E+01	1.55E+00	1.60E-01	4.84E+00
1.43E+04	7.00E-01	1.57E+01	1.35E+00	1.70E-01	3.97E+00
1.67E+04	6.00E-01	8.77E+00	1.37E+00	2.30E-01	2.97E+00
2.00E+04	5.00E-01	2.68E+00	3.09E+00	8.40E-01	1.84E+00
2.22E+04	4.50E-01	1.57E+00	5.26E+00	1.40E+00	1.88E+00

TABLE 3. Au, GOLD (Continued)
G. P. Motulevich and A. A. Shubin, Soviet Phys. JETP 20, 560 (1965).

ω(cm⁻¹)	λ(μm)	-ε1	ε2	n	k
8.33E+02	1.20E+01	6.24E+03	2.48E+03	1.54E+01	8.05E+01
1.00E+03	1.00E+01	4.42E+03	1.55E+03	1.15E+01	6.75E+01
1.25E+03	8.00E+00	2.92E+03	8.54E+02	7.82E+00	5.46E+01
1.67E+03	6.00E+00	1.72E+03	3.92E+02	4.70E+00	4.17E+01
2.00E+03	5.00E+00	1.23E+03	2.30E+02	3.27E+00	3.52E+01
2.50E+03	4.00E+00	7.74E+02	1.14E+02	2.04E+00	2.79E+01
3.33E+03	3.00E+00	4.40E+02	4.91E+01	1.17E+00	2.10E+01
4.00E+03	2.50E+00	2.99E+02	2.84E+01	8.20E-01	1.73E+01
5.00E+03	2.00E+00	1.93E+02	1.52E+01	5.46E-01	1.39E+01
6.67E+03	1.50E+00	1.08E+02	7.43E+00	3.57E-01	1.04E+01
1.00E+04	1.00E+00	4.50E+01	3.01E+00	2.24E-01	6.71E+00

TABLE 3. Au, GOLD (Continued)
V. G. Padalka and I. N. Shklyarevskii, Opt. Spectr. U.S.S.R. 11, 285 (1961).

ω(cm⁻¹)	λ(μm)	-ε1	ε2	n	k
9.09E+02	1.10E+01	3.31E+03	1.01E+03	8.71E+00	5.82E+01
1.00E+03	1.00E+01	2.80E+03	7.91E+02	7.41E+00	5.34E+01
1.11E+03	9.00E+00	2.32E+03	6.04E+02	6.21E+00	4.86E+01
1.25E+03	8.00E+00	1.87E+03	4.39E+02	5.05E+00	4.35E+01
1.43E+03	7.00E+00	1.45E+03	3.04E+02	3.97E+00	3.83E+01
1.67E+03	6.00E+00	1.08E+03	1.99E+02	3.01E+00	3.30E+01
2.00E+03	5.00E+00	7.62E+02	1.21E+02	2.19E+00	2.77E+01
2.50E+03	4.00E+00	4.91E+02	6.62E+01	1.49E+00	2.22E+01
3.33E+03	3.00E+00	2.78E+02	3.11E+01	9.30E-01	1.67E+01
5.00E+03	2.00E+00	1.25E+02	1.21E+01	5.40E-01	1.12E+01
1.00E+04	1.00E+00	3.10E+01	3.46E+00	3.10E-01	5.58E+00

TABLE 3. Au, GOLD (Continued)
G. A. Bolotin, A. N. Voloshinskii, M. M. Neskov, A. V. Sokolov, and B. A. Charikov, Phys. Met. and Met. 13, 823 (1962).

ω(cm⁻¹)	λ(μm)	-ε1	ε2	n	k
1.05E+03	9.50E+00	2.44E+03	1.10E+03	1.09E+01	5.06E+01
1.11E+03	9.00E+00	2.19E+03	9.58E+02	1.00E+01	4.79E+01
1.18E+03	8.50E+00	1.98E+03	8.86E+02	9.72E+00	4.56E+01
1.25E+03	8.00E+00	1.87E+03	6.95E+02	7.90E+00	4.40E+01
1.43E+03	7.00E+00	1.51E+03	5.22E+02	6.62E+00	3.94E+01
1.54E+03	6.50E+00	1.37E+03	4.10E+02	5.48E+00	3.74E+01
1.67E+03	6.00E+00	1.17E+03	3.25E+02	4.71E+00	3.45E+01
2.00E+03	5.00E+00	8.05E+02	1.54E+02	2.71E+00	2.85E+01
2.22E+03	4.50E+00	6.35E+02	1.15E+02	2.28E+00	2.53E+01
2.50E+03	4.00E+00	5.35E+02	8.72E+01	1.88E+00	2.32E+01
3.33E+03	3.00E+00	3.08E+02	4.40E+01	1.25E+00	1.76E+01
4.00E+03	2.50E+00	2.07E+02	1.99E+01	6.90E-01	1.44E+01

TABLE 3. Au, Gold (Continued)
G. Brandli and A. J. Sievers, Phy. Rev. B 5, 3550 (1972).

ω(cm⁻¹)	λ(μm)	-ε1	ε2	n	k
3.14E+01	3.18E+02	8.62E+04	6.23E+05	5.21E+02	5.98E+02
3.72E+01	2.69E+02	8.74E+04	5.37E+05	4.78E+02	5.62E+02
4.24E+01	2.36E+02	9.47E+04	4.81E+05	4.45E+02	5.41E+02
5.00E+01	2.00E+02	9.18E+04	4.00E+05	3.99E+02	5.01E+02
6.06E+01	1.65E+02	9.87E+04	3.37E+05	3.55E+02	4.74E+02
6.99E+01	1.43E+02	9.60E+04	2.82E+05	3.18E+02	4.44E+02
8.00E+01	1.25E+02	9.97E+04	2.47E+05	2.89E+02	4.28E+02
9.01E+01	1.11E+02	1.00E+05	2.15E+05	2.62E+02	4.11E+02
1.00E+02	1.00E+02	1.06E+05	1.93E+05	2.39E+02	4.04E+02
1.10E+02	9.09E+01	1.03E+05	1.68E+05	2.17E+02	3.88E+02
1.20E+02	8.33E+01	1.04E+05	1.49E+05	1.97E+02	3.78E+02
1.30E+02	7.69E+01	9.72E+04	1.30E+05	1.80E+02	3.60E+02
1.40E+02	7.14E+01	9.66E+04	1.14E+05	1.63E+02	3.51E+02
1.50E+02	6.67E+01	8.51E+04	1.00E+05	1.52E+02	3.29E+02

TABLE 3. Au, Gold (Continued)
J. H. Weaver, C. Krafka, D. W. Lynch, and E. E. Koch (with C. G. Olson), Physics Data, Optical Properties of Metals, (Fach-Information Zentrum, Kalsrube, FOR, 1981).

ω(cm⁻¹)	λ(μm)	-ε1	ε2	n	k
8.07E+02	1.24E+01	6.79E+03	1.35E+03	8.17E+00	8.28E+01
1.21E+03	8.27E+00	3.07E+03	4.12E+02	3.71E+00	5.56E+01
1.61E+03	6.20E+00	1.74E+03	1.78E+02	2.13E+00	4.17E+01
2.02E+03	4.96E+00	1.11E+03	9.29E+01	1.39E+00	3.34E+01
2.42E+03	4.13E+00	7.73E+02	5.51E+01	9.90E-01	2.78E+01
2.82E+03	3.54E+00	5.67E+02	3.57E+01	7.50E-01	2.38E+01
3.23E+03	3.10E+00	4.34E+02	2.46E+01	5.90E-01	2.08E+01
3.63E+03	2.76E+00	3.42E+02	1.74E+01	4.70E-01	1.85E+01
4.03E+03	2.48E+00	2.76E+02	1.30E+01	3.90E-01	1.66E+01
4.44E+03	2.25E+00	2.27E+02	9.95E+00	3.30E-01	1.51E+01
4.84E+03	2.07E+00	1.90E+02	7.72E+00	2.80E-01	1.38E+01
5.24E+03	1.91E+00	1.61E+02	6.09E+00	2.40E-01	1.27E+01
5.65E+03	1.77E+00	1.38E+02	5.17E+00	2.20E-01	1.18E+01
6.05E+03	1.65E+00	1.19E+02	4.15E+00	1.90E-01	1.09E+01
6.45E+03	1.55E+00	1.04E+02	3.68E+00	1.80E-01	1.02E+01
6.86E+03	1.46E+00	9.16E+01	3.06E+00	1.60E-01	9.57E+00
7.26E+03	1.38E+00	8.12E+01	2.70E+00	1.50E-01	9.01E+00
7.66E+03	1.31E+00	7.21E+01	2.38E+00	1.40E-01	8.49E+00
8.07E+03	1.24E+00	6.45E+01	2.09E+00	1.30E-01	8.03E+00
1.21E+04	8.27E-01	2.48E+01	7.97E-01	8.00E-02	4.98E+00
1.61E+04	6.20E-01	9.97E+00	8.22E-01	1.30E-01	3.16E+00

TABLE 4. Pb, LEAD
G. Brandli and A. J. Sievers, Phys. Rev. B 5, 3550 (1972).

ω(cm⁻¹)	λ(μm)	-ε1	ε2	n	k
6.25E+00	1.60E+03	1.99E+03	4.43E+05	4.69E+02	4.71E+02
1.17E+01	8.57E+02	1.74E+03	2.21E+05	3.31E+02	3.34E+02
1.78E+01	5.63E+02	2.21E+03	1.64E+05	2.85E+02	2.89E+02
2.61E+01	3.83E+02	2.40E+03	1.17E+05	2.39E+02	2.44E+02
3.38E+01	2.96E+02	2.14E+03	8.49E+04	2.03E+02	2.09E+02
4.41E+01	2.27E+02	2.10E+03	6.44E+04	1.77E+02	1.82E+02
5.38E+01	1.86E+02	2.09E+03	5.27E+04	1.59E+02	1.66E+02
6.28E+01	1.59E+02	2.05E+03	4.47E+04	1.46E+02	1.53E+02
7.19E+01	1.39E+02	2.01E+03	3.87E+04	1.35E+02	1.43E+02
7.96E+01	1.26E+02	2.02E+03	3.50E+04	1.28E+02	1.36E+02
8.92E+01	1.12E+02	1.85E+03	2.98E+04	1.18E+02	1.26E+02
1.02E+02	9.80E+01	1.71E+03	2.51E+04	1.08E+02	1.16E+02
1.12E+02	8.96E+01	1.64E+03	2.24E+04	1.02E+02	1.10E+02
1.21E+02	8.25E+01	1.61E+03	2.05E+04	9.72E+01	1.05E+02

TABLE 4. Pb, LEAD (Continued)
A. I. Golovashkin and G. P. Motulevich, Soviet Physics JETP 26, 881 (1968)

ω(cm⁻¹)	λ(μm)	-ε1	ε2	n	k
8.33E+02	1.20E+01	1.04E+03	1.99E+03	2.46E+01	4.05E+01
9.09E+02	1.10E+01	9.98E+02	1.82E+03	2.32E+01	3.92E+01
1.00E+03	1.00E+01	9.58E+02	1.57E+03	2.10E+01	3.74E+01
1.11E+03	9.00E+00	9.32E+02	1.34E+03	1.87E+01	3.58E+01
1.25E+03	8.00E+00	8.60E+02	1.10E+03	1.64E+01	3.36E+01
1.43E+03	7.00E+00	7.56E+02	8.71E+02	1.41E+01	3.09E+01
1.67E+03	6.00E+00	6.53E+02	6.58E+02	1.17E+01	2.81E+01
2.00E+03	5.00E+00	5.33E+02	4.48E+02	9.04E+00	2.48E+01
2.50E+03	4.00E+00	3.89E+02	2.74E+02	6.58E+00	2.08E+01
2.86E+03	3.50E+00	3.17E+02	2.01E+02	5.39E+00	1.86E+01
3.33E+03	3.00E+00	2.51E+02	1.40E+02	4.27E+00	1.64E+01
3.85E+03	2.60E+00	1.95E+02	9.94E+01	3.45E+00	1.44E+01
4.00E+03	2.50E+00	1.83E+02	8.95E+01	3.22E+00	1.39E+01
4.17E+03	2.40E+00	1.65E+02	8.00E+01	3.03E+00	1.32E+01
4.35E+03	2.30E+00	1.56E+02	7.27E+01	2.84E+00	1.28E+01
4.55E+03	2.20E+00	1.42E+02	6.42E+01	2.63E+00	1.22E+01
4.76E+03	2.10E+00	1.31E+02	5.78E+01	2.47E+00	1.17E+01
5.00E+03	2.00E+00	1.20E+02	5.20E+01	2.32E+00	1.12E+01
5.88E+03	1.70E+00	8.61E+01	3.58E+01	1.89E+00	9.47E+00
6.67E+03	1.50E+00	6.62E+01	2.72E+01	1.64E+00	8.30E+00
7.69E+03	1.30E+00	7.43E-01	5.19E+00	1.50E+00	1.73E+00
1.00E+04	1.00E+00	2.64E+01	1.47E+01	1.38E+00	5.32E+00
1.11E+04	9.00E-01	1.99E+01	1.31E+01	1.40E+00	4.68E+00
1.18E+04	8.50E-01	1.68E+01	1.25E+01	1.44E+00	4.35E+00
1.25E+04	8.00E-01	1.45E+01	1.23E+01	1.50E+00	4.09E+00
1.33E+04	7.50E-01	1.17E+01	1.21E+01	1.60E+00	3.78E+00
1.43E+04	7.00E-01	9.58E+00	1.27E+01	1.78E+00	3.57E+00
1.54E+04	6.50E-01	8.67E+00	1.34E+01	1.91E+00	3.51E+00
1.67E+04	6.00E-01	8.25E+00	1.32E+01	1.91E+00	3.45E+00
1.82E+04	5.50E-01	8.21E+00	1.24E+01	1.83E+00	3.40E+00
2.00E+04	5.00E-01	8.00E+00	1.12E+01	1.70E+00	3.30E+00
2.22E+04	4.50E-01	8.04E+00	9.16E+00	1.44E+00	3.18E+00

TABLE 5. Ag, SILVER
H. E. Bennett and J. M. Bennett in Optical Properties and Electronic Structure of Metals and Alloys, edited by F. Abeles (North-Holland, Amsterdam, 1966), p. 175.

ω(cm⁻¹)	λ(μm)	-ε1	ε2	n	k
3.13E+02	3.20E+01	4.44E+04	2.06E+04	4.78E+01	2.16E+02
3.33E+02	3.00E+01	3.98E+04	1.74E+04	4.26E+01	2.04E+02
3.57E+02	2.80E+01	3.55E+04	1.44E+04	3.76E+01	1.92E+02
3.85E+02	2.60E+01	3.10E+04	1.17E+04	3.28E+01	1.79E+02
4.17E+02	2.40E+01	2.71E+04	9.45E+03	2.83E+01	1.67E+02
4.55E+02	2.20E+01	2.31E+04	7.39E+03	2.40E+01	1.54E+02
5.00E+02	2.00E+01	1.95E+04	5.67E+03	2.01E+01	1.41E+02
5.56E+02	1.80E+01	1.59E+04	4.17E+03	1.64E+01	1.27E+02
6.25E+02	1.60E+01	1.28E+04	2.99E+03	1.31E+01	1.14E+02
7.14E+02	1.40E+01	9.90E+03	2.02E+03	1.01E+01	1.00E+02
8.33E+02	1.20E+01	7.34E+03	1.28E+03	7.46E+00	8.60E+01
1.00E+03	1.00E+01	5.14E+03	7.49E+02	5.21E+00	7.19E+01
1.25E+03	8.00E+00	3.32E+03	3.87E+02	3.35E+00	5.77E+01
1.43E+03	7.00E+00	2.55E+03	2.60E+02	2.57E+00	5.06E+01
1.67E+03	6.00E+00	1.88E+03	1.64E+02	1.89E+00	4.34E+01
2.00E+03	5.00E+00	1.31E+03	9.56E+01	1.32E+00	3.62E+01
2.50E+03	4.00E+00	8.34E+02	4.88E+01	8.44E-01	2.89E+01
3.33E+03	3.00E+00	4.71E+02	2.06E+01	4.74E-01	2.17E+01
5.00E+03	2.00E+00	2.10E+02	6.15E+00	2.12E-01	1.45E+01

TABLE 5. Ag, SILVER (Continued)
L. G. Schulz, J. Opt. Soc. Am. 44, p. 357 and 362 (1954).

ω(cm⁻¹)	λ(μm)	-ε1	ε2	n	k
1.05E+04	9.50E-01	4.30E+01	1.44E+00	1.10E-01	6.56E+00
1.11E+04	9.00E-01	3.87E+01	1.31E+00	1.05E-01	6.22E+00
1.18E+04	8.50E-01	3.42E+01	1.17E+00	1.00E-01	5.85E+00
1.25E+04	8.00E-01	2.97E+01	9.81E-01	9.00E-02	5.45E+00
1.33E+04	7.50E-01	2.55E+01	8.08E-01	8.00E-02	5.05E+00
1.43E+04	7.00E-01	2.13E+01	6.93E-01	7.50E-02	4.62E+00
1.54E+04	6.50E-01	1.76E+01	5.88E-01	7.00E-02	4.20E+00
1.67E+04	6.00E-01	1.41E+01	4.50E-01	6.00E-02	3.75E+00
1.82E+04	5.50E-01	1.10E+01	3.65E-01	5.50E-02	3.32E+00
2.00E+04	5.00E-01	8.23E+00	2.87E-01	5.00E-02	2.87E+00
2.22E+04	4.50E-01	5.55E+00	2.66E+00	5.50E-01	2.42E+00
2.50E+04	4.00E-01	3.72E+00	2.90E-01	7.50E-02	1.93E+00

TABLE 5. Ag, Silver (Continued)
H. J. Hageman, W. Gudat, and C. Kunz, J. Opt. Soc. Am. 65, 742 (1975).

ω(cm⁻¹)	λ(μm)	-ε1	ε2	n	k
8.07E+02	1.24E+01	8.05E+03	1.79E+03	9.91E+00	9.03E+01
1.61E+03	6.20E+00	2.08E+03	2.60E+02	2.84E+00	4.57E+01
2.42E+03	4.13E+00	9.29E+02	8.60E+01	1.41E+00	3.05E+01
3.23E+03	3.10E+00	5.23E+02	4.17E+01	9.10E-01	2.29E+01
4.03E+03	2.48E+00	3.35E+02	2.45E+01	6.70E-01	1.83E+01
8.07E+03	1.24E+00	8.15E+01	5.06E+00	2.80E-01	9.03E+00
1.21E+04	8.27E-01	3.35E+01	3.13E+00	2.70E-01	5.79E+00
1.61E+04	6.20E-01	1.74E+01	2.26E+00	2.70E-01	4.18E+00

TABLE 6. Co, COBALT
M. M. Kirillova and B. A. Charikov, Opt. Spectry. 17, 134 (1964).

ω(cm⁻¹)	λ(μm)	-ε1	ε2	n	k
5.00E+02	2.00E+01	2.44E+03	1.57E+03	1.52E+01	5.17E+01
5.26E+02	1.90E+01	2.18E+03	1.46E+03	1.49E+01	4.90E+01
5.88E+02	1.70E+01	1.84E+03	1.22E+03	1.35E+01	4.50E+01
6.67E+02	1.50E+01	1.51E+03	9.07E+02	1.12E+01	4.05E+01
7.14E+02	1.40E+01	1.34E+03	7.75E+02	1.02E+01	3.80E+01
8.33E+02	1.20E+01	1.12E+03	6.25E+02	9.00E+00	3.47E+01
9.09E+02	1.10E+01	9.97E+02	5.28E+02	8.10E+00	3.26E+01
1.00E+03	1.00E+01	8.20E+02	4.19E+02	7.10E+00	2.95E+01
1.11E+03	9.00E+00	6.97E+02	3.57E+02	6.56E+00	2.72E+01
1.25E+03	8.00E+00	5.42E+02	2.78E+02	5.80E+00	2.40E+01
1.43E+03	7.00E+00	4.08E+02	2.26E+02	5.40E+00	2.09E+01
1.54E+03	6.50E+00	3.45E+02	2.01E+02	5.20E+00	1.93E+01
1.67E+03	6.00E+00	2.81E+02	1.75E+02	5.00E+00	1.75E+01
1.82E+03	5.50E+00	2.40E+02	1.54E+02	4.76E+00	1.62E+01
2.00E+03	5.00E+00	1.94E+02	1.38E+02	4.70E+00	1.47E+01
2.22E+03	4.50E+00	1.36E+02	1.20E+02	4.78E+00	1.26E+01
2.50E+03	4.00E+00	9.89E+01	1.03E+02	4.70E+00	1.10E+01
3.33E+03	3.00E+00	4.78E+01	8.26E+01	4.88E+00	8.46E+00
4.00E+03	2.50E+00	3.48E+01	7.96E+01	5.10E+00	7.80E+00

TABLE 6. Co, COBALT (Continued)
P. B. Johnson and R. W. Christy, Phys. B 9, 5056 (1974).

ω(cm⁻¹)	λ(μm)	-ε1	ε2	n	k
5.16E+03	1.94E+00	4.57E+01	6.03E+01	3.87E+00	7.79E+00
6.21E+03	1.61E+00	3.97E+01	5.24E+01	3.61E+00	7.26E+00
7.18E+03	1.39E+00	3.41E+01	4.63E+01	3.42E+00	6.77E+00
8.23E+03	1.22E+00	2.98E+01	4.00E+01	3.17E+00	6.31E+00
9.19E+03	1.09E+00	2.59E+01	3.46E+01	2.94E+00	5.88E+00
1.02E+04	9.84E-01	2.25E+01	3.06E+01	2.78E+00	5.50E+00
1.12E+04	8.92E-01	1.96E+01	2.73E+01	2.65E+00	5.16E+00
1.22E+04	8.21E-01	1.74E+01	2.47E+01	2.53E+00	4.88E+00
1.32E+04	7.56E-01	1.58E+01	2.23E+01	2.40E+00	4.64E+00
1.42E+04	7.04E-01	1.45E+01	2.06E+01	2.31E+00	4.45E+00
1.52E+04	6.59E-01	1.32E+01	1.92E+01	2.25E+00	4.27E+00
1.62E+04	6.17E-01	1.21E+01	1.80E+01	2.19E+00	4.11E+00
1.72E+04	5.82E-01	1.11E+01	1.69E+01	2.13E+00	3.96E+00
1.82E+04	5.49E-01	1.04E+01	1.57E+01	2.05E+00	3.82E+00
1.92E+04	5.21E-01	9.66E+00	1.45E+01	1.97E+00	3.68E+00
2.02E+04	4.96E-01	9.07E+00	1.33E+01	1.88E+00	3.55E+00
2.12E+04	4.71E-01	8.35E+00	1.23E+01	1.81E+00	3.41E+00
2.22E+04	4.51E-01	7.73E+00	1.14E+01	1.74E+00	3.28E+00
2.32E+04	4.30E-01	7.26E+00	1.06E+01	1.67E+00	3.17E+00
2.42E+04	4.13E-01	6.71E+00	9.82E+00	1.61E+00	3.05E+00
2.52E+04	3.97E-01	6.12E+00	9.20E+00	1.57E+00	2.93E+00
2.62E+04	3.81E-01	5.61E+00	8.63E+00	1.53E+00	2.82E+00
2.72E+04	3.68E-01	5.09E+00	8.13E+00	1.50E+00	2.71E+00
2.82E+04	3.54E-01	4.59E+00	7.78E+00	1.49E+00	2.61E+00
2.92E+04	3.42E-01	4.16E+00	7.46E+00	1.48E+00	2.52E+00
3.02E+04	3.31E-01	3.82E+00	7.12E+00	1.46E+00	2.44E+00
3.12E+04	3.20E-01	3.51E+00	6.87E+00	1.45E+00	2.37E+00
3.22E+04	3.11E-01	3.26E+00	6.65E+00	1.44E+00	2.31E+00
3.32E+04	3.01E-01	2.99E+00	6.48E+00	1.44E+00	2.25E+00
3.42E+04	2.92E-01	2.72E+00	6.31E+00	1.44E+00	2.19E+00
3.52E+04	2.84E-01	2.51E+00	6.16E+00	1.44E+00	2.14E+00
3.62E+04	2.76E-01	2.29E+00	6.02E+00	1.44E+00	2.09E+00
3.72E+04	2.69E-01	2.09E+00	5.88E+00	1.44E+00	2.04E+00
3.82E+04	2.62E-01	1.97E+00	5.79E+00	1.44E+00	2.01E+00
3.92E+04	2.55E-01	1.78E+00	5.71E+00	1.45E+00	1.97E+00
4.02E+04	2.49E-01	1.62E+00	5.60E+00	1.45E+00	1.93E+00
4.12E+04	2.43E-01	1.52E+00	5.58E+00	1.46E+00	1.91E+00
4.22E+04	2.37E-01	1.41E+00	5.56E+00	1.47E+00	1.89E+00
4.32E+04	2.31E-01	1.34E+00	5.50E+00	1.47E+00	1.87E+00
4.42E+04	2.26E-01	1.36E+00	5.39E+00	1.45E+00	1.86E+00
4.52E+04	2.21E-01	1.38E+00	5.29E+00	1.43E+00	1.85E+00
4.62E+04	2.16E-01	1.40E+00	5.19E+00	1.41E+00	1.84E+00
4.72E+04	2.12E-01	1.41E+00	5.02E+00	1.38E+00	1.82E+00
4.82E+04	2.07E-01	1.32E+00	4.84E+00	1.36E+00	1.78E+00
4.92E+04	2.03E-01	1.32E+00	4.62E+00	1.32E+00	1.75E+00
5.02E+04	1.99E-01	1.26E+00	4.41E+00	1.29E+00	1.71E+00
5.12E+04	1.95E-01	1.20E+00	4.21E+00	1.26E+00	1.67E+00
5.22E+04	1.92E-01	1.19E+00	3.94E+00	1.21E+00	1.63E+00
5.32E+04	1.88E-01	1.18E+00	3.69E+00	1.16E+00	1.59E+00

TABLE 6. Co, COBALT (Continued)
J. H. Weaver, E. Colavita, D. W. Lynch and R. Rosei, Phys. Rev. B 19, 3850 (1979).

ω(cm⁻¹)	λ(μm)	-ε1	ε2	n	k
8.07E+02	1.24E+01	1.39E+03	5.08E+02	6.71E+00	3.79E+01
1.05E+03	9.54E+00	9.05E+02	3.29E+02	5.38E+00	3.06E+01
1.21E+03	8.27E+00	6.27E+02	2.37E+02	4.66E+00	2.55E+01
1.61E+03	6.20E+00	3.40E+02	1.33E+02	3.55E+00	1.88E+01
2.02E+03	4.96E+00	1.97E+02	1.16E+02	3.98E+00	1.46E+01
2.42E+03	4.13E+00	1.32E+02	9.83E+01	4.04E+00	1.22E+01
2.82E+03	3.54E+00	9.03E+01	8.68E+01	4.18E+00	1.04E+01
3.23E+03	3.10E+00	6.54E+01	7.74E+01	4.24E+00	9.13E+00
3.63E+03	2.76E+00	4.80E+01	6.89E+01	4.24E+00	8.12E+00
4.03E+03	2.48E+00	3.22E+01	6.34E+01	4.41E+00	7.19E+00
4.84E+03	2.07E+00	1.35E+01	6.02E+01	4.91E+00	6.13E+00
5.65E+03	1.77E+00	6.76E+00	6.13E+01	5.24E+00	5.85E+00
6.45E+03	1.55E+00	7.96E+00	6.09E+01	5.17E+00	5.89E+00
7.26E+03	1.38E+00	1.10E+01	5.88E+01	4.94E+00	5.95E+00
8.07E+03	1.24E+00	1.44E+01	5.23E+01	4.46E+00	5.86E+00
9.68E+03	1.03E+00	1.42E+01	4.08E+01	3.81E+00	5.36E+00
1.21E+04	8.27E-01	1.50E+01	3.08E+01	3.10E+00	4.96E+00
1.61E+04	6.20E-01	1.11E+01	1.77E+01	2.21E+00	4.00E+00

TABLE 7. Fe, Iron
J. H. Weaver, E. Colavita, D. W. Lynch, and R. Rosei, Phys. Rev. B 19, 3850 (1979).

ω(cm⁻¹)	λ(μm)	-ε1	ε2	n	k
8.07E+02	1.24E+01	1.05E+03	4.24E+02	6.41E+00	3.31E+01
1.05E+03	9.54E+00	6.79E+02	3.36E+02	6.26E+00	2.68E+01
1.21E+03	8.27E+00	4.82E+02	2.86E+02	6.26E+00	2.28E+01
1.37E+03	7.29E+00	3.82E+02	2.58E+02	6.28E+00	2.05E+01
1.61E+03	6.20E+00	3.19E+02	1.34E+02	3.68E+00	1.82E+01
1.77E+03	5.64E+00	2.16E+02	1.48E+02	4.80E+00	1.55E+01
1.94E+03	5.17E+00	1.88E+02	1.45E+02	4.96E+00	1.46E+01
2.10E+03	4.77E+00	1.62E+02	1.36E+02	4.98E+00	1.37E+01
2.26E+03	4.43E+00	1.43E+02	1.23E+02	4.78E+00	1.29E+01
2.42E+03	4.13E+00	1.21E+02	1.17E+02	4.87E+00	1.21E+01
2.58E+03	3.87E+00	1.11E+02	1.09E+02	4.73E+00	1.15E+01
2.74E+03	3.65E+00	9.69E+01	1.03E+02	4.70E+00	1.09E+01
2.90E+03	3.44E+00	8.71E+01	9.77E+01	4.68E+00	1.04E+01
3.06E+03	3.26E+00	8.00E+01	9.32E+01	4.63E+00	1.01E+01
3.23E+03	3.10E+00	7.55E+01	8.62E+01	4.42E+00	9.75E+00
4.03E+03	2.48E+00	4.72E+01	6.64E+01	4.14E+00	8.02E+00
4.84E+03	2.07E+00	3.29E+01	5.46E+01	3.93E+00	6.95E+00
5.65E+03	1.77E+00	2.38E+01	4.66E+01	3.78E+00	6.17E+00
6.45E+03	1.55E+00	1.80E+01	4.09E+01	3.65E+00	5.60E+00
7.26E+03	1.38E+00	1.42E+01	3.63E+01	3.52E+00	5.16E+00
8.07E+03	1.24E+00	1.12E+01	3.29E+01	3.43E+00	4.79E+00
8.87E+03	1.13E+00	1.03E+01	3.08E+01	3.33E+00	4.62E+00
9.68E+03	1.03E+00	7.65E+00	2.76E+01	3.24E+00	4.26E+00
1.05E+04	9.54E-01	6.58E+00	2.57E+01	3.16E+00	4.07E+00
1.13E+04	8.86E-01	5.24E+00	2.41E+01	3.12E+00	3.87E+00
1.21E+04	8.27E-01	4.91E+00	2.30E+01	3.05E+00	3.77E+00
1.29E+04	7.75E-01	3.96E+00	2.16E+01	3.00E+00	3.60E+00
1.37E+04	7.29E-01	3.51E+00	2.10E+01	2.98E+00	3.52E+00
1.45E+04	6.89E-01	3.45E+00	2.02E+01	2.92E+00	3.46E+00
1.53E+04	6.53E-01	3.00E+00	1.95E+01	2.89E+00	3.37E+00
1.61E+04	6.20E-01	3.11E+00	1.92E+01	2.86E+00	3.36E+00

TABLE 7. Fe, Iron (Continued)
G. A. Bolotin, M. M. Kirillova, and V. M. Mayevskiy, Phys. Met. Metall, 27(2) 31 (1969).

ω(cm⁻¹)	λ(μm)	-ε1	ε2	n	k
5.26E+02	1.90E+01	1.92E+03	1.09E+03	1.20E+01	4.54E+01
5.56E+02	1.80E+01	1.58E+03	9.52E+02	1.15E+01	4.14E+01
5.88E+02	1.70E+01	1.41E+03	8.70E+02	1.11E+01	3.92E+01
6.25E+02	1.60E+01	1.27E+03	8.04E+02	1.08E+01	3.72E+01
6.67E+02	1.50E+01	1.15E+03	7.62E+02	1.07E+01	3.56E+01
7.14E+02	1.40E+01	1.06E+03	7.18E+02	1.05E+01	3.42E+01
7.69E+02	1.30E+01	9.52E+02	6.63E+02	1.02E+01	3.25E+01
8.33E+02	1.20E+01	8.43E+02	5.47E+02	9.00E+00	3.04E+01
9.09E+02	1.10E+01	7.20E+02	4.48E+02	8.00E+00	2.80E+01
1.00E+03	1.00E+01	6.06E+02	3.58E+02	7.00E+00	2.56E+01
1.11E+03	9.00E+00	4.67E+02	2.98E+02	6.60E+00	2.26E+01
1.25E+03	8.00E+00	3.46E+02	2.56E+02	6.50E+00	1.97E+01
1.43E+03	7.00E+00	2.68E+02	1.94E+02	5.60E+00	1.73E+01
1.67E+03	6.00E+00	1.89E+02	1.35E+02	4.65E+00	1.45E+01
2.00E+03	5.00E+00	1.39E+02	1.04E+02	4.15E+00	1.25E+01
2.50E+03	4.00E+00	8.36E+01	8.10E+01	4.05E+00	1.00E+01
3.33E+03	3.00E+00	4.72E+01	6.16E+01	3.90E+00	7.90E+00
4.17E+03	2.40E+00	4.01E+01	4.37E+01	3.10E+00	7.05E+00
5.00E+03	2.00E+00	2.98E+01	3.97E+01	3.15E+00	6.30E+00
6.67E+03	1.50E+00	2.00E+01	3.02E+01	2.85E+00	5.30E+00
1.00E+04	1.00E+00	1.51E+01	2.08E+01	2.30E+00	4.52E+00

TABLE 8. Ni, NICKEL
D. W. Lynch, R. Rosei and J. H. Weaver, Solid State Commun. 9, 2195 (1971).

ω(cm⁻¹)	λ(μm)	-ε1	ε2	n	k
8.07E+02	1.24E+01	2.01E+03	8.74E+02	9.54E+00	4.58E+01
8.87E+02	1.13E+01	1.68E+03	6.79E+02	8.12E+00	4.18E+01
9.03E+03	1.11E+00	1.41E+03	5.44E+02	7.11E+00	3.83E+01
1.05E+03	9.54E+00	1.21E+03	4.55E+02	6.44E+00	3.53E+01
1.13E+03	8.86E+00	1.04E+03	3.82E+02	5.83E+00	3.28E+01
1.21E+03	8.27E+00	9.04E+02	3.33E+02	5.45E+00	3.06E+01
1.29E+03	7.75E+00	7.95E+02	2.86E+02	5.00E+00	2.86E+01
1.37E+03	7.29E+00	6.98E+02	2.51E+02	4.68E+00	2.68E+01
1.45E+03	6.89E+00	6.17E+02	2.25E+02	4.45E+00	2.52E+01
1.53E+03	6.53E+00	5.48E+02	2.05E+02	4.30E+00	2.38E+01
1.61E+03	6.20E+00	4.88E+02	1.85E+02	4.12E+00	2.25E+01
1.69E+03	5.90E+00	4.35E+02	1.76E+02	4.13E+00	2.13E+01
1.77E+03	5.64E+00	3.92E+02	1.66E+02	4.11E+00	2.02E+01
1.86E+03	5.39E+00	3.54E+02	1.60E+02	4.14E+00	1.93E+01
1.94E+03	5.17E+00	3.22E+02	1.53E+02	4.16E+00	1.84E+01
2.02E+03	4.96E+00	2.95E+02	1.50E+02	4.25E+00	1.77E+01
2.10E+03	4.77E+00	2.73E+02	1.46E+02	4.29E+00	1.71E+01
2.18E+03	4.59E+00	2.54E+02	1.42E+02	4.30E+00	1.65E+01
2.26E+03	4.43E+00	2.37E+02	1.38E+02	4.30E+00	1.60E+01
2.34E+03	4.28E+00	2.22E+02	1.32E+02	4.26E+00	1.55E+01
2.42E+03	4.13E+00	2.09E+02	1.26E+02	4.19E+00	1.51E+01
2.66E+03	3.76E+00	1.73E+02	1.13E+02	4.10E+00	1.38E+01
2.82E+03	3.54E+00	1.54E+02	1.05E+02	4.03E+00	1.31E+01
2.98E+03	3.35E+00	1.38E+02	9.84E+01	3.97E+00	1.24E+01
3.15E+03	3.18E+00	1.23E+02	9.12E+01	3.88E+00	1.18E+01
3.23E+03	3.10E+00	1.16E+02	8.78E+01	3.84E+00	1.14E+01
3.63E+03	2.76E+00	8.62E+01	8.56E+01	4.20E+00	1.02E+01
4.03E+03	2.48E+00	7.67E+01	7.77E+01	4.03E+00	9.64E+00
4.44E+03	2.25E+00	6.44E+01	6.96E+01	3.90E+00	8.92E+00
4.84E+03	2.07E+00	5.50E+01	6.41E+01	3.84E+00	8.35E+00
5.24E+03	1.91E+00	4.91E+01	5.84E+01	3.69E+00	7.92E+00
5.65E+03	1.77E+00	4.31E+01	5.37E+01	3.59E+00	7.48E+00
6.05E+03	1.65E+00	3.87E+01	4.98E+01	3.49E+00	7.13E+00
6.45E+03	1.55E+00	3.51E+01	4.61E+01	3.38E+00	6.82E+00
6.86E+03	1.46E+00	3.17E+01	4.26E+01	3.27E+00	6.51E+00
7.26E+03	1.38E+00	2.87E+01	3.96E+01	3.18E+00	6.23E+00
7.66E+03	1.31E+00	2.61E+01	3.72E+01	3.11E+00	5.98E+00
8.07E+03	1.24E+00	2.36E+01	3.51E+01	3.06E+00	5.74E+00
8.47E+03	1.18E+00	2.17E+01	3.34E+01	3.01E+00	5.55E+00
8.87E+03	1.13E+00	2.01E+01	3.20E+01	2.97E+00	5.38E+00
9.28E+03	1.08E+00	1.90E+01	3.05E+01	2.91E+00	5.24E+00
9.68E+03	1.03E+00	1.79E+01	2.91E+01	2.85E+00	5.10E+00
1.01E+04	9.92E-01	1.69E+01	2.78E+01	2.80E+00	4.97E+00
1.05E+04	9.54E-01	1.60E+01	2.66E+01	2.74E+00	4.85E+00
1.09E+04	9.18E-01	1.51E+01	2.54E+01	2.69E+00	4.73E+00
1.13E+04	8.86E-01	1.44E+01	2.45E+01	2.65E+00	4.63E+00
1.17E+04	8.55E-01	1.40E+01	2.36E+01	2.59E+00	4.55E+00
1.21E+04	8.27E-01	1.36E+01	2.26E+01	2.53E+00	4.47E+00
1.25E+04	8.00E-01	1.30E+01	2.17E+01	2.48E+00	4.38E+00
1.29E+04	7.75E-01	1.27E+01	2.09E+01	2.43E+00	4.31E+00

TABLE 8. Ni, Nickel (Continued)
B. Johnson and R. W. Christy, Phys. Rev. B 9, 5056 (1974).

ω(cm⁻¹)	λ(μm)	-ε1	ε2	n	k
5.16E+03	1.94E+00	7.06E+01	6.31E+01	3.47E+00	9.09E+00
6.21E+03	1.61E+00	5.35E+01	5.00E+01	3.14E+00	7.96E+00
7.18E+03	1.39E+00	4.14E+01	4.19E+01	2.96E+00	7.08E+00
8.23E+03	1.22E+00	3.36E+01	3.59E+01	2.79E+00	6.43E+00
9.19E+03	1.09E+00	2.81E+01	3.14E+01	2.65E+00	5.93E+00
1.02E+04	9.84E-01	2.47E+01	2.75E+01	2.48E+00	5.55E+00
1.12E+04	8.92E-01	2.16E+01	2.51E+01	2.40E+00	5.23E+00
1.22E+04	8.21E-01	1.96E+01	2.25E+01	2.26E+00	4.97E+00
1.32E+04	7.56E-01	1.78E+01	2.01E+01	2.13E+00	4.73E+00
1.42E+04	7.04E-01	1.60E+01	1.85E+01	2.06E+00	4.50E+00
1.52E+04	6.59E-01	1.42E+01	1.70E+01	1.99E+00	4.26E+00
1.62E+04	6.17E-01	1.22E+01	1.60E+01	1.99E+00	4.02E+00
1.72E+04	5.82E-01	1.06E+01	1.49E+01	1.96E+00	3.80E+00
1.82E+04	5.49E-01	9.35E+00	1.39E+01	1.92E+00	3.61E+00
1.92E+04	5.21E-01	8.27E+00	1.27E+01	1.85E+00	3.42E+00
2.02E+04	4.96E-01	7.25E+00	1.18E+01	1.82E+00	3.25E+00

TABLE 9. Pd, Palladium
J. H. Weaver and R. L. Bendow, Phys. Rev. B 12, 3509 (1975).

ω(cm⁻¹)	λ(μm)	-ε1	ε2	n	k
8.07E+02	1.24E+01	2.92E+03	4.47E+02	4.13E+00	5.42E+01
8.87E+02	1.13E+01	2.41E+03	3.79E+02	3.85E+00	4.92E+01
9.68E+02	1.03E+01	2.02E+03	3.25E+02	3.60E+00	4.51E+01
1.05E+03	9.54E+00	1.71E+03	2.79E+02	3.36E+00	4.15E+01
1.13E+03	8.86E+00	1.47E+03	2.55E+02	3.31E+00	3.85E+01
1.21E+03	8.27E+00	1.27E+03	2.24E+02	3.13E+00	3.58E+01
1.61E+03	6.20E+00	6.98E+02	1.63E+02	3.07E+00	2.66E+01
2.42E+03	4.13E+00	2.86E+02	1.23E+02	3.56E+00	1.73E+01
3.23E+03	3.10E+00	1.58E+02	1.13E+02	4.27E+00	1.33E+01
4.03E+03	2.48E+00	1.14E+02	9.38E+01	4.10E+00	1.14E+01
4.84E+03	2.07E+00	8.48E+01	7.57E+01	3.80E+00	9.96E+00
6.45E+03	1.55E+00	5.37E+01	5.40E+01	3.35E+00	8.06E+00
8.07E+03	1.24E+00	3.85E+01	4.12E+01	2.99E+00	6.89E+00
1.21E+04	8.27E-01	2.25E+01	2.27E+01	2.17E+00	5.22E+00
1.61E+04	6.20E-01	1.44E+01	1.46E+01	1.75E+00	4.18E+00

TABLE 9. Pd, PALLADIUM (Continued)
B. A. Bolotin, M. M. Kirilova, L. V. Namerovannaya, and M. M. Noskov, Fiz. Metal. Metalloved 23, 463 (1967).

ω(cm⁻¹)	λ(μm)	-ε1	ε2	n	k
5.56E+02	1.80E+01	7.70E+02	6.84E+02	1.14E+01	3.00E+01
6.25E+02	1.60E+01	6.49E+02	5.69E+02	1.04E+01	2.75E+01
7.14E+02	1.40E+01	5.64E+02	4.74E+02	9.30E+00	2.55E+01
8.33E+02	1.20E+01	4.91E+02	3.67E+02	7.80E+00	2.35E+01
9.09E+02	1.10E+01	4.59E+02	3.11E+02	6.90E+00	2.25E+01
1.00E+03	1.00E+01	4.04E+02	2.56E+02	6.10E+00	2.10E+01
1.11E+03	9.00E+00	3.37E+02	1.84E+02	4.85E+00	1.90E+01
1.25E+03	8.00E+00	2.69E+02	1.53E+02	4.50E+00	1.70E+01
1.43E+03	7.00E+00	2.22E+02	1.33E+02	4.30E+00	1.55E+01
1.67E+03	6.00E+00	1.59E+02	8.32E+01	3.20E+00	1.30E+01
2.00E+03	5.00E+00	1.03E+02	5.67E+01	2.70E+00	1.05E+01
2.50E+03	4.00E+00	5.68E+01	3.45E+01	2.20E+00	7.85E+00
3.33E+03	3.00E+00	2.61E+01	2.58E+01	2.30E+00	5.60E+00

TABLE 9. Pd, PALLADIUM (Continued)
P. B. Johnson and R. W. Christy, Phys. Rev. B 9, 5056 (1974).

ω(cm⁻¹)	λ(μm)	-ε1	ε2	n	k
5.16E+03	1.94E+00	8.67E+01	6.61E+01	3.34E+00	9.89E+00
6.21E+03	1.61E+00	6.47E+01	5.17E+01	3.01E+00	8.59E+00
7.18E+03	1.39E+00	5.07E+01	4.28E+01	2.80E+00	7.65E+00
8.23E+03	1.22E+00	4.05E+01	3.67E+01	2.66E+00	6.90E+00
9.19E+03	1.09E+00	3.37E+01	3.19E+01	2.52E+00	6.33E+00
1.02E+04	9.84E-01	2.92E+01	2.76E+01	2.34E+00	5.89E+00
1.12E+04	8.92E-01	2.53E+01	2.45E+01	2.23E+00	5.50E+00
1.22E+04	8.21E-01	2.27E+01	2.14E+01	2.06E+00	5.19E+00
1.32E+04	7.56E-01	2.01E+01	1.91E+01	1.95E+00	4.89E+00
1.42E+04	7.04E-01	1.82E+01	1.73E+01	1.86E+00	4.65E+00
1.52E+04	6.59E-01	1.63E+01	1.59E+01	1.80E+00	4.42E+00
1.62E+04	6.17E-01	1.47E+01	1.47E+01	1.75E+00	4.21E+00
1.72E+04	5.82E-01	1.33E+01	1.35E+01	1.68E+00	4.02E+00
1.82E+04	5.49E-01	1.21E+01	1.26E+01	1.64E+00	3.84E+00
1.92E+04	5.21E-01	1.11E+01	1.16E+01	1.57E+00	3.68E+00
2.02E+04	4.96E-01	1.02E+01	1.08E+01	1.52E+00	3.54E+00
2.12E+04	4.71E-01	9.36E+00	9.90E+00	1.46E+00	3.39E+00
2.22E+04	4.51E-01	8.64E+00	9.19E+00	1.41E+00	3.26E+00
2.32E+04	4.30E-01	7.98E+00	8.60E+00	1.37E+00	3.14E+00
2.42E+04	4.13E-01	7.41E+00	8.06E+00	1.33E+00	3.03E+00
2.52E+04	3.97E-01	6.89E+00	7.62E+00	1.30E+00	2.93E+00
2.62E+04	3.81E-01	6.42E+00	7.13E+00	1.26E+00	2.83E+00
2.72E+04	3.68E-01	5.97E+00	6.80E+00	1.24E+00	2.74E+00
2.82E+04	3.54E-01	5.51E+00	6.52E+00	1.23E+00	2.65E+00
2.92E+04	3.42E-01	5.12E+00	6.27E+00	1.22E+00	2.57E+00
3.02E+04	3.31E-01	4.81E+00	6.00E+00	1.20E+00	2.50E+00
3.12E+04	3.20E-01	4.39E+00	5.86E+00	1.21E+00	2.42E+00
3.22E+04	3.11E-01	4.06E+00	5.69E+00	1.21E+00	2.35E+00
3.32E+04	3.01E-01	3.80E+00	5.50E+00	1.20E+00	2.29E+00
3.42E+04	2.92E-01	3.58E+00	5.26E+00	1.18E+00	2.23E+00
3.52E+04	2.84E-01	3.36E+00	5.14E+00	1.18E+00	2.18E+00
3.62E+04	2.76E-01	3.12E+00	5.07E+00	1.19E+00	2.13E+00
3.72E+04	2.69E-01	3.06E+00	4.87E+00	1.16E+00	2.10E+00
3.82E+04	2.62E-01	3.01E+00	4.68E+00	1.13E+00	2.07E+00
3.92E+04	2.55E-01	2.89E+00	4.51E+00	1.11E+00	2.03E+00
4.02E+04	2.49E-01	2.79E+00	4.30E+00	1.08E+00	1.99E+00
4.12E+04	2.43E-01	2.72E+00	4.06E+00	1.04E+00	1.95E+00
4.22E+04	2.37E-01	2.65E+00	3.82E+00	1.00E+00	1.91E+00
4.32E+04	2.31E-01	2.52E+00	3.61E+00	9.70E-01	1.86E+00
4.42E+04	2.26E-01	2.39E+00	3.40E+00	9.40E-01	1.81E+00
4.52E+04	2.21E-01	2.25E+00	3.24E+00	9.20E-01	1.76E+00
4.62E+04	2.16E-01	2.06E+00	3.09E+00	9.10E-01	1.70E+00
4.72E+04	2.12E-01	1.93E+00	2.94E+00	8.90E-01	1.65E+00
4.82E+04	2.07E-01	1.80E+00	2.78E+00	8.70E-01	1.60E+00

TABLE 10. Pt, Platinum
J. H. Weaver, Phys. Rev. B 11, 1416 (1975).

ω(cm⁻¹)	λ(μm)	-ε1	ε2	n	k
8.07E+02	1.24E+01	1.83E+03	1.18E+03	1.32E+01	4.47E+01
1.05E+03	9.54E+00	1.25E+03	7.28E+02	9.91E+00	3.67E+01
1.21E+03	8.27E+00	9.04E+02	5.10E+02	8.18E+00	3.12E+01
1.37E+03	7.29E+00	6.92E+02	3.68E+02	6.78E+00	2.72E+01
1.61E+03	6.20E+00	5.39E+02	2.83E+02	5.90E+00	2.40E+01
2.42E+03	4.13E+00	2.46E+02	1.27E+02	3.92E+00	1.62E+01
3.23E+03	3.10E+00	1.22E+02	6.40E+01	2.81E+00	1.14E+01
4.03E+03	2.48E+00	4.42E+01	6.03E+01	3.91E+00	7.71E+00
4.84E+03	2.07E+00	1.92E+01	6.93E+01	5.13E+00	6.75E+00
5.65E+03	1.77E+00	1.40E+01	7.80E+01	5.71E+00	6.83E+00
6.45E+03	1.55E+00	2.14E+01	7.48E+01	5.31E+00	7.04E+00
8.07E+03	1.24E+00	2.58E+01	5.63E+01	4.25E+00	6.62E+00
1.21E+04	8.27E-01	1.72E+01	2.96E+01	2.92E+00	5.07E+00
1.61E+04	6.20E-01	1.13E+01	1.87E+01	2.30E+00	4.07E+00

TABLE 10. Pt, PLATINUM (Continued)
J. H. Weaver, D. W. Lynch, and C. G. Olson, Phys. Rev. B 10, 501 (1974).

ω(cm⁻¹)	λ(μm)	-ε1	ε2	n	k
8.06E+02	1.24E+01	1.62E+03	9.28E+02	1.11E+01	4.18E+01
1.20E+03	8.30E+00	8.02E+02	4.16E+02	7.12E+00	2.92E+01
1.61E+03	6.20E+00	4.75E+02	2.30E+02	5.14E+00	2.24E+01
2.42E+03	4.13E+00	2.17E+02	1.02E+02	3.39E+00	1.51E+01
2.82E+03	3.54E+00	1.56E+02	7.19E+01	2.81E+00	1.28E+01
3.23E+03	3.10E+00	1.08E+02	5.24E+01	2.45E+00	1.07E+01
3.62E+03	2.76E+00	6.93E+01	4.77E+01	2.72E+00	8.76E+00
4.03E+03	2.48E+00	4.33E+01	5.47E+01	3.64E+00	7.52E+00
4.44E+03	2.25E+00	3.09E+01	5.59E+01	4.06E+00	6.88E+00
4.83E+03	2.07E+00	2.21E+01	6.01E+01	4.58E+00	6.56E+00
5.24E+03	1.91E+00	1.89E+01	6.26E+01	4.82E+00	6.49E+00
5.65E+03	1.77E+00	1.86E+01	6.35E+01	4.88E+00	6.51E+00
6.06E+03	1.65E+00	2.00E+01	6.32E+01	4.81E+00	6.57E+00
6.45E+03	1.55E+00	2.18E+01	6.11E+01	4.64E+00	6.58E+00
6.85E+03	1.46E+00	2.37E+01	5.74E+01	4.38E+00	6.55E+00
7.25E+03	1.38E+00	2.47E+01	5.28E+01	4.10E+00	6.44E+00
8.06E+03	1.24E+00	2.40E+01	4.49E+01	3.67E+00	6.12E+00
8.85E+03	1.13E+00	2.22E+01	3.87E+01	3.35E+00	5.78E+00
9.71E+03	1.03E+00	2.04E+01	3.35E+01	3.07E+00	5.46E+00
1.05E+04	9.50E-01	1.85E+01	2.96E+01	2.86E+00	5.17E+00
1.12E+04	8.90E-01	1.68E+01	2.63E+01	2.68E+00	4.90E+00
1.20E+04	8.30E-01	1.55E+01	2.35E+01	2.52E+00	4.67E+00
1.30E+04	7.70E-01	1.41E+01	2.13E+01	2.39E+00	4.45E+00
1.37E+04	7.30E-01	1.30E+01	1.93E+01	2.27E+00	4.26E+00
1.45E+04	6.90E-01	1.19E+01	1.77E+01	2.17E+00	4.08E+00
1.49E+04	6.70E-01	1.15E+01	1.70E+01	2.12E+00	4.00E+00
1.54E+04	6.50E-01	1.11E+01	1.64E+01	2.09E+00	3.93E+00
1.56E+04	6.40E-01	1.11E+01	1.57E+01	2.02E+00	3.89E+00
1.61E+04	6.20E-01	1.06E+01	1.49E+01	1.96E+00	3.80E+00

TABLE 11. Ti, TITANIUM
M. M. Kirillova and B. A. Charikov, Opt. Spectry 17, 134 (1964).

ω(cm⁻¹)	λ(μm)	-ε1	ε2	n	k
5.00E+02	2.00E+01	8.43E+02	1.17E+03	1.73E+01	3.38E+01
5.26E+02	1.90E+01	6.85E+02	1.04E+03	1.68E+01	3.11E+01
5.56E+02	1.80E+01	6.54E+02	8.82E+02	1.49E+01	2.96E+01
5.88E+02	1.70E+01	5.96E+02	7.67E+02	1.37E+01	2.80E+01
6.25E+02	1.60E+01	5.65E+02	7.05E+02	1.30E+01	2.71E+01
6.67E+02	1.50E+01	5.11E+02	6.14E+02	1.20E+01	2.56E+01
7.14E+02	1.40E+01	4.74E+02	5.25E+02	1.08E+01	2.43E+01
8.33E+02	1.20E+01	3.36E+02	3.77E+02	9.20E+00	2.05E+01
9.09E+02	1.10E+01	3.24E+02	3.38E+02	8.50E+00	1.99E+01
1.00E+03	1.00E+01	2.81E+02	2.90E+02	7.85E+00	1.85E+01
1.11E+03	9.00E+00	2.22E+02	2.42E+02	7.30E+00	1.66E+01
1.18E+03	8.50E+00	2.11E+02	2.24E+02	6.96E+00	1.61E+01
1.25E+03	8.00E+00	1.76E+02	1.94E+02	6.56E+00	1.48E+01
1.33E+03	7.50E+00	1.53E+02	1.75E+02	6.31E+00	1.39E+01
1.43E+03	7.00E+00	1.38E+02	1.58E+02	5.99E+00	1.32E+01
1.54E+03	6.50E+00	1.17E+02	1.37E+02	5.63E+00	1.22E+01
1.67E+03	6.00E+00	9.87E+01	1.22E+02	5.38E+00	1.13E+01
1.82E+03	5.50E+00	8.04E+01	1.04E+02	5.07E+00	1.03E+01
2.00E+03	5.00E+00	6.06E+01	8.94E+01	4.87E+00	9.18E+00
2.22E+03	4.50E+00	4.32E+01	7.51E+01	4.66E+00	8.06E+00
2.50E+03	4.00E+00	3.11E+01	6.78E+01	4.66E+00	7.27E+00
2.86E+03	3.50E+00	2.25E+01	6.00E+01	4.56E+00	6.58E+00
3.33E+03	3.00E+00	1.31E+01	5.33E+01	4.57E+00	5.83E+00
4.00E+03	2.50E+00	8.17E+00	4.93E+01	4.57E+00	5.39E+00

TABLE 11. Ti, TITANIUM (Continued)
D. W. Lynch, C. G. Olson, and J. H. Weaver, Phys. Rev. B 11, 3617 (1975).

ω(cm⁻¹)	λ(μm)	-ε1	ε2	n	k
8.07E+02	1.24E+01	5.21E+02	2.35E+02	5.03E+00	2.34E+01
9.68E+02	1.03E+01	3.76E+02	1.54E+02	3.90E+00	1.98E+01
1.05E+03	9.54E+00	3.20E+02	1.27E+02	3.49E+00	1.82E+01
1.21E+03	8.27E+00	2.38E+02	9.43E+01	3.00E+00	1.57E+01
1.61E+03	6.20E+00	1.24E+02	4.81E+01	2.12E+00	1.13E+01
1.69E+03	5.90E+00	1.08E+02	4.33E+01	2.04E+00	1.06E+01

TABLE 11. Ti, TITANIUM (Continued)
P. B. Johnson and R. W. Christy, Phys. Rev. B 9, 5056 (1974).

ω(cm⁻¹)	λ(μm)	-ε1	ε2	n	k
5.16E+03	1.94E+00	1.46E+01	3.64E+01	3.51E+00	5.19E+00
6.21E+03	1.61E+00	8.47E+00	3.47E+01	3.69E+00	4.70E+00
7.18E+03	1.39E+00	5.63E+00	3.21E+01	3.67E+00	4.37E+00
8.23E+03	1.22E+00	4.12E+00	3.00E+01	3.62E+00	4.15E+00
9.19E+03	1.09E+00	3.91E+00	2.81E+01	3.50E+00	4.02E+00
1.02E+04	9.84E-01	4.54E+00	2.66E+01	3.35E+00	3.97E+00
1.12E+04	8.92E-01	4.86E+00	2.61E+01	3.29E+00	3.96E+00
1.22E+04	8.21E-01	5.78E+00	2.57E+01	3.21E+00	4.01E+00

TABLE 11. Ti, TITANIUM (Continued)
M. M. Kirillova and B. A. Charikov, Phys. Met. 15, 138 (1963).

ω(cm⁻¹)	λ(μm)	-ε1	ε2	n	k
2.50E+03	4.00E+00	3.17E+01	6.79E+01	4.65E+00	7.30E+00
2.86E+03	3.50E+00	2.29E+01	6.01E+01	4.55E+00	6.60E+00
3.33E+03	3.00E+00	1.44E+01	5.21E+01	4.45E+00	5.85E+00
4.00E+03	2.50E+00	8.20E+00	4.62E+01	4.40E+00	5.25E+00
4.17E+03	2.40E+00	9.17E+00	4.61E+01	4.35E+00	5.30E+00
4.35E+03	2.30E+00	6.94E+00	4.25E+01	4.25E+00	5.00E+00
4.55E+03	2.20E+00	7.36E+00	4.20E+01	4.20E+00	5.00E+00
5.00E+03	2.00E+00	7.12E+00	3.93E+01	4.05E+00	4.85E+00
5.56E+03	1.80E+00	4.76E+00	3.73E+01	4.05E+00	4.60E+00
5.88E+03	1.70E+00	5.81E+00	3.42E+01	3.80E+00	4.50E+00
6.25E+03	1.60E+00	5.36E+00	3.38E+01	3.80E+00	4.45E+00
6.45E+03	1.55E+00	6.56E+00	3.33E+01	3.70E+00	4.50E+00
6.67E+03	1.50E+00	4.48E+00	3.31E+01	3.80E+00	4.35E+00
6.90E+03	1.45E+00	4.37E+00	3.15E+01	3.70E+00	4.25E+00
7.14E+03	1.40E+00	5.04E+00	2.98E+01	3.55E+00	4.20E+00
7.41E+03	1.35E+00	3.75E+00	2.80E+01	3.50E+00	4.00E+00
7.69E+03	1.30E+00	4.84E+00	2.75E+01	3.40E+00	4.05E+00
8.00E+03	1.25E+00	8.47E+00	2.90E+01	3.30E+00	4.40E+00
8.33E+03	1.20E+00	5.60E+00	2.42E+01	3.10E+00	3.90E+00

TABLE 11. Ti, TITANIUM (Continued)
G. A. Bolotin, A. N. Voloshinskii, M. M. Neskov, A. V. Sokolov, and B. A. Charikov, Phys. Met. and Met. 13, 823 (1962).

ω(cm⁻¹)	λ(μm)	-ε1	ε2	n	k
1.00E+03	1.00E+01	2.36E+02	3.21E+02	9.01E+00	1.78E+01
1.05E+03	9.50E+00	2.19E+02	2.93E+02	8.56E+00	1.71E+01
1.11E+03	9.00E+00	2.18E+02	2.51E+02	7.56E+00	1.66E+01
1.18E+03	8.50E+00	2.11E+02	2.24E+02	6.96E+00	1.61E+01
1.25E+03	8.00E+00	1.76E+02	1.94E+02	6.56E+00	1.48E+01
1.33E+03	7.50E+00	1.53E+02	1.75E+02	6.31E+00	1.39E+01
1.43E+03	7.00E+00	1.38E+02	1.58E+02	5.99E+00	1.32E+01
1.54E+03	6.50E+00	1.17E+02	1.37E+02	5.63E+00	1.22E+01
1.67E+03	6.00E+00	9.87E+01	1.22E+02	5.38E+00	1.13E+01
1.82E+03	5.50E+00	8.04E+01	1.04E+02	5.07E+00	1.03E+01
2.00E+03	5.00E+00	6.06E+01	8.94E+01	4.87E+00	9.18E+00
2.22E+03	4.50E+00	4.34E+01	7.52E+01	4.66E+00	8.07E+00
2.50E+03	4.00E+00	3.11E+01	6.78E+01	4.66E+00	7.27E+00
2.86E+03	3.50E+00	2.25E+01	6.00E+01	4.56E+00	6.58E+00
3.33E+03	3.00E+00	1.31E+01	5.33E+01	4.57E+00	5.83E+00
4.00E+03	2.50E+00	8.17E+00	4.93E+01	4.57E+00	5.39E+00
5.00E+03	2.00E+00	4.24E+00	4.24E+01	4.38E+00	4.84E+00

$$\epsilon_1(0) = -\left(\frac{\omega_p}{\omega_\tau}\right)^2. \tag{7}$$

The dc conductivity σ_0 is related to ω_p and ω_τ by

$$\sigma_0 = \omega_p^2/(4\pi\omega_\tau) \tag{8}$$

with σ_0 having units of cm^{-1}. This can be expressed in terms of the dc resistivity ρ_0:

$$\sigma_0(\mathrm{cm}^{-1}) = 1/[2\pi c\rho_0(\mathrm{s})] = (9\times 10^{11})/[2\pi c\rho_0(\Omega\,\mathrm{cm})]. \tag{9}$$

To analyze the data of Brandli, and Sievers[1] it is convenient to write the surface impedance $Z(\omega)$ for the Drude model[2]:

$$Z(\omega) = R(\omega) + iX(\omega) = \frac{4\pi}{c}(1+i)\left(\frac{\omega\omega_\tau}{2\omega_p^2}\right)^{1/2}\left(1+i\frac{\omega}{\omega_\tau}\right)^{1/2}. \tag{10}$$

We shall need only $R(\omega)$:

$$R(\omega) = \frac{4\pi}{c}\left(\frac{\omega\omega_\tau}{2\omega_p^2}\right)^{1/2}\left[-\frac{\omega}{\omega_\tau} + \left(1+\frac{\omega^2}{\omega_\tau^2}\right)^{1/2}\right]^{1/2}. \tag{11}$$

III. Determination of Drude Model Parameters

All data in the form of n and k were changed to ϵ_1 and ϵ_2. Equations (3) and (4) were solved for ω_τ, eliminating ω_p:

$$\omega_\tau = \frac{\omega\epsilon_2}{(1-\epsilon_1)}. \tag{12}$$

This equation was solved to determine ω_τ using ϵ_1 and ϵ_2 at some frequency ω. Then ω_p was obtained from

$$\omega_p^2 = (1-\epsilon_1)(\omega^2+\omega_\tau^2). \tag{13}$$

This was done for several values of ω to obtain several pairs of ω_τ and ω_p, which produce the curve with the best eyeball fit to the data.

TABLE 12. W, TUNGSTEN
L. V. Nomerovannaya, M. M. Kirillova, and M.M. Noskov, Opt. Spectry. 17, 134 (1964).

ω(cm⁻¹)	λ(μm)	-ε1	ε2	n	k
5.00E+02	2.00E+01	4.32E+03	2.38E+03	1.75E+01	6.80E+01
5.26E+02	1.90E+01	3.70E+03	2.05E+03	1.63E+01	6.30E+01
5.56E+02	1.80E+01	3.56E+03	1.90E+03	1.54E+01	6.16E+01
5.88E+02	1.70E+01	3.37E+03	1.80E+03	1.50E+01	6.00E+01
6.25E+02	1.60E+01	3.32E+03	1.91E+03	1.60E+01	5.98E+01
6.67E+02	1.50E+01	3.19E+03	1.69E+03	1.45E+01	5.83E+01
7.14E+02	1.40E+01	2.94E+03	1.43E+03	1.28E+01	5.57E+01
7.69E+02	1.30E+01	2.65E+03	1.13E+03	1.07E+01	5.26E+01
8.33E+02	1.20E+01	2.42E+03	1.10E+03	1.09E+01	5.04E+01
9.09E+02	1.10E+01	2.05E+03	8.80E+02	9.50E+00	4.63E+01
1.00E+03	1.00E+01	1.65E+03	6.85E+02	8.25E+00	4.15E+01
1.05E+03	9.50E+00	1.51E+03	5.85E+02	7.40E+00	3.95E+01
1.11E+03	9.00E+00	1.36E+03	5.49E+02	7.30E+00	3.76E+01
1.18E+03	8.50E+00	1.18E+03	4.48E+02	6.40E+00	3.50E+01
1.21E+03	8.25E+00	1.13E+03	4.10E+02	6.00E+00	3.42E+01
1.25E+03	8.00E+00	1.07E+03	4.06E+02	6.10E+00	3.33E+01
1.29E+03	7.76E+00	1.01E+03	3.49E+02	5.40E+00	3.23E+01
1.33E+03	7.50E+00	9.34E+02	3.19E+02	5.15E+00	3.10E+01
1.38E+03	7.25E+00	8.43E+02	3.07E+02	5.20E+00	2.95E+01
1.43E+03	7.00E+00	7.72E+02	3.03E+02	5.35E+00	2.83E+01
1.48E+03	6.75E+00	6.68E+02	2.85E+02	5.40E+00	2.64E+01
1.54E+03	6.50E+00	5.90E+02	2.49E+02	5.03E+00	2.48E+01
1.60E+03	6.25E+00	5.42E+02	2.33E+02	4.90E+00	2.38E+01
1.67E+03	6.00E+00	4.87E+02	2.19E+02	4.85E+00	2.26E+01
1.74E+03	5.75E+00	5.00E+02	2.05E+02	4.50E+00	2.28E+01
1.82E+03	5.50E+00	4.82E+02	2.01E+02	4.48E+00	2.24E+01
1.90E+03	5.25E+00	4.80E+02	1.83E+02	4.11E+00	2.23E+01
2.00E+03	5.00E+00	4.37E+02	1.48E+02	3.48E+00	2.12E+01
2.11E+03	4.75E+00	3.81E+02	1.32E+02	3.33E+00	1.98E+01
2.22E+03	4.50E+00	3.88E+02	1.13E+02	2.85E+00	1.99E+01
2.27E+03	4.40E+00	3.85E+02	1.05E+02	2.65E+00	1.98E+01
2.38E+03	4.20E+00	3.53E+02	9.50E+01	2.50E+00	1.90E+01
2.44E+03	4.10E+00	3.48E+02	8.65E+01	2.30E+00	1.88E+01
2.50E+03	4.00E+00	3.30E+02	8.16E+01	2.23E+00	1.83E+01
2.56E+03	3.90E+00	3.15E+02	7.95E+01	2.22E+00	1.79E+01
2.70E+03	3.70E+00	2.81E+02	7.44E+01	2.20E+00	1.69E+01
2.78E+03	3.60E+00	2.68E+02	6.60E+01	2.00E+00	1.65E+01
2.94E+03	3.40E+00	2.35E+02	7.19E+01	2.32E+00	1.55E+01
3.03E+03	3.30E+00	2.17E+02	6.73E+01	2.26E+00	1.49E+01
3.13E+03	3.20E+00	2.08E+02	6.48E+01	2.22E+00	1.46E+01
3.23E+03	3.10E+00	1.97E+02	6.25E+01	2.20E+00	1.42E+01
3.33E+03	3.00E+00	1.84E+02	7.18E+01	2.60E+00	1.38E+01
3.45E+03	2.90E+00	1.76E+02	6.89E+01	2.55E+00	1.35E+01
3.57E+03	2.80E+00	1.80E+02	6.26E+01	2.30E+00	1.36E+01
3.70E+03	2.70E+00	1.54E+02	5.29E+01	2.10E+00	1.26E+01
3.85E+03	2.60E+00	1.39E+02	5.16E+01	2.15E+00	1.20E+01
4.00E+03	2.50E+00	1.28E+02	4.71E+01	2.05E+00	1.15E+01
4.17E+03	2.40E+00	1.28E+02	4.95E+01	2.15E+00	1.15E+01

TABLE 12. W, TUNGSTEN (Continued)

ω(cm⁻¹)	λ(μm)	-ε1	ε2	n	k
4.35E+03	2.30E+00	9.80E+01	4.04E+01	2.00E+00	1.01E+01
4.55E+03	2.20E+00	8.85E+01	3.65E+01	1.90E+00	9.60E+00
4.76E+03	2.10E+00	7.58E+01	3.29E+01	1.85E+00	8.90E+00
5.00E+03	2.00E+00	6.09E+01	2.80E+01	1.75E+00	8.00E+00
5.26E+03	1.90E+00	4.86E+01	2.90E+01	2.00E+00	7.25E+00
5.56E+03	1.80E+00	4.12E+01	2.84E+01	2.10E+00	6.75E+00
5.71E+03	1.75E+00	3.89E+01	2.62E+01	2.00E+00	6.55E+00
5.88E+03	1.70E+00	3.34E+01	2.58E+01	2.10E+00	6.15E+00
6.02E+03	1.66E+00	3.27E+01	2.98E+01	2.40E+00	6.20E+00
6.25E+03	1.60E+00	3.88E+01	3.51E+01	2.60E+00	6.75E+00
6.45E+03	1.55E+00	2.51E+01	2.80E+01	2.50E+00	5.60E+00
6.67E+03	1.50E+00	2.08E+01	3.13E+01	2.90E+00	5.40E+00
6.90E+03	1.45E+00	1.75E+01	3.09E+01	3.00E+00	5.15E+00
7.14E+03	1.40E+00	1.73E+01	3.36E+01	3.20E+00	5.25E+00
7.41E+03	1.35E+00	1.64E+01	3.30E+01	3.20E+00	5.16E+00
7.69E+03	1.30E+00	1.53E+01	3.23E+01	3.20E+00	5.05E+00
8.33E+03	1.20E+00	1.15E+01	2.85E+01	3.10E+00	4.60E+00
9.09E+03	1.10E+00	9.78E+00	2.61E+01	3.01E+00	4.34E+00
1.00E+04	1.00E+00	3.25E+00	2.10E+01	3.00E+00	3.50E+00

TABLE 12. W, TUNGSTEN (Continued)
J. H. Weaver, D. W. Lynch and C. G. Olson, Phys. Rev. B 12, 1293 (1975).

ω(cm⁻¹)	λ(μm)	-ε1	ε2	n	k
4.84E+02	2.07E+01	5.68E+03	5.71E+03	3.45E+01	8.29E+01
5.65E+02	1.77E+01	4.75E+03	3.91E+03	2.65E+01	7.39E+01
6.45E+02	1.55E+01	3.83E+03	2.73E+03	2.09E+01	6.53E+01
7.26E+02	1.38E+01	3.31E+03	2.04E+03	1.70E+01	6.00E+01
8.07E+02	1.24E+01	2.80E+03	1.54E+03	1.41E+01	5.47E+01
9.68E+02	1.03E+01	2.05E+03	9.37E+02	1.01E+01	4.64E+01
1.13E+03	8.86E+00	1.56E+03	6.09E+02	7.58E+00	4.02E+01
1.29E+03	7.75E+00	1.21E+03	4.18E+02	5.92E+00	3.53E+01
1.61E+03	6.20E+00	7.86E+02	2.19E+02	3.87E+00	2.83E+01
2.42E+03	4.13E+00	3.32E+02	6.71E+01	1.83E+00	1.83E+01
3.23E+03	3.10E+00	1.70E+02	5.11E+01	1.94E+00	1.32E+01
4.03E+03	2.48E+00	1.09E+02	2.95E+01	1.40E+00	1.05E+01
4.84E+03	2.07E+00	6.19E+01	1.93E+01	1.21E+00	7.96E+00
5.65E+03	1.77E+00	3.50E+01	1.95E+01	1.59E+00	6.13E+00
6.61E+03	1.51E+00	1.57E+01	2.18E+01	2.36E+00	4.61E+00
7.26E+03	1.38E+00	1.00E+01	2.76E+01	3.11E+00	4.44E+00
8.07E+03	1.24E+00	8.80E+00	2.71E+01	3.14E+00	4.32E+00
1.21E+04	8.27E-01	-4.33E+00	1.94E+01	3.48E+00	2.79E+00
1.61E+04	6.20E-01	-4.61E+00	2.08E+01	3.60E+00	2.89E+00

Table 13. Optical Parameters Found using a Drude Model Fit of the Experimental Dielectric Functions for Six Metals for which the Dielectric Functions could be Fit; here ω_r is the Frequency at which the Fit is Forced, and $-\epsilon_1(0)$ is $-\epsilon_1(\omega)$ at dc; the Crossover Frequency Applies to $-\epsilon_1 = \epsilon_2$.

	ω_p (cm^{-1}) for fit of data in IR	ω_p (cm^{-1}) IR fit	ω_p (cm^{-1}) UV fit	$-\epsilon_1(0) = -(\omega_p/\omega_\tau)^2$	ω_τ (cm^{-1}) from dc resistivities and ω_p	ω_τ (cm^{-1}) crossover on $-\epsilon_1, \epsilon_2$ plot
Noble Metals and Al and Pb						
Al	1.11x10^{5}	6.47x10^{2}	1.19x10^{5}	3.37x10^{4}	6.45x10^{2}	7.00x10^{2}
Cu	2.00x10^{5}	1.76x10^{5}	6.38x10^{4}	5.27x10^{4}	1.15x10^{2}	2.55x10^{2}
Au	8.06x10^{2}	2.16x10^{2}	7.25x10^{4}	1.13x10^{5}	1.93x10^{2}	2.16x10^{2}
Pb	5.00x10^{1}	1.45x10^{3}	6.20x10^{4}	1.33x10^{3}	1.35x10^{3}	1.55x10^{3}
Ag	1.00x10^{3}	1.45x10^{2}	7.25x10^{4}	2.50x10^{5}	1.41x10^{2}	1.52x10^{2}
Transition Metals						
W	8.06x10^{2}	4.33x10^{2}	4.84x10^{4}	1.25x10^{4}	2.16x10^{2}	4.30x10^{2}

The one exception to this process was the measurements of Brandli and Sievers[1] for Au and Pb. They reported values of $R(\omega)/Z_0$ where $Z_0 = (4\pi)/c$. For the far IR, Eq. (11) reduces to

$$\frac{R(\omega)}{Z_0} = \left(\frac{\omega\omega_\tau}{2\omega_p^2}\right)^{1/2}. \tag{14}$$

ω_τ was obtained from this data using ω_n from the near IR fit. This value of ω_τ was used for gold and lead rather than the ω_τ obtained from the near IR fit.

We note from Eq. (12) the frequency for which $-\epsilon_1(\omega) = \epsilon_2(\omega)$ is very nearly $\omega = \omega_\tau$ since $-\epsilon_1 \gg 1$. With $\omega = \omega_\tau$ both components ($-\epsilon_1$ and ϵ_2) of the dielectric function are $\omega_p^2/(2\omega_\tau^2)$. Thus the Drude parameters, ω_τ and ω_p, can be determined at the crossover from $\omega = \omega_\tau$ and the value of the dielectric function. Note that $-\epsilon_1(0) \simeq \omega_p^2/\omega_\tau^2$; so $-\frac{1}{2}\epsilon_1(0) \simeq -\epsilon_1(\omega_\tau)$.

IV. Data

Figures 1-12 are plots of $-\epsilon_1(\omega)$ and $\epsilon_2(\omega)$ for the twelve metals. The high frequency termination occurs where the Drude model becomes invalid. The solid lines are calculated from the Drude model with the parameters listed in Table 13. Tables 1-12 present the collected values of ϵ_1, ϵ_2, n and k. Table 13 summarizes the Drude model parameters from our fit (for Ag, Au, Cu, Al, Pb, and W) as well as ω_τ calculated from ω_p and the AIP Handbook[19] values of the dc resistivity. Dielectric functions for all metals considered in this article except Pb have been tabulated by Weaver *et al.* for the UV, visible, and near IR.

Finally, we disclaim any physical signficance for the Drude model. The intent is only to parametrize the optical constants for these metals even when there is

some question as to the physical meaning of the parameters. The transition metals show interband transitions and cannot be fit with a Drude model in the IR (with the exception of *W*). Even the noble metals in the IR can have small interband contributions to the dielectric constants.[20]

References

1. G. Brandli and A. J. Sievers, Phys. Rev. B **5**, 3550 (1972).
2. P. Drude, *Theory of Optics* (Longmans, Green, New York, 1922; Dover, New York, 1968). A more modern reference is F. Wooten, *Optical Properties of Solids* (Academic, New York, 1972), p. 52. For the Drude model and surface impedance see B. Donovan, *Elementary Theory of Metals* (Pergamon, New York, 1967), p. 220.
3. J. H. Weaver, C. Krafka, D. W. Lynch, and E. E. Koch, "Part 1: The Transition Metals," "Part 2, Noble Metals, Aluminum, Scandium, Yttrium, the Lanthanides, and the Actinides," in *Physics Data, Optical Properties of Metals* (Fachinformationszentrum 7514 Eggenstein-Leopoldshafen 2, Karlsruhe, Federal Republic of Germany, 1981).
4. G. Haas and L. Hadley, in *American Institute of Physics Handbook*, D. E. Gray, Ed. (McGraw-Hill, New York, 1972), p. 6-118.
5. H. E. Bennett and J. M. Bennett, in *Optical Properties and Electronic Structure of Metals and Alloys*, F. Abeles, Ed., (North-Holland, Amsterdam; Wiley, New York, 1966), Sec. II.6, p. 175. For Ag, Au, and Al, for ω, they estimated 145, 216, and 663 cm^{-1}, respectively.
6. For a single carrier type (electrons) the plasma frequency ω_p is as given in Eq. (5) where the dielectric constant is ϵ_∞ (the contribution from the core electrons at high frequencies). Often $m^* = m$ and $\epsilon_\infty = 1$ are assumed. For discussion see H. Ehrenreich and M. H. Cohen, Phys. Rev. **115**, 786 (1959); the last paragraph on p. 790 is most relevant.
7. Al: E. Shiles, T. Sasaki, M. Inokuti, and D. Y. Smith, Phys. Rev. B **22**, 1612 (1980); H. E. Bennett and J. M. Bennett, *Optical Properties and Electronic Structure of Metals and Alloys*, F. Abeles, Ed. (North Holland, Amsterdam, 1966), p. 175; L. G. Schulz, J. Opt. Soc. Am. **44**, 357, 362 (1954).
8. Cu: L. G. Schulz, J. Opt. Soc. Am. **44**, 357, 362 (1954); A. P. Lenham and D. M. Treherne, J. Opt. Soc. Am. **56**, 683 (1966); P. F. Robusto and R. Braunstein, Phys. Status Solidi B **107**, 443 (1981); H. J. Hageman, W. Gudat, and C. Kunz, J. Opt. Soc. Am. **65**, 742 (1975); B. Dold and R. Mecke, Optik **22**, 435 (1965).
9. Au: H. E. Bennett and J. M. Bennett, *Optical Properties and Electronic Structure of Metals and Alloys*, F. Abeles, Ed. (North Holland, Amsterdam, 1966), p. 75; L. G. Schulz, J. Opt. Soc. Am **44**, 357, 362 (1954); G. P. Motulevich and A. A. Shubin, Sov. Phys. JETP **20**, 560 (1965); V. G. Padalka and I. N. Shklyarevskii, Opt. Spectrosc. **11**, 285 (1961); G. A. Bolotin, A. N. Voloshinskii, M. M. Kirilbra, M. M. Neskov, A. V. Sokolov, and B. A. Charikov, Fiz. Met. Metalloved. **13**, 823 (1962); G. Brandli and A. J. Sievers, Phys. Rev. B **5**, 3550 (1972).
10. Pb: G. Brandli and A. J. Sievers, Phys. Rev. B **5**, 3550 (1972); A. I. Golovashkin and G. P. Motulevich, Sov. Phys. JETP **26**, 881 (1968).
11. Ag: H. E. Bennett and J. M. Bennett, in *Optical Properties and Electronic Structure of Metals and Alloys* F. Abeles, Ed. (North-Holland, Amsterdam, 1966), p. 175; L. G. Schulz, J. Opt. Soc. Am. **44**, 357, and 362 (1954); H. J. Hagemann, W. Endat, and C. Kunz, J. Opt. Soc. Am. **65**, 742 (1975).
12. Co: M. M. Kirillova and B. A. Charikov, Opt. Spectrosc. **17**, 134 (1964); P. B. Johnson and R. W. Christy, Phys. Rev. B **9**, 5056 (1974); J. H. Weaver, E. Colavita, D. W. Lynch, and R. Rosei, Phys. Rev. B **19**, 3850 (1979).
13. Fe: J. H. Weaver, E. Colavita, D. W. Lynch, and R. Rosei, Phys. Rev. B **19**, 3850 (1979); G. A. Bolotin, M. M. Krillova, and V. M. Mayevskiy, Phys. Met. Mettalogr. USSR **27**, No. 2, 31 (1969).
14. Ni: D. W. Lynch, R. Rosei, and J. H. Weaver, Solid State Commun. **9**, 2195 (1973); P. B. Johnson and R. W. Christy, Phys. Rev. B **9**, 5056 (1974).
15. Pd: J. H. Weaver and R. L. Benbow, Phys. Rev. B **12**, 3509 (1975); G. A. Bolotin, M. M. Kirillova, L. V. Nomerovannaya, and M. M. Noskov, Fiz. Met. Mettalloved. **23**, 463 (1967); P. B. Johnson and R. W. Christy, Phys. Rev. B **9**, 5056 (1974).
16. Pt: J. H. Weaver, Phys. Rev. B **11**, 1416 (1975); J. H. Weaver, C. G. Olson, and D. W. Lynch, Phys. Rev. B **10**, 501 (1974).
17. Ti: M. M. Kirillova and B. A. Charikov, Opt. Spectrosc. **17**, 134 (1964); D. W. Lynch, C. G. Olson, and J. H. Weaver, Phys. Rev. B **11**, 3617 (1975); P. B. Johnson and R. W. Christy, Phys. Rev. B **9**, 5056 (1974); M. M. Kirillova and B. A. Charikov, Phys. Met. **15**, 138 (1963); G. A. Bolotin, A. N. Voloshinskii, M. M. Noskov, A. V. Sokolov, and B. A. Charikov, Phys. Met. Metallogr. USSR **13**, 823 (1962).
18. W: L. V. Nomerovannaya, M. M. Kirillova, and M. M. Noskov, Opt. Spectrosc. **17**, 134 (1964); J. H. Weaver, D. W. Lynch, and C. G. Olson, Phys. Rev. B **12**, 1293 (1975).
19. J. Babiskin and J. R. Anderson, in *American Institute of Physics Handbook*, (McGraw-Hill, New York, 1972), p. 9-39.
20. G. R. Parkins, W. E. Lawrence, and R. W. Christy, Phys. Rev. B **23**, 6408 (1981).

This work was partially supported by the U.S. Army, DAAK-11-82-C-0052. We gratefully acknowledge the valuable advice of Jean M. Bennett, David Begley, David Bryan, Kul Bhasin, and W. F. Parks.

BLANK

APPENDIX B

PROGRAM FOR KRAMERS-KRONIG ANALYSIS

```
OPTION BASE 1
DIM R(4800),W(4800),F(4800),THETA(600)
'       ************************************************
'       ***********Program Name KKtrap.CBS**************
'       ************************************************
'       ***  Kramers Kronig analysis of reflection   ***
'       ***  data. This program is designed to       ***
'       ***  calculate the phase, and the real       ***
'       ***  and imaginary parts of the complex      ***
'       ***  refractive index.  These corrections    ***
'       ***  are done by evaluating the integeral    ***
'       ***  from  zero to the lowest exp. point for ***
'       ***  the lower wing, and then evaluate the   ***
'       ***  integeral from the last exp. data point ***
'       ***  to infinity for the upper wing.         ***
'       ***                                          ***
'       ***  The upper and lower constant reflectance***
'       ***  is computed by averaging over the first ***
'       ***  five data points for the lower wing and ***
'       ***  the last five for the upper wing.       ***
'       ***                                          ***
'       ***   This spectrum is then used to compute  ***
'       ***   the phase by doing a Trapezoidal       ***
'       ***   integeration over the data and wing    ***
'       ***   corrections for the low and high ends. ***
'       ***                                          ***
'       ***                                          ***
'       ***                                          ***
'       ***            INFRARED LAB.  5/83           ***
'       ***      UNIVERSITY OF MISSOURI AT ROLLA     ***
'       ***           PHYSICS DEPTARTMENT            ***
'       ************************************************
'       ************************************************
'       ************************************************
'
'          VARIABLES ARRAYS & STRINGS USED IN PROGRAM
'-------------------------------------------------------------------
'|                                                                  |
'|  ARRAYS                                                          |
'|        R(I%)------REFLECTANCE                                    |
'|        W(I%)------WAVE NUMBER (1/CM)                             |
'|        F(I%)------INTERGRAND                                     |
'|        THETA(I%)--PHASE ANGLE                                    |
'|        F(I%)------ALSO USED TO STORE THE PHASE                   |
'|                                                                  |
'|  VARIABLES                                                       |
'|        SUM--------INTERMEDIATE RESULTS OF INTEGRATION            |
'|        SUM1-------RESULTS OF INDIVIDUAL TERMS OF INTEGRATION     |
'|        DERR-------DERIVATIVE OF R(W)                             |
'|        DELTAX-----USED IN SIMPSON INTERGRATION                   |
'|        DENOM------DENOMINATOR OF EQUATIONS FOR N AND K           |
'|        RLOW-------CONSTANT REFLECTION COEF.USED FOR LOWER WING   |
'|        REXT-------CONSTANT    "       "   "   "   "   "          |
'|        PI---------3.14159265                                     |
'|                                                                  |
```

```
'|  STRINGS                                                          |
'|        FILENAME$--FILENAME OF RATIO DATA                          |
'|        RNAME$-----FILENAME FOR RESULTS  W,N,K,E1,E2,3r3}          |
'|        SNAME$-----FILENAME FOR SCRATCH FILES                      |
'-------------------------------------------------------------------
'
'
   CLS : GOTO 3
1  BEEP : CLS : RESUME 3
'
'
3  INPUT "FILENAME OF RATIO DATA ";FILENAME$
     ON ERROR GOTO 1
       OPEN "I",#1,FILENAME$
     ON ERROR GOTO 0
'
5  INPUT "IF k IS LESS THAN ZERO SET k EQUAL TO ZERO?  Y(es)/N(o) ";FLAG1$
'
   IF FLAG1$<>"Y" AND FLAG1$<>"y" AND FLAG1$<>"N" AND FLAG1$<>"n"_
       THEN CLS :_
            PRINT "FILENAME OF RATIO DATA ";FILENAME$:_
             GOTO 5
'
   INPUT "SCRATCH FILES TO DISK ";DISK$
       IF DISK$="" THEN SNAME$="SCRATCH"_
                        ELSE SNAME$=DISK$+":SCRATCH"
'
INPUT "MAXIUM WAVE NUMBER TO COMPUTE RESULTS (RETURN FOR ENTIRE RANGE) ";_
                                                          LASTWAVE
'
      GOSUB 1800      ' GET FILENAME FOR RESULTS
'
'
 ENDPOINT%=0
    NPTS%=1
20      IF EOF(1) THEN 30
          INPUT #1,W(NPTS%),R(NPTS%)
           R(NPTS%)=SQR(R(NPTS%))
           IF LASTWAVE>0.0 THEN_
              IF W(NPTS%)<LASTWAVE  THEN ENDPOINT%=NPTS%
           NPTS%=NPTS%+1
IF NPTS%=4801 THEN PRINT "**********ARRAYS FULL*********":_
INPUT "STRIKE ANY KEY TO CONTINUE OR Ctrl Break TO TERMINATE ";FLAG2$ :_
GOTO 30
        GOTO 20
30     CLOSE #1
   NPTS%=NPTS%-1
'
'  EVALUATE THE INTERGRAND OF THE PHASE ANGLE
'
   PI=3.141592653589793
'  COMPUTE AVERAGE SEPERATION OF WAVE NUMBERS
   DELTAX=.5
'
'
```

```
      GOSUB 1600  '  AVERAGE FIRST 5 AND LAST 5 POINTS FOR WINGS
'
      IF NPTS%/2=INT(NPTS%/2) THEN NPTS%=NPTS%-1  'MAKE TOTAL NUMBER OF
      WU=W(NPTS%)+DELTAX                          '  DATA POINTS ODD
      WL=W(1)-DELTAX
'
      IF LASTWAVE=0 THEN ENDPOINT%=NPTS%
      LOCATE 15,15,0
      PRINT "DATA POINT ____ OF ";NPTS%;" DOING ";ENDPOINT%;" TOTAL POINTS";
'
'
      K%=1       ' INITIALIZE THETA COUNTER
      IF ENDPOINT%<600 THEN 35
      OPEN "O",#3,SNAME$
35     FOR I%=1 TO ENDPOINT%
          FOR J%=1 TO NPTS%
            IF  I%=J% THEN GOSUB 1500 :GOTO 40 ' COMPUTE DERIVATIVE
             F(J%)=LOG(R(J%)/R(I%))/(W(I%)*W(I%)-W(J%)*W(J%))
40        NEXT J%
'
' USE TRAPEZOID RULE TO EVALUATE THE DEFINITE INTEGRAL
'
     SUM=0.0
       FOR J%=1 TO NPTS%-1
         SUM1=(W(J%+1)-W(J%))*(F(J%+1)+F(J%))
          SUM=SUM+SUM1
       NEXT J%
        CORRECT=F(1)+F(NPTS)
        THETAL=LOG(R(I%)/RLOW)*LOG((W(I%)+WL)/(W(I%)-WL))
        THETAU=LOG(R(I%)/REXT)*LOG((WU-W(I%))/(WU+W(I%)))
        THETA(K%) = (SUM*W(I%)+CORRECT*2*DELTAX-THETAU-THETAL)/PI
        IF K%=600 THEN GOSUB 2200 ' WRITE PHASE TO SCRATCH FILE
        K%=K%+1
     LOCATE 15,26,0
     PRINT USING "####";I%
  NEXT I%
           K%=K%-1
           IF FLAG3$<>"SET" THEN 50
           GOSUB 2200  ' FINISH WRITING SCRATCH FILE TO DISK
           CLOSE #3
           GOSUB 2400  ' READ PHASE IN OVER F ARRAY
           KILL SNAME$
           GOTO 60
'
'
'      IF NO SCRATCH FILE THEN TRANSFER ARRAY FROM THETA TO F
50     FOR I%=1 TO ENDPOINT% : F(I%)=THETA(I%) : NEXT I%

60     PRINT " " : PRINT "WRITING DATA TO DISK"
'
       GOSUB 2000     'WRITE DATA TO DISK
'
                        END
'
'
```

```
'
1500 ' ******************************************
'  *                                            *
'  *     SUBROUTINE TO COMPUTE DERIVATIVE       *
'  *                                            *
'  ******************************************
'
'  COMPUTE DERIVATIVE OF R(W) SO AS TO COMPUTE
'  F(I%) WHEN J%=I%
'  where F(I%)=-R'(I%)/[2*W(I%)*R(I%)]
'
     DERR=(R(I%+1)-R(I%))/(W(I%+1)-W(I%))
     F(J%)=-DERR/(2*W(I%)*R(I%))
   RETURN
                        END
'
'
1600 '   ************************************************************
'    *                                                          *
'    *  SUBROUTINE TO AVERAGE FIRST FIVE AND LAST FIVE POINTS   *
'    *                                                          *
'    ************************************************************
'
'                  AVERAGE FIRST FIVE DATA POINTS
'
'
     PRINT " "
      RLOW=0.0
       FOR I%=1 TO 5
         RLOW=RLOW+R(I%)
       NEXT I% : RLOW=RLOW/5
     PRINT "LOWER REFLECTANCE=";
     PRINT USING "#.######";RLOW^2; : PRINT "                ";
'
'            AVERAGE LAST FIVE POINTS FOR UPPER WING
'
      REXT=0
        FOR I%=NPTS%-4 TO NPTS%
          REXT=REXT+R(I%)
        NEXT I% : REXT=REXT/5
     PRINT "UPPER REFLECTANCE=";
     PRINT USING "#.######";REXT^2
'
'
     RETURN
     END
'
'
```

```
'
'
1800 '   ************************************************************
     '   *                                                          *
     '   *              FILENAME FOR OUTPUT                         *
     '   *                                                          *
     '   ************************************************************
     '
     '
         INPUT "FILENAME FOR RESULTS w,n,k,E1,E2 & |r|^2 ";RNAME$
         PRINT " "
         PRINT "ONE LINE COMMENT 80 CHARACTERS OR LESS "
         LINE INPUT ONELINE$
         RETURN
         END
     '
     '
     '
     '
2000 '   ************************************************************
     '   *                                                          *
     '   *            WRITE DATA TO ONE DISK FILE                   *
     '   *                                                          *
     '   ************************************************************
     '
     '
                   OPEN "O",#2,RNAME$
                   PRINT #2,ONELINE$
                   PRINT #2, "UPPER REFLECTANCE= ";
                   PRINT #2,USING "#.#####";REXT^2
                   PRINT #2, "LOWER REFLECTANCE= ";
                   PRINT #2,USING "#.#####";RLOW^2
       FOR I%=1 TO ENDPOINT%
           DENOM=1.0-2.0*R(I%)*COS(F(I%))+R(I%)*R(I%)
           K=2.0*R(I%)*SIN(F(I%))/DENOM
           IF K<0.0 AND (FLAG1$="Y" OR FLAG1$="y") THEN K=0.0
           N=(1.0-R(I%)*R(I%))/DENOM
              PRINT #2,USING "####.####    ";W(I%) , N , K ,_
                                              N^2-K^2 , 2*N*K ,_
                                                        R(I%)*R(I%)
       NEXT I%
            CLOSE #2
            RETURN
            END
     '
     '
```

```
'
'
2200 '   ********************************************************
     '   *                                                      *
     '   *      SUBROUTINE TO WRITE SCRATCH FILES TO DISK       *
     '   *                                                      *
     '   ********************************************************
     '
     '
     '
         FLAG3$="SET"      ' SET FLAG TO INDICATE SCRATCH FILE
        FOR L%=1 TO K%
         PRINT #3, THETA(L%)
        NEXT L%
          K%=0
          RETURN
          END
     '
     '
2400 '   ********************************************************
     '   *                                                      *
     '   *      SUBROUTINE TO READ PHASE OVER ARRAY F           *
     '   *                                                      *
     '   ********************************************************
     '
     '
     '
         OPEN "I",#3,SNAME$
          FOR I%=1 TO NPTS%
                INPUT #3,F(I%)
          NEXT I%
         CLOSE #3
          RETURN
          END
```

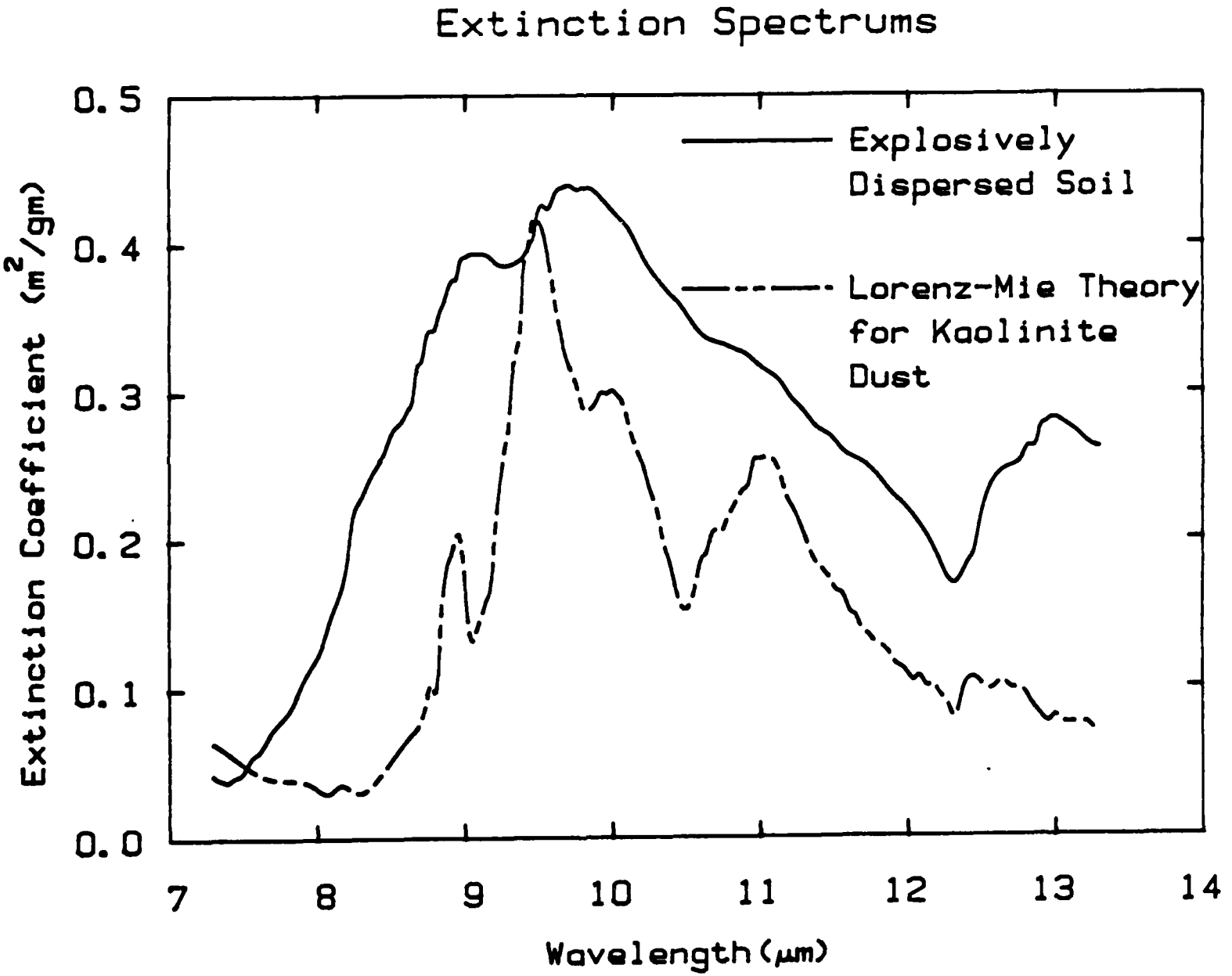

Figure 1. Extinction Spectrum for Explosively Dispersed Soil (measured) and for Kaolinite (calculated). Adapted from Ref. 2.

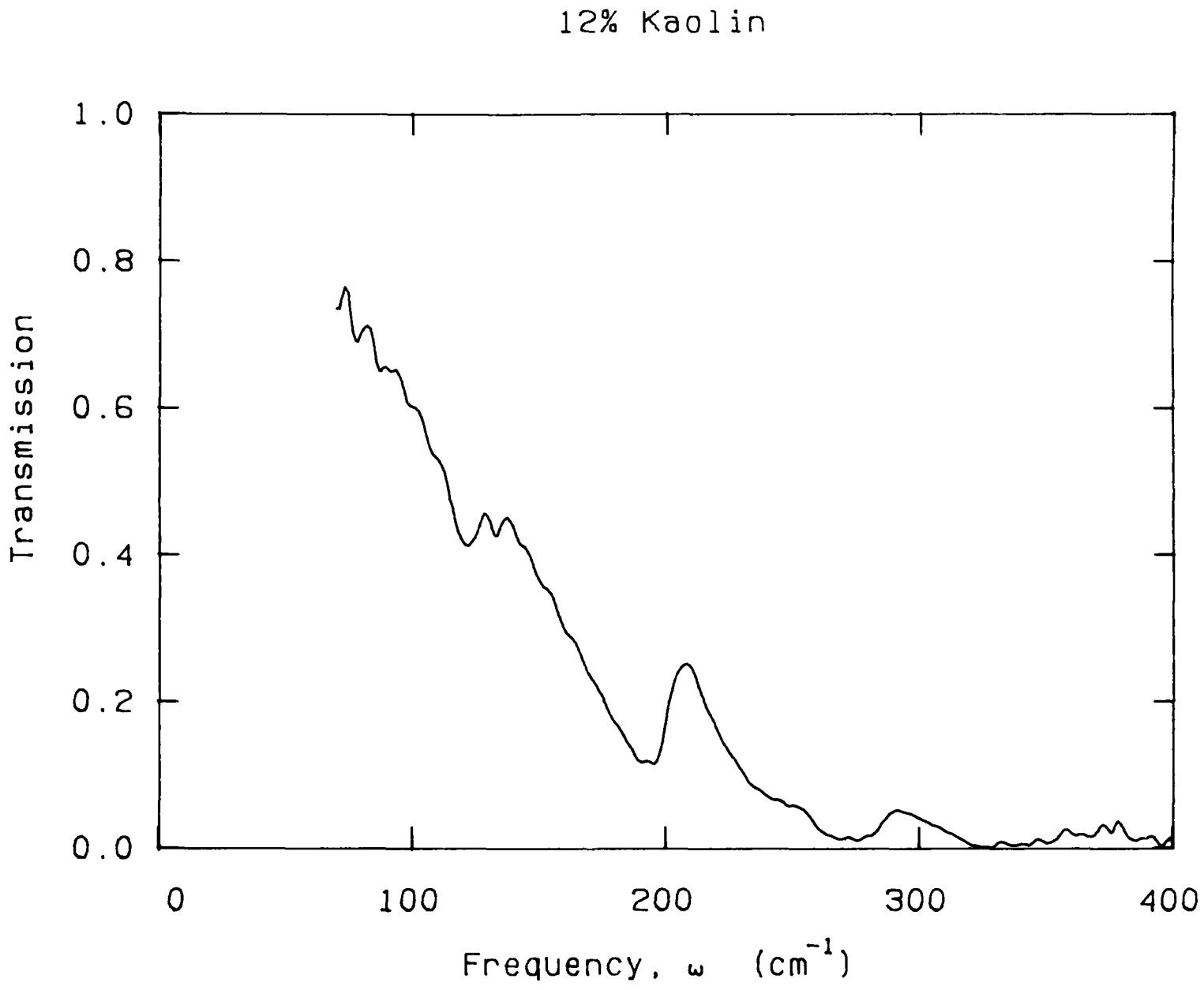

Figure 2. Transmission spectrum for a KBr pressed pellet containing 12% Kaolin by weight.

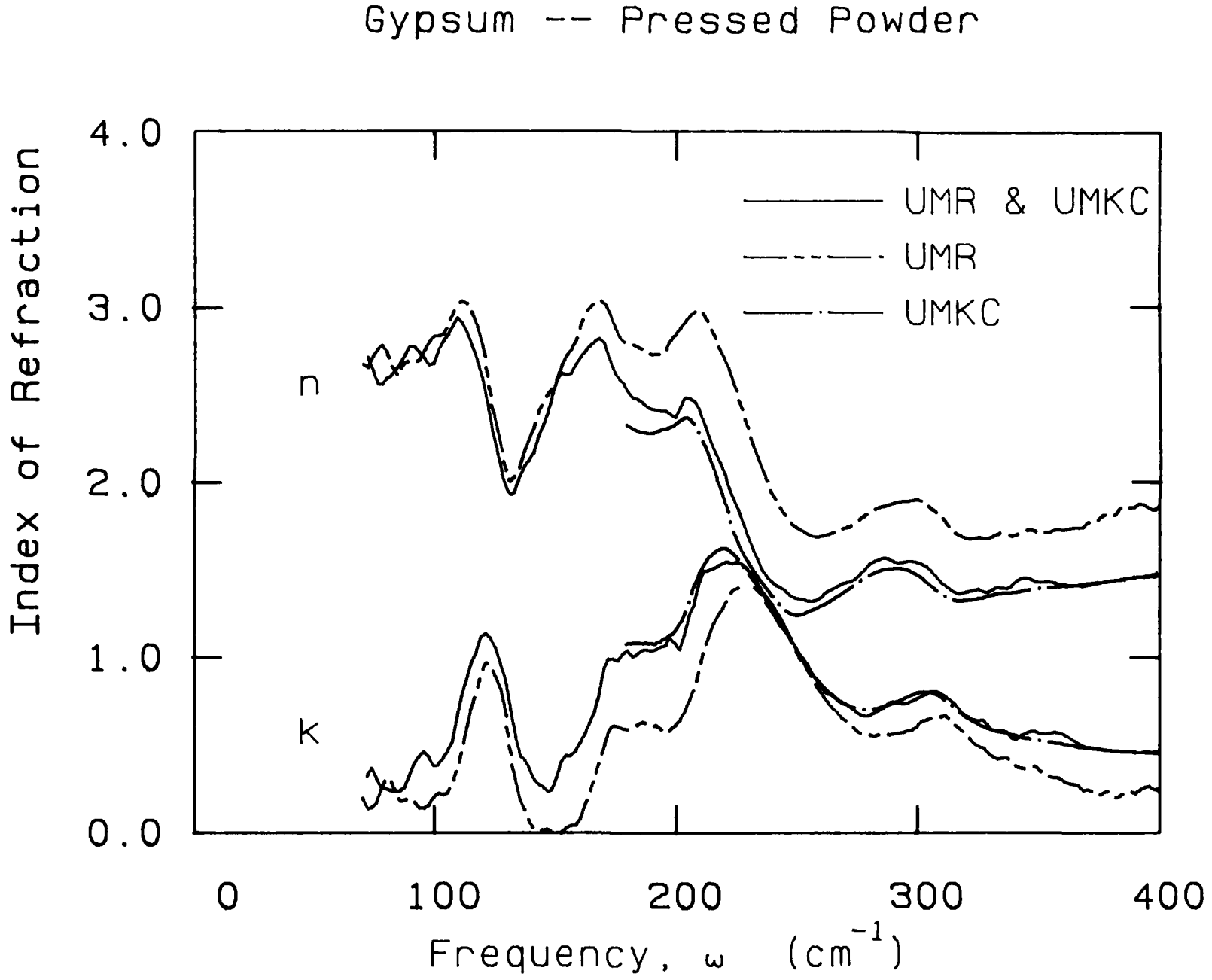

Figure 3. Index of Refraction of Gypsum showing KK analysis of UMR, UMKC and Combined Data Sets.

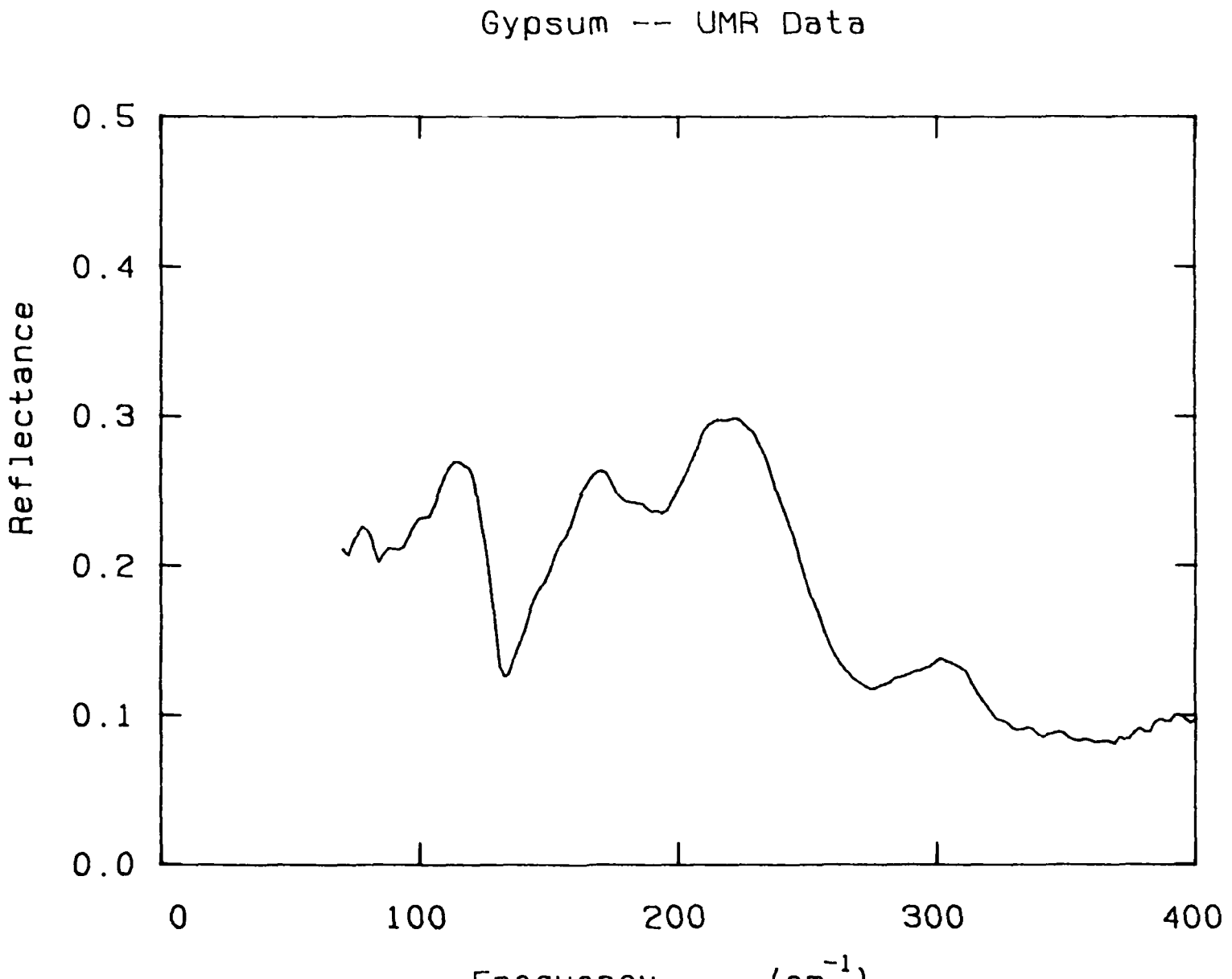

Figure 4. Reflectance of Gypsum from 0-400 cm^{-1}.

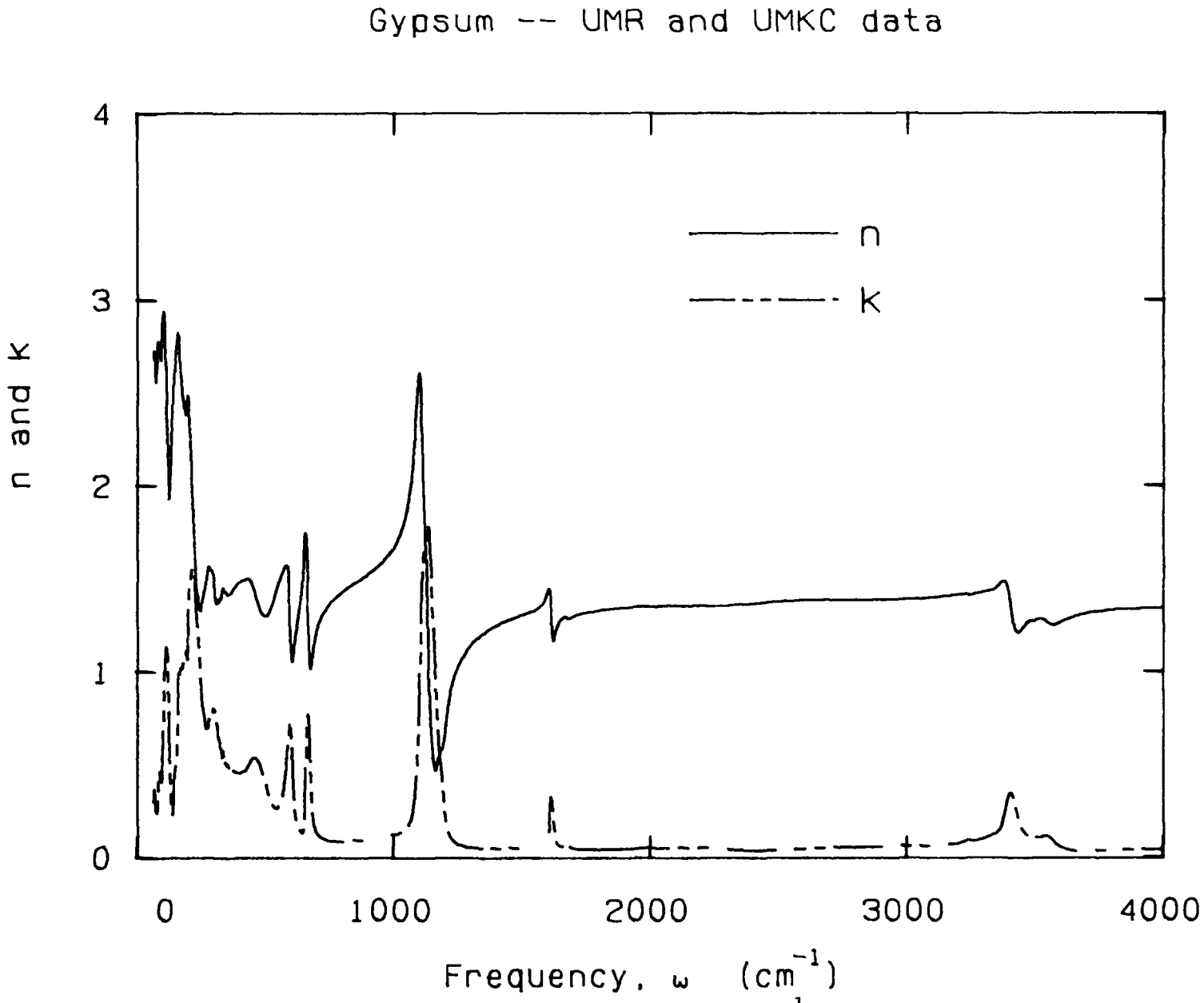

Figure 5. Index of Refraction for Gypsum, 0-4000 cm^{-1}.

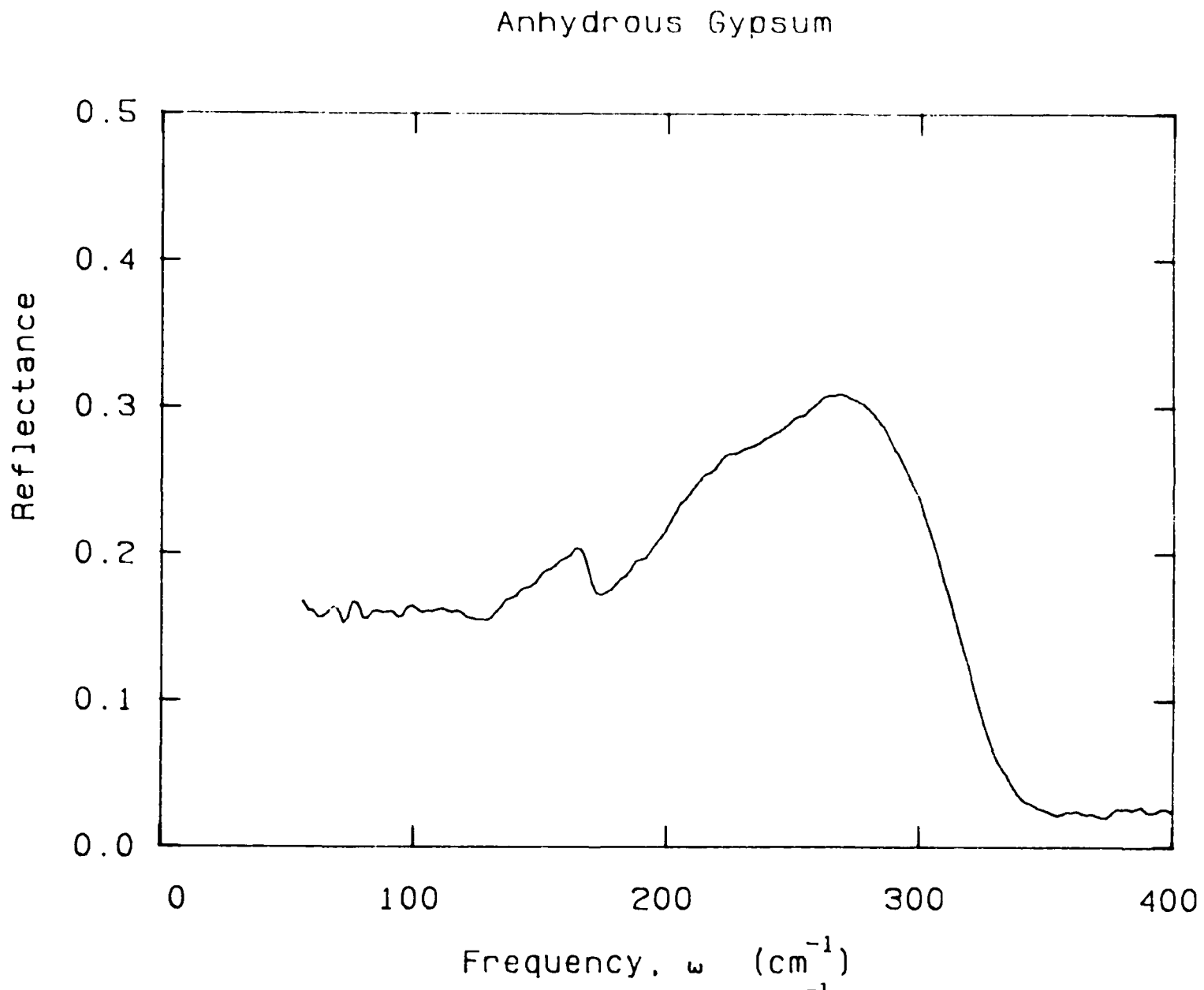

Figure 6. Reflectance of Anhydrous Gypsum, 0-400 cm^{-1}.

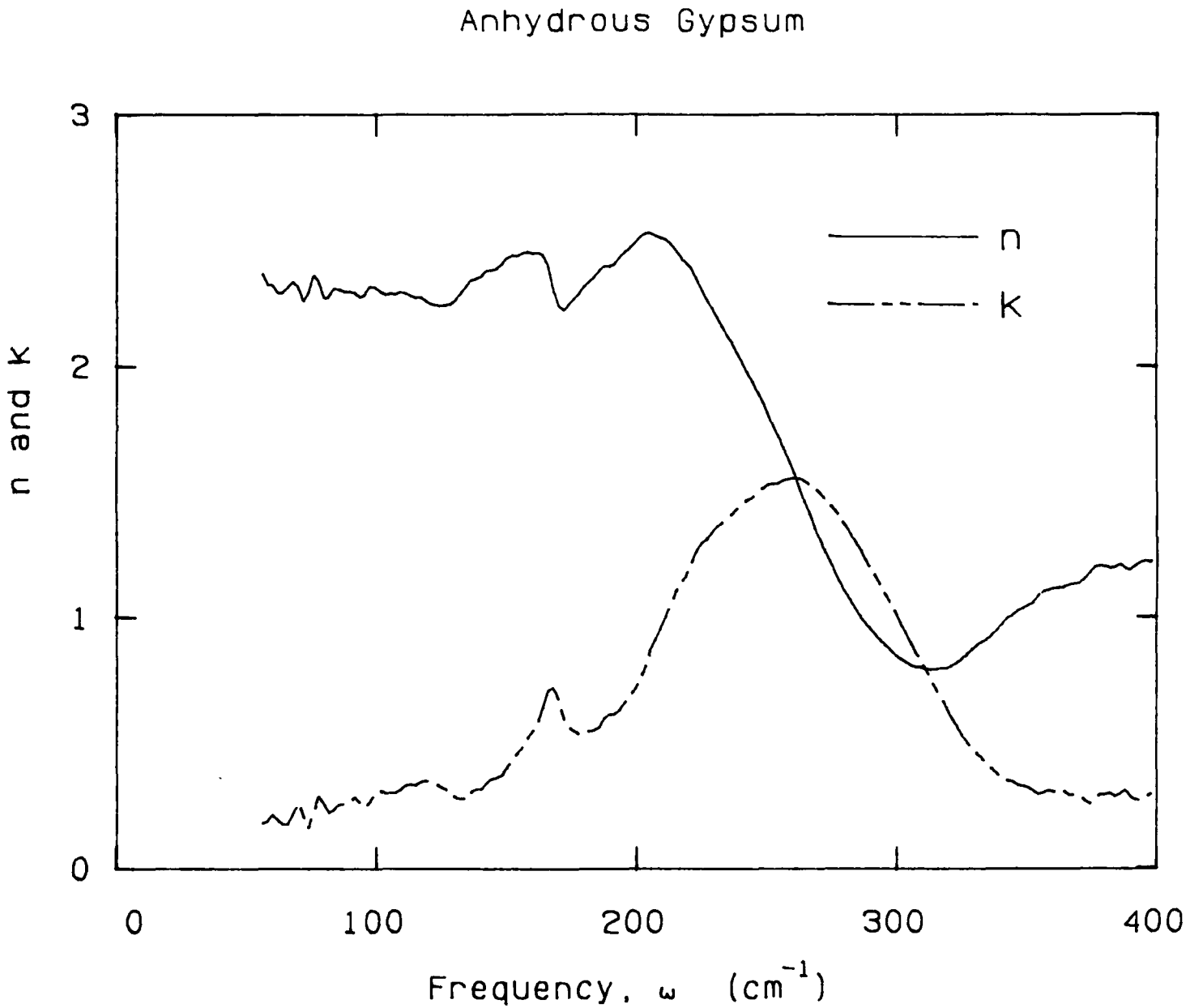

Figure 7. Index of Refraction for Anhydrous Gypsum 0-400 cm^{-1}.

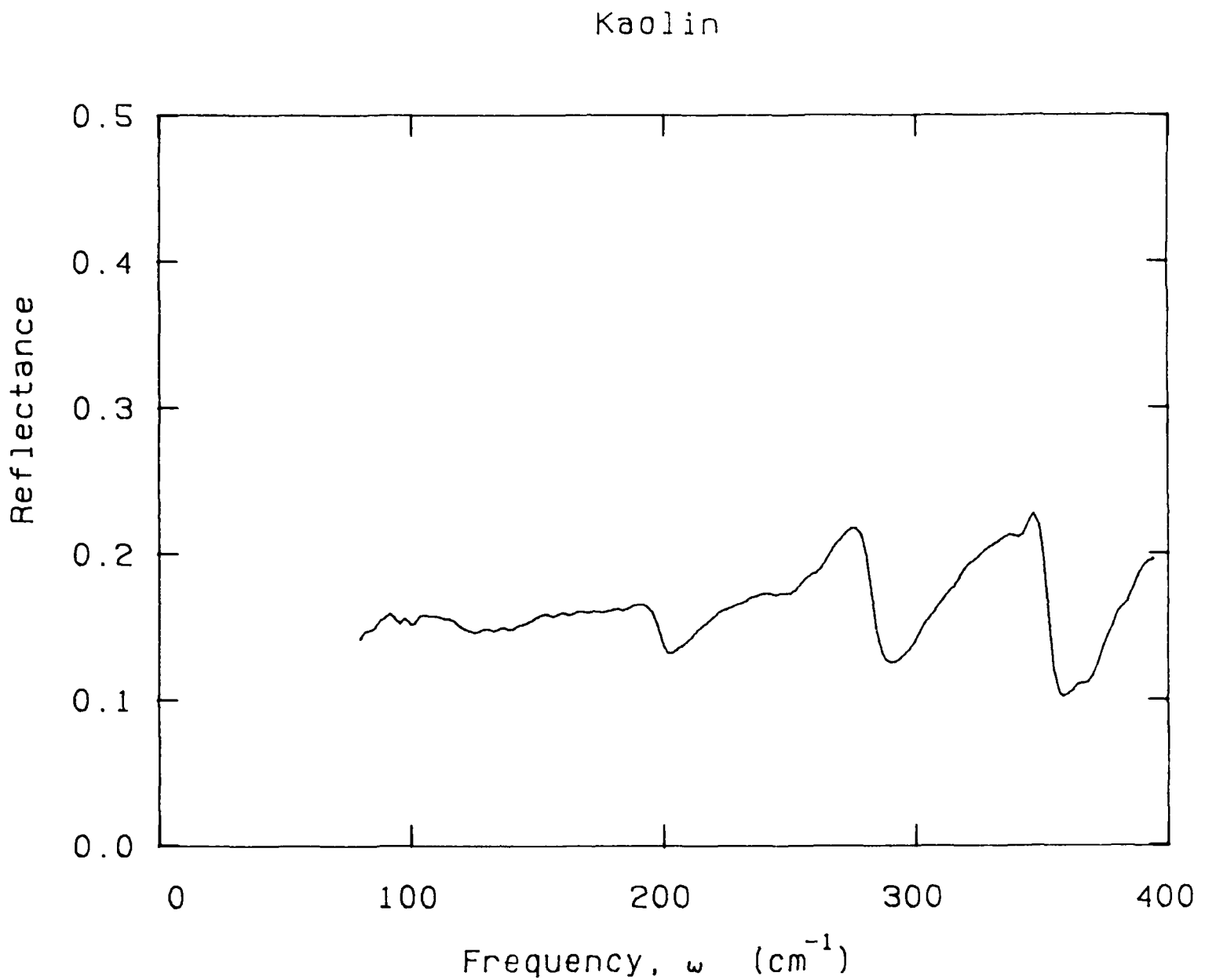

Figure 8. Reflectance of Kaolin, 0-400 cm^{-1}.

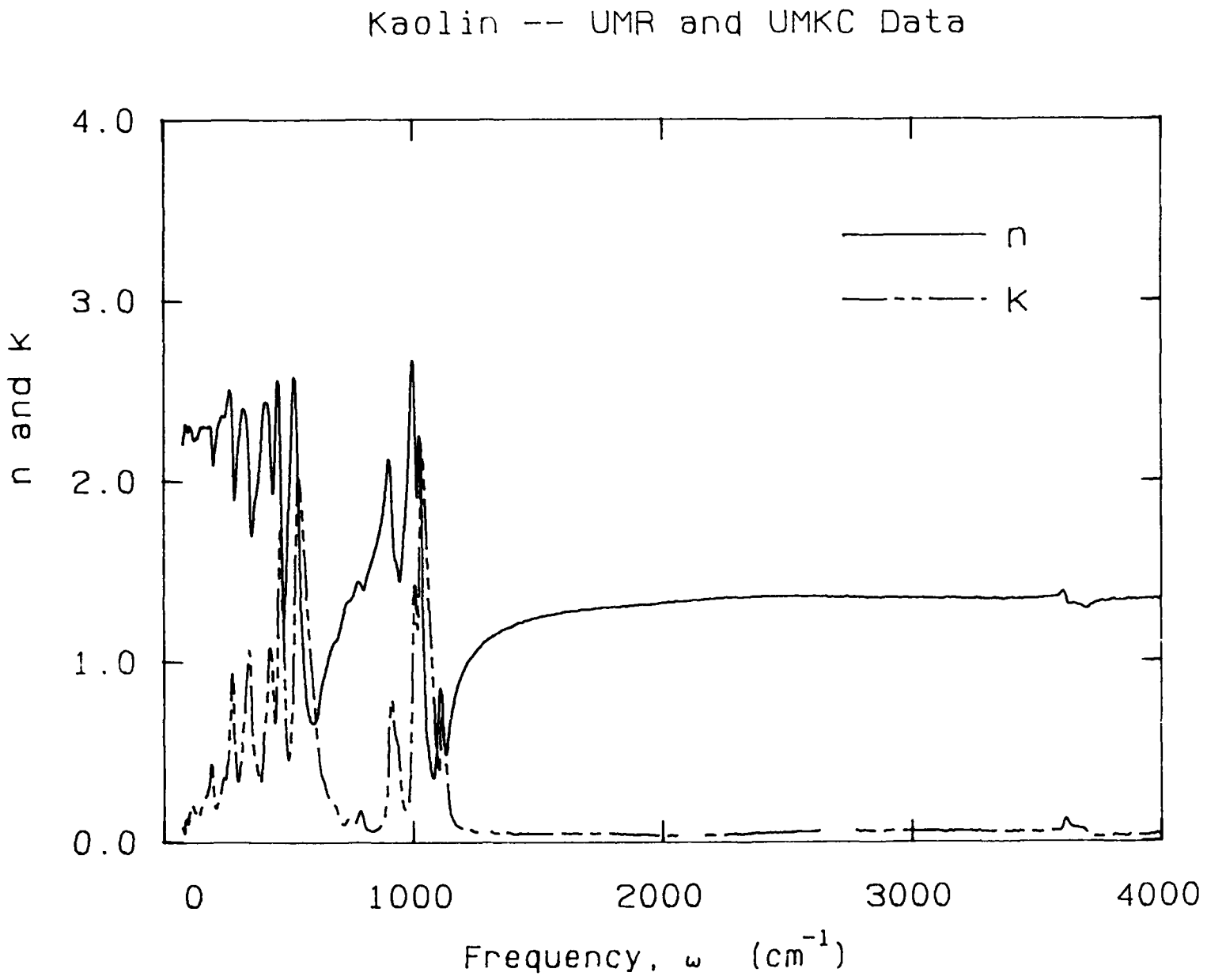

Figure 9. Index of Refraction for Kaolin, 0-4000 cm^{-1}.

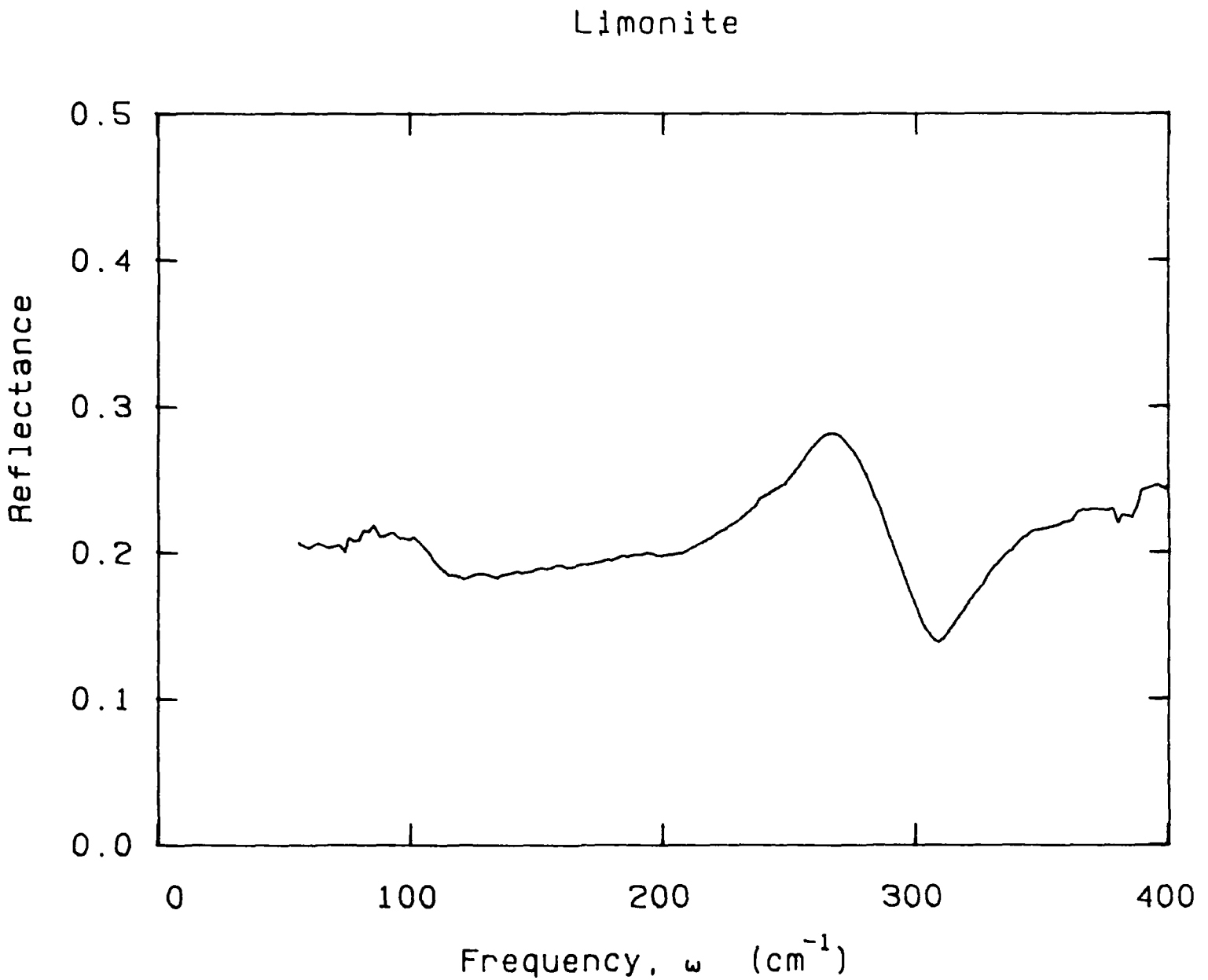

Figure 10. Reflectance of Limonite, 0-400 cm^{-1}.

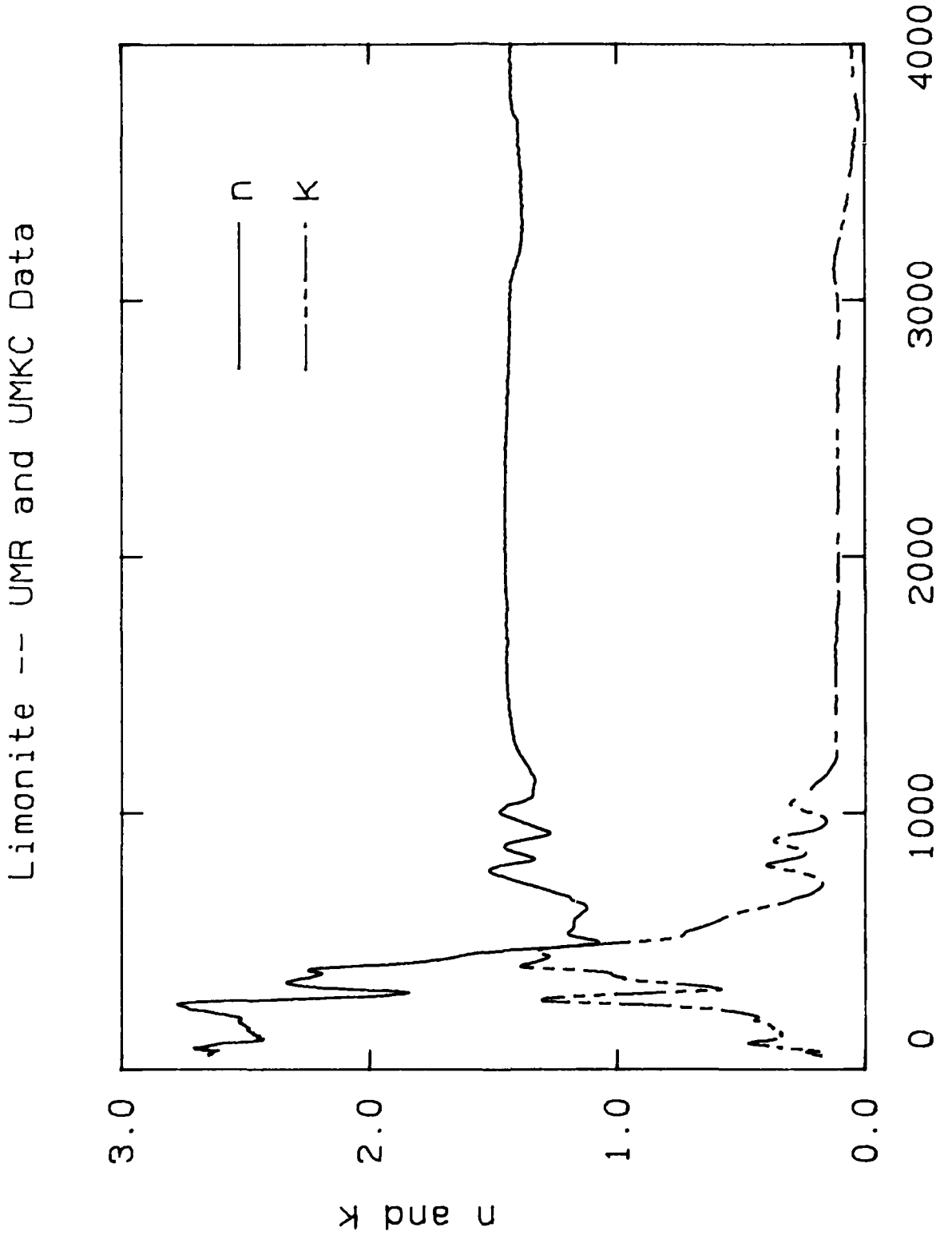

Figure 11. Index of Refraction for Limonite, 0-4000 cm^{-1}.

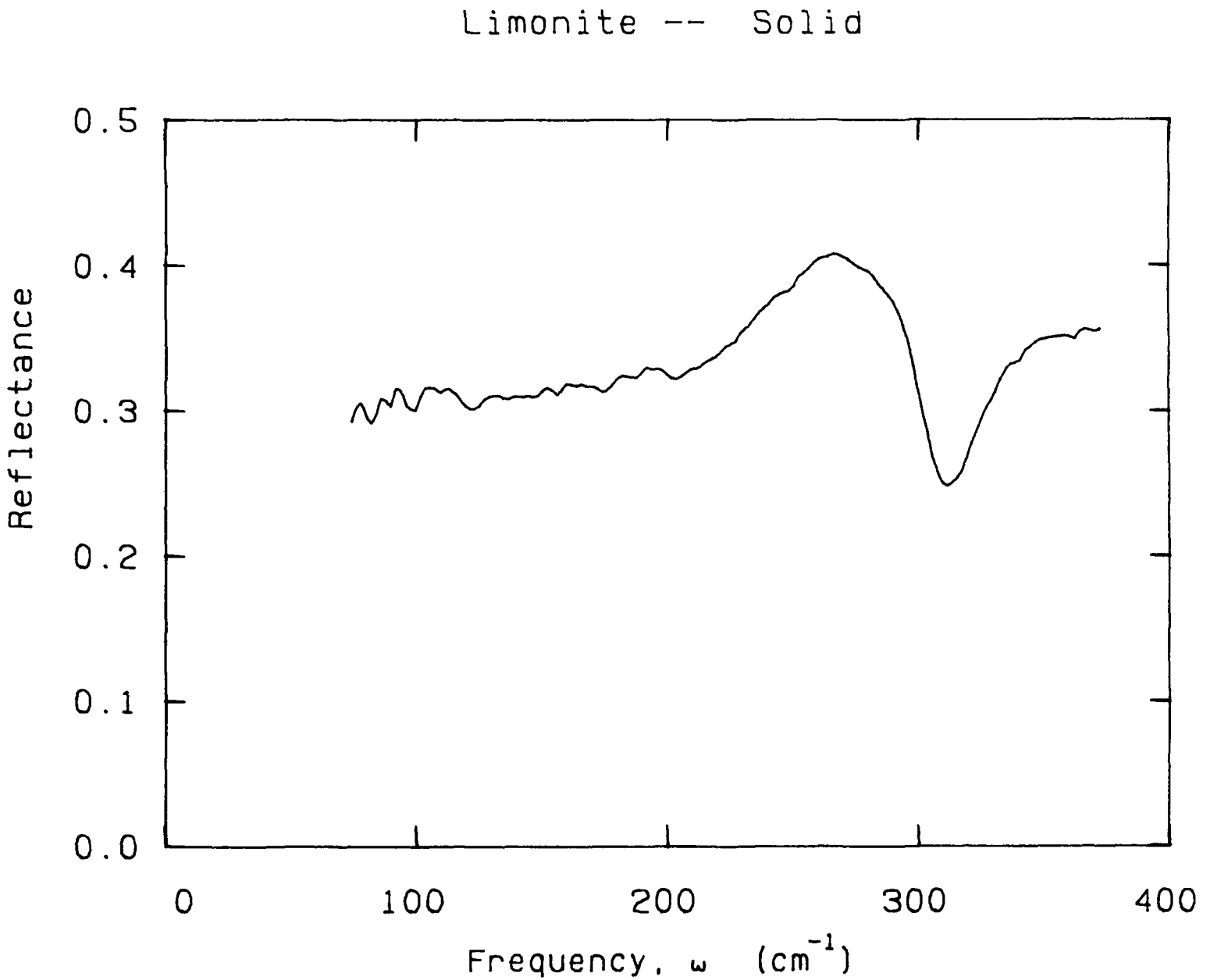

Figure 12. Reflectance Rock Sample of Limonite, 0-400 cm^{-1}.

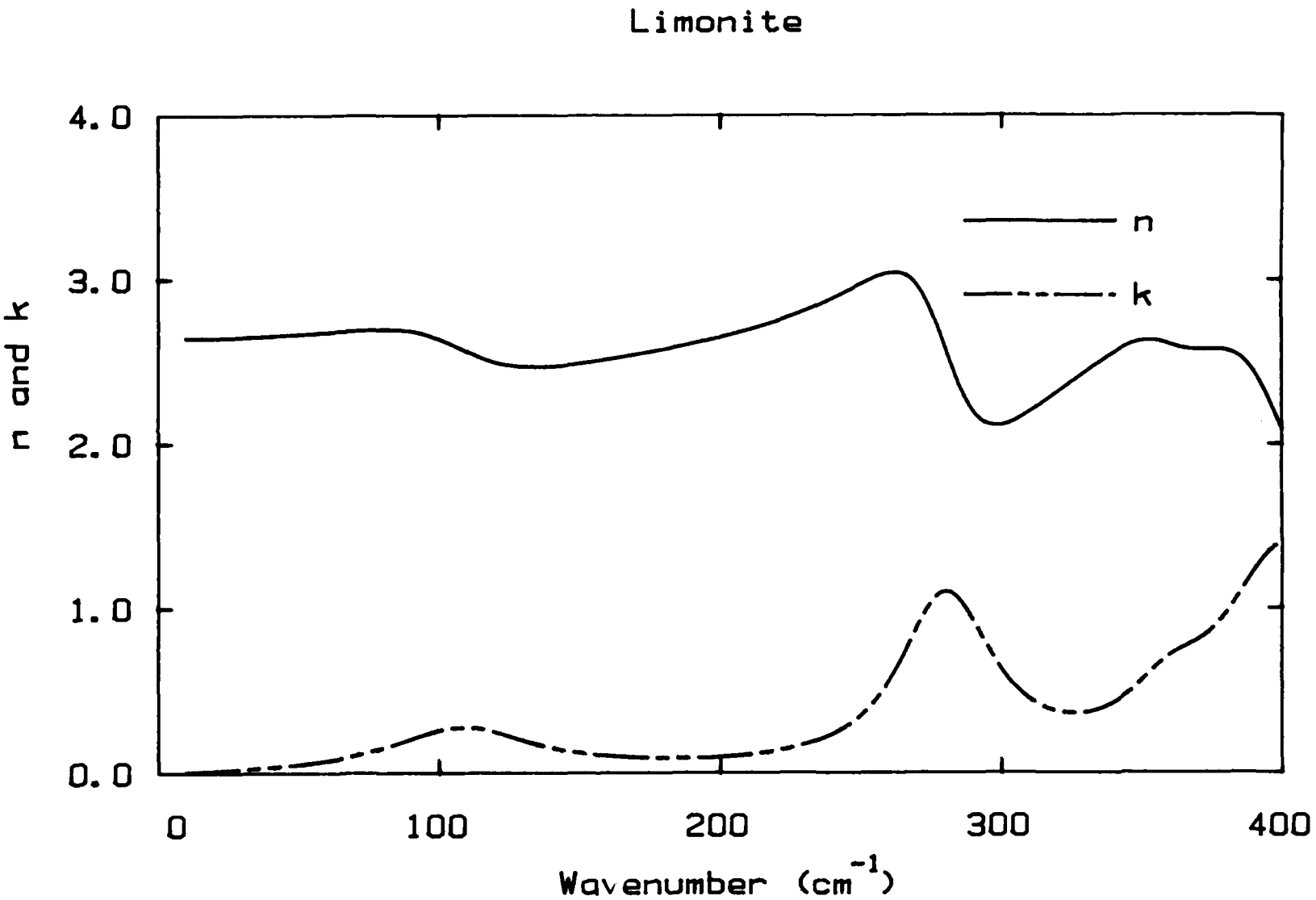

Figure 13. Index of Refraction for Rock Limonite, 0-400 cm^{-1}.

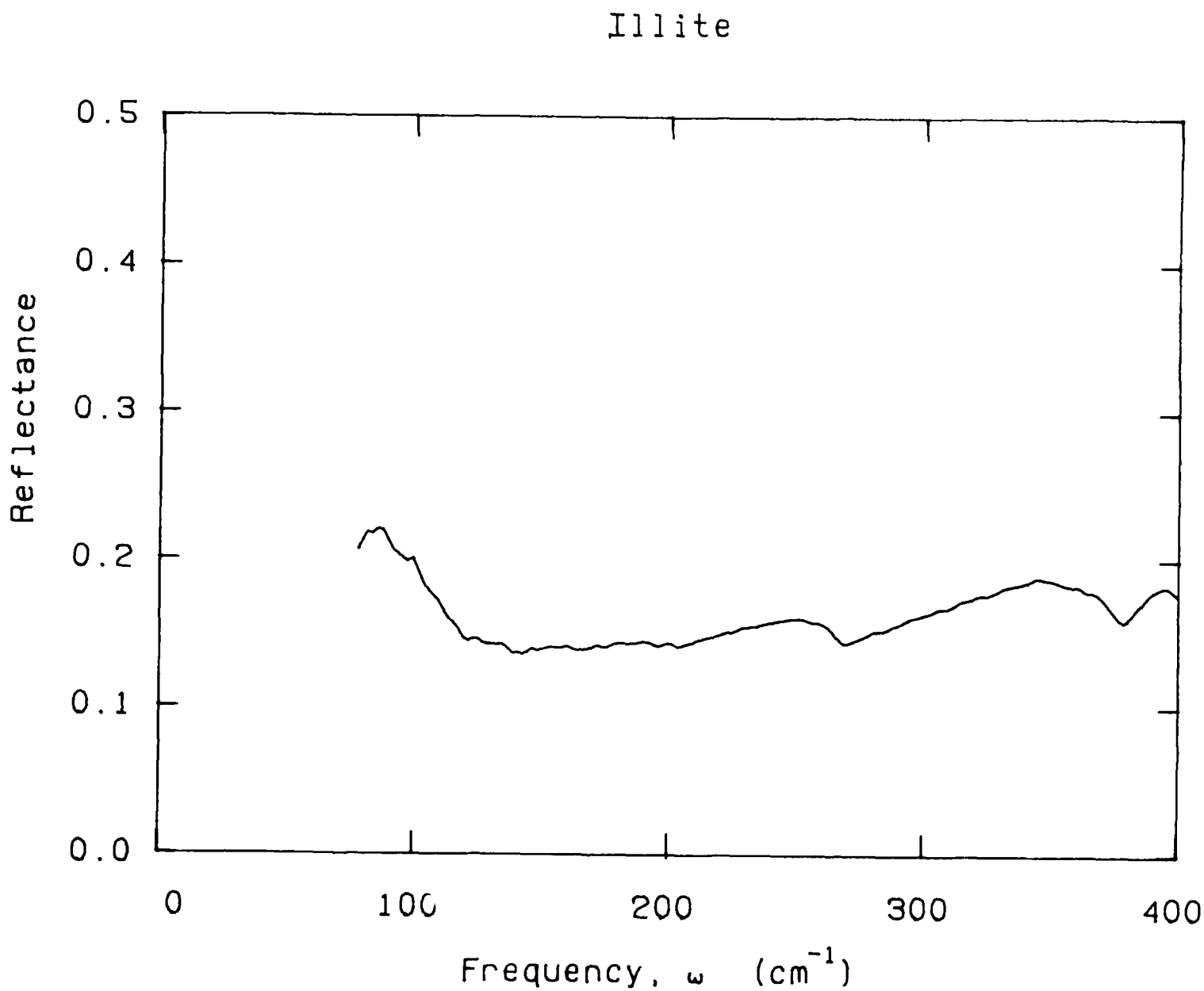

Figure 14. Reflectance Illite, 0-400 cm^{-1}.

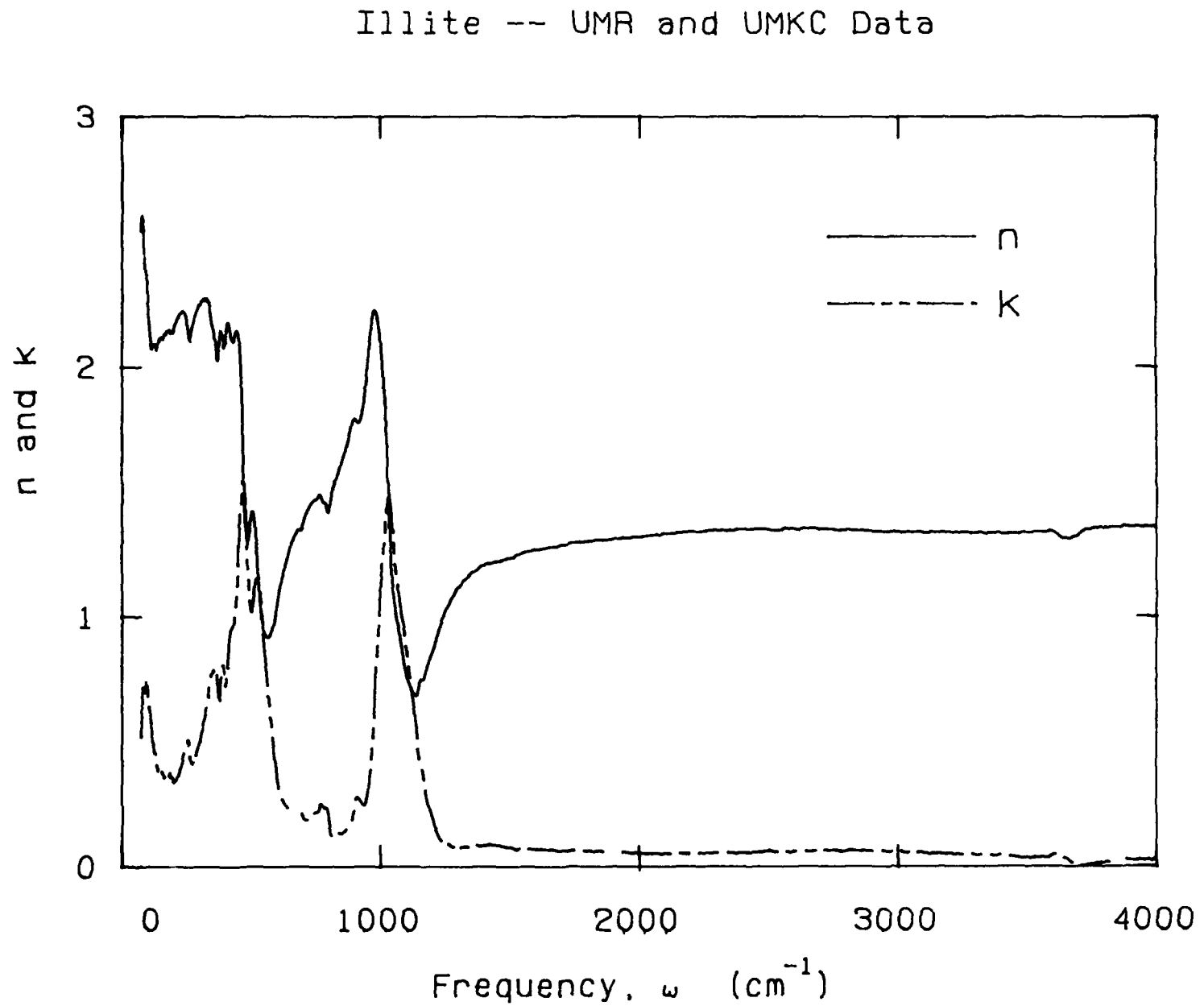

Figure 15. Index of Refraction for Illite, 0-4000 cm^{-1}.

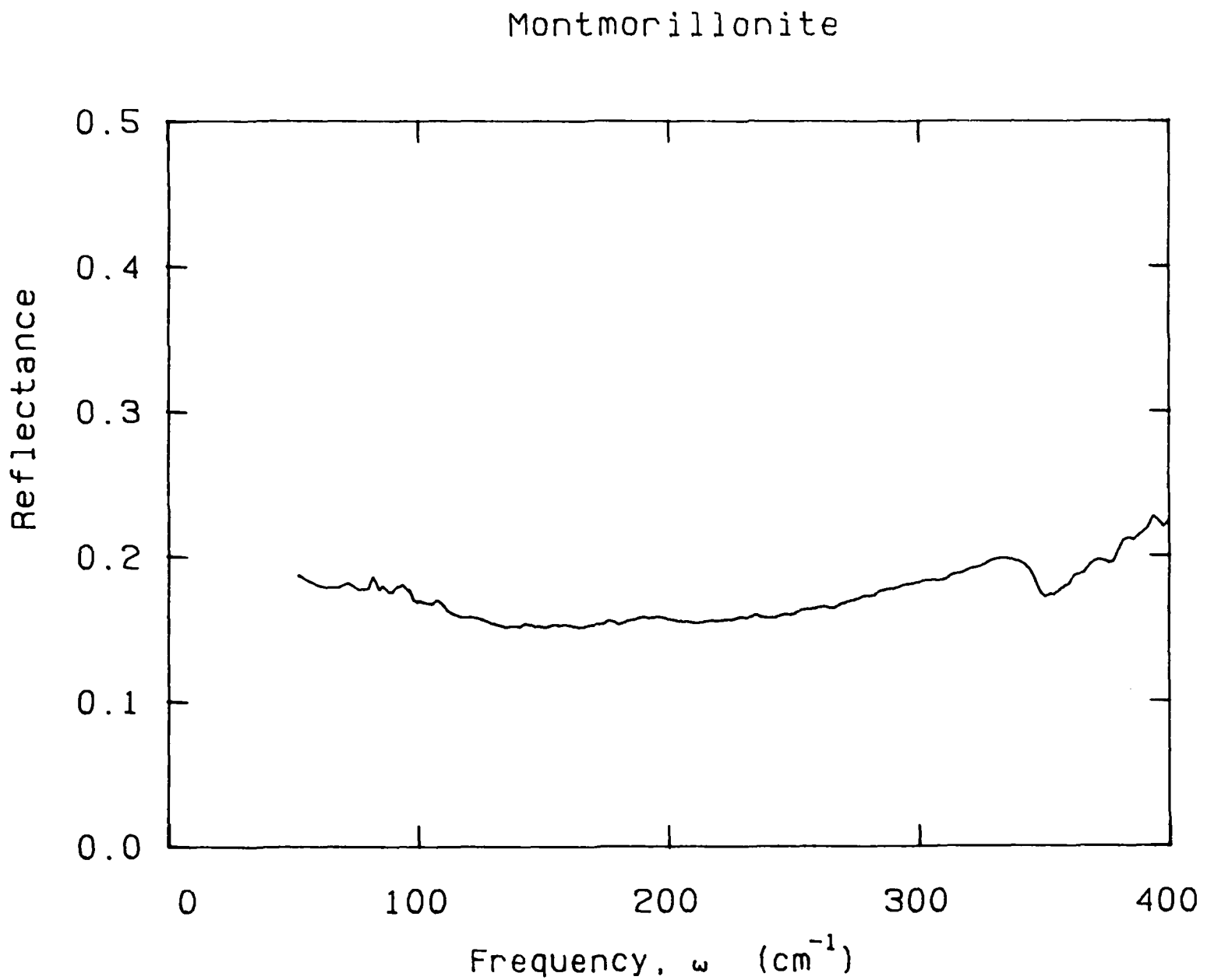

Figure 16. Reflectance for Montmorillonite, 0-400 cm^{-1}.

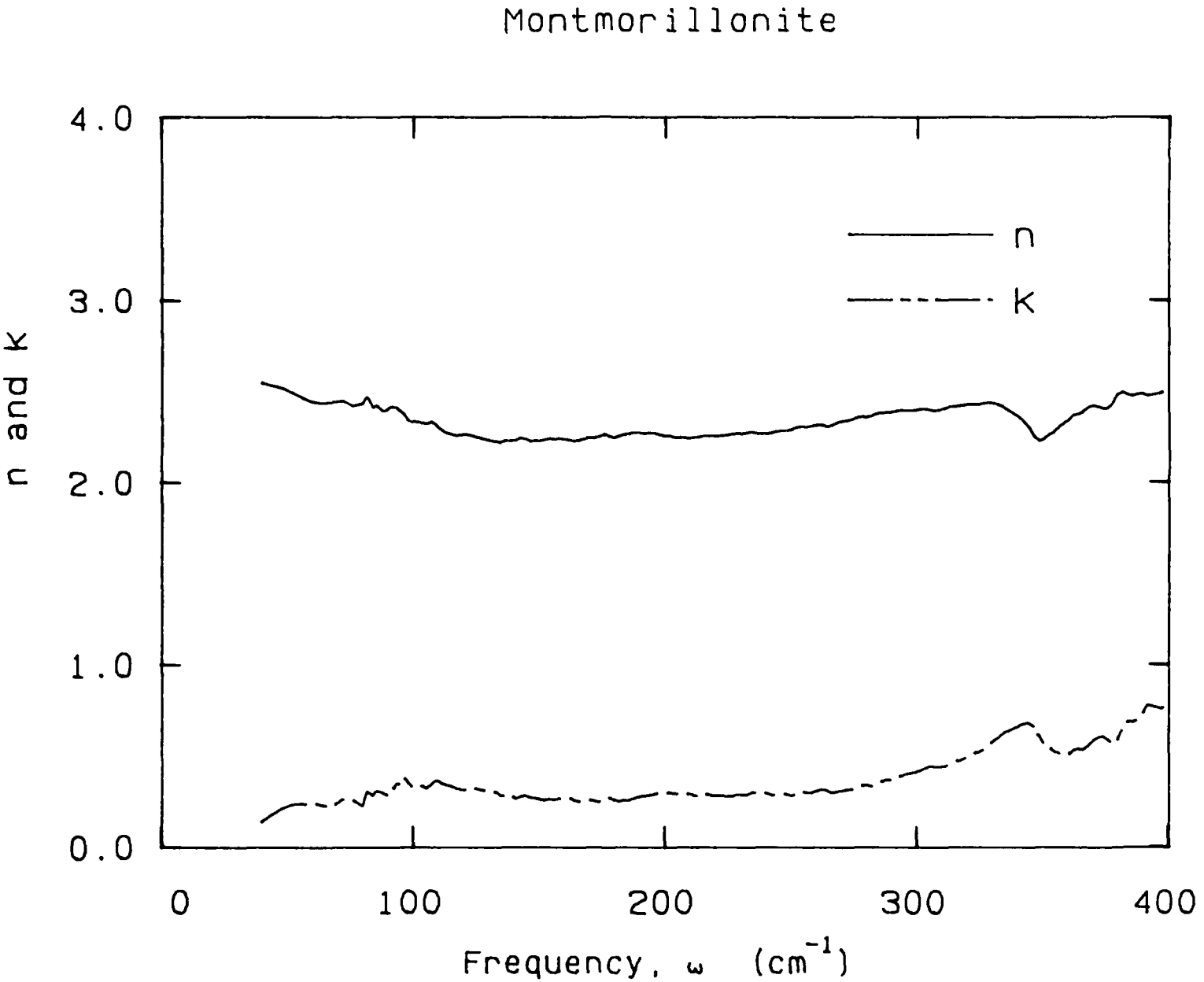

Figure 17. Index of Refraction for Montmorillonite, 0-4000 cm^{-1}.

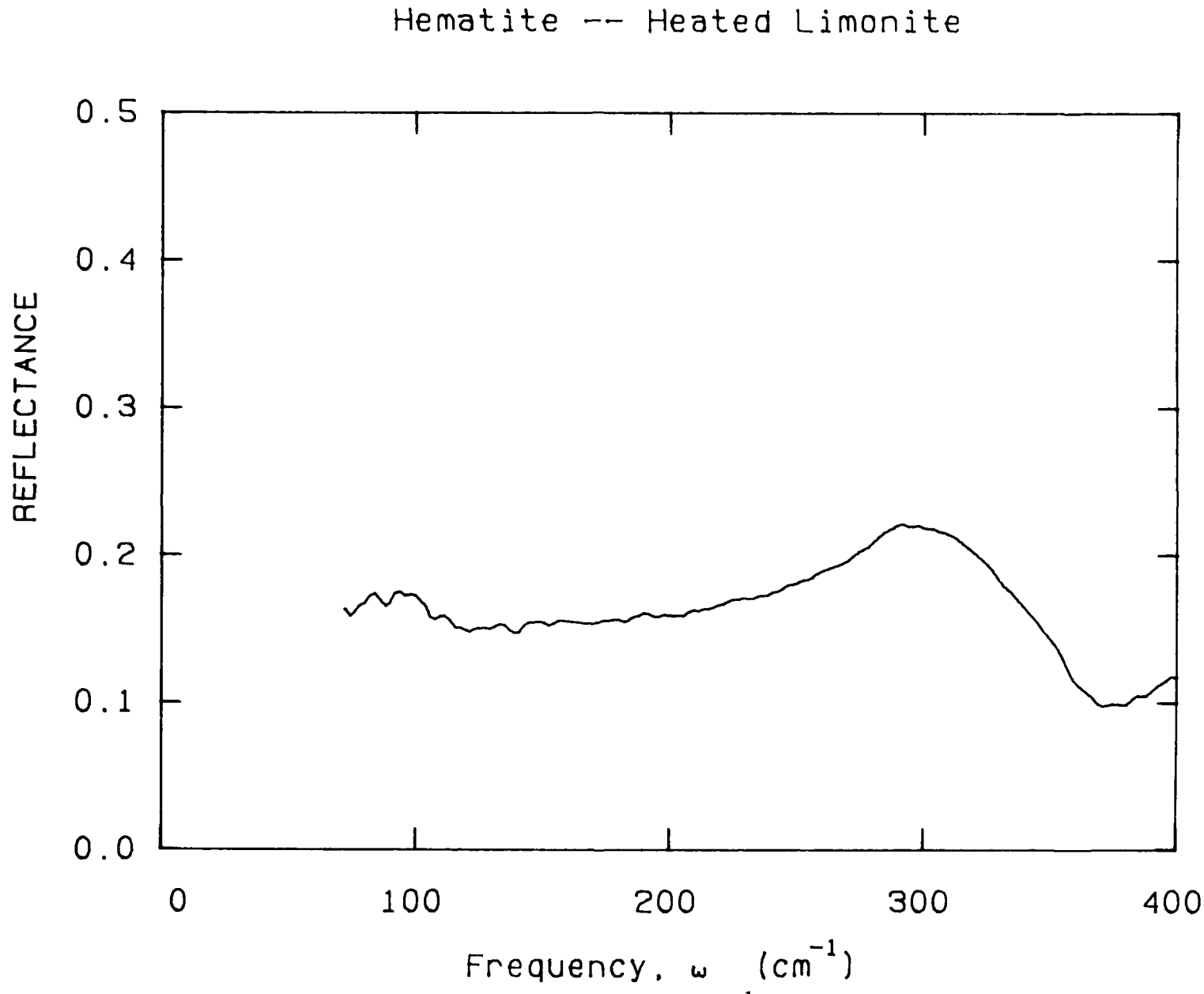

Figure 18. Reflectance of Hematite, 0-400 cm^{-1}.

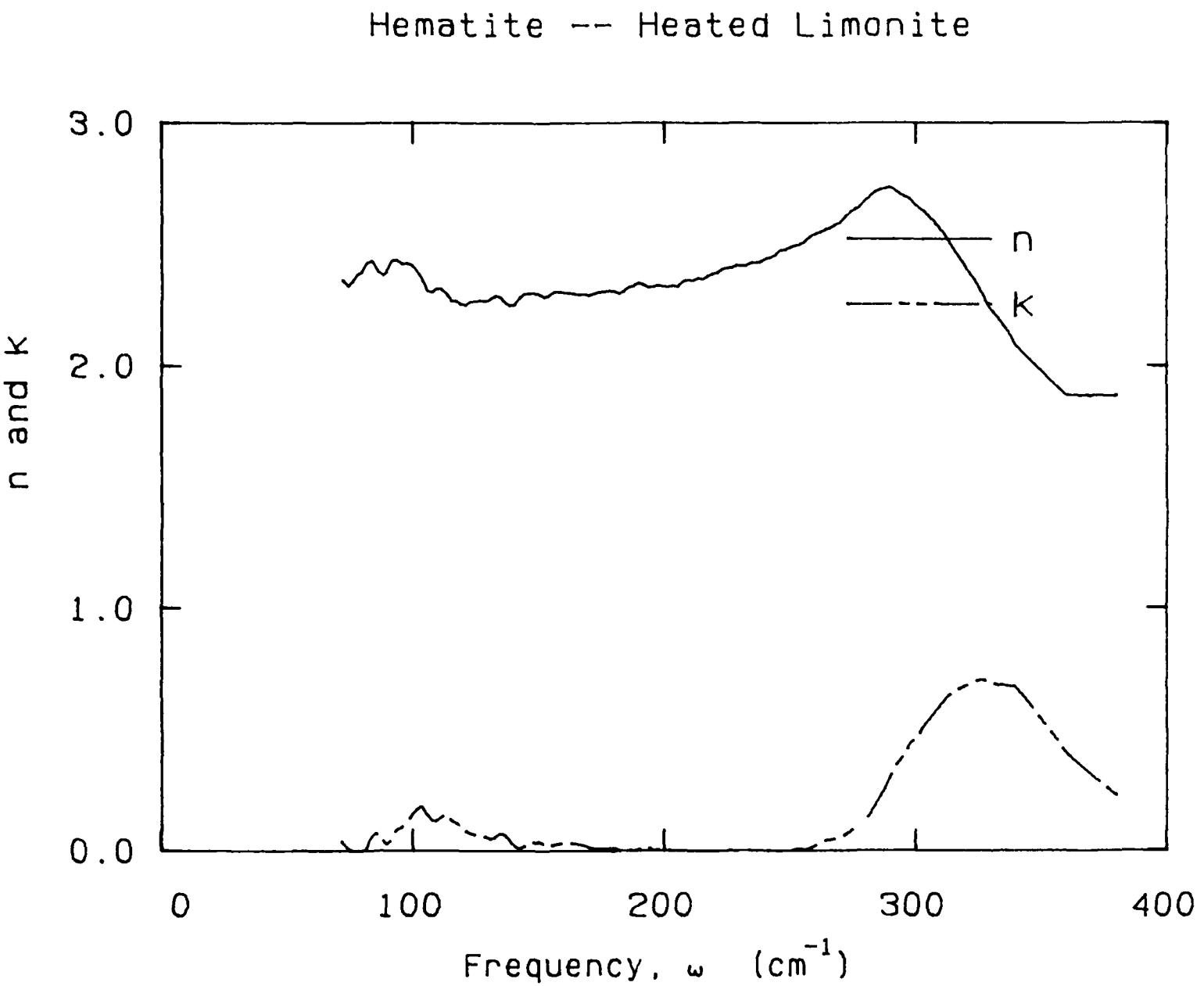

Figure 19. Index of Refraction for Hematite, 0-400 cm^{-1}.

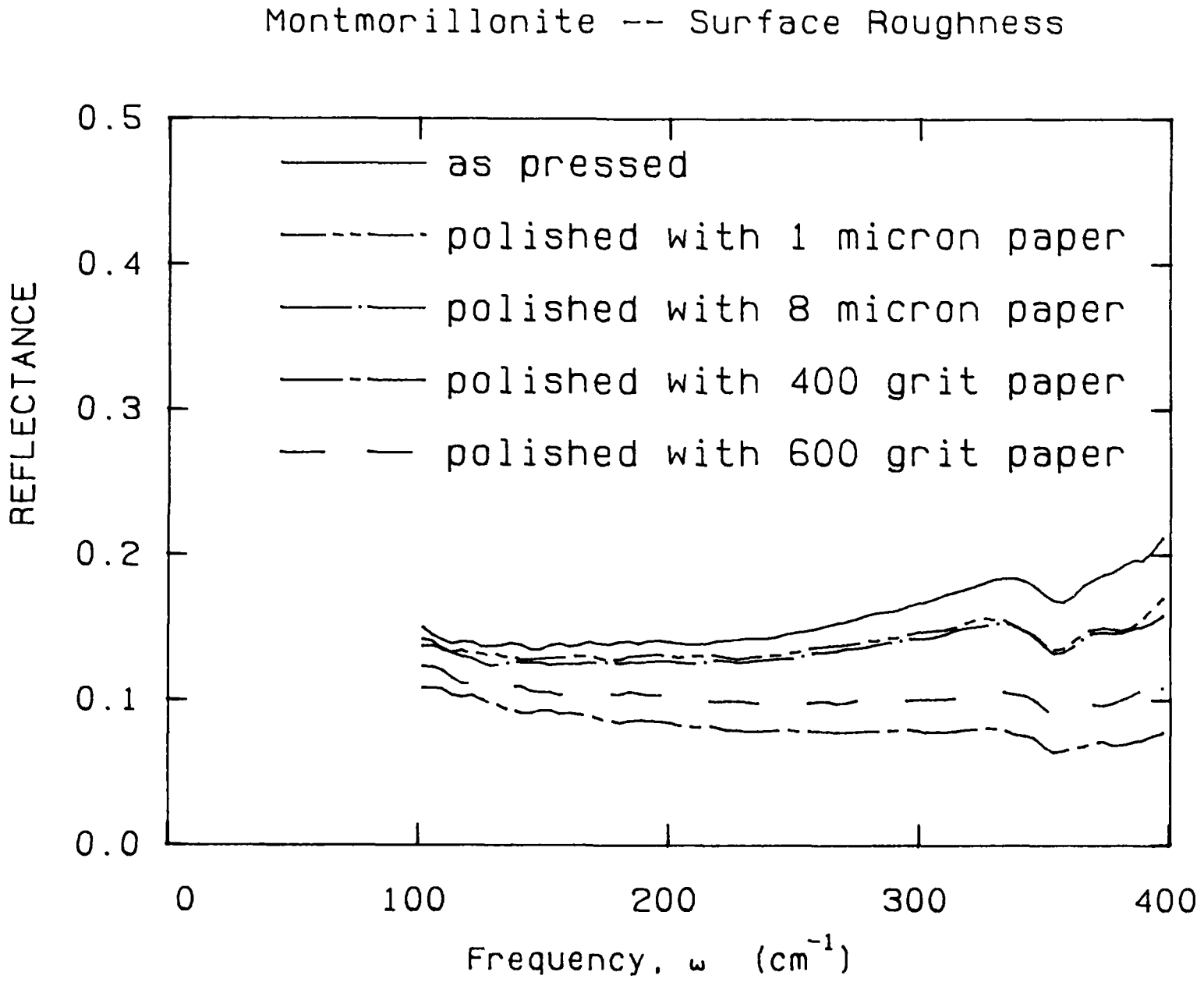

Figure 20. Montmorillonite with Various Grit Polishes from 1 Micrometer to #400 Grit.

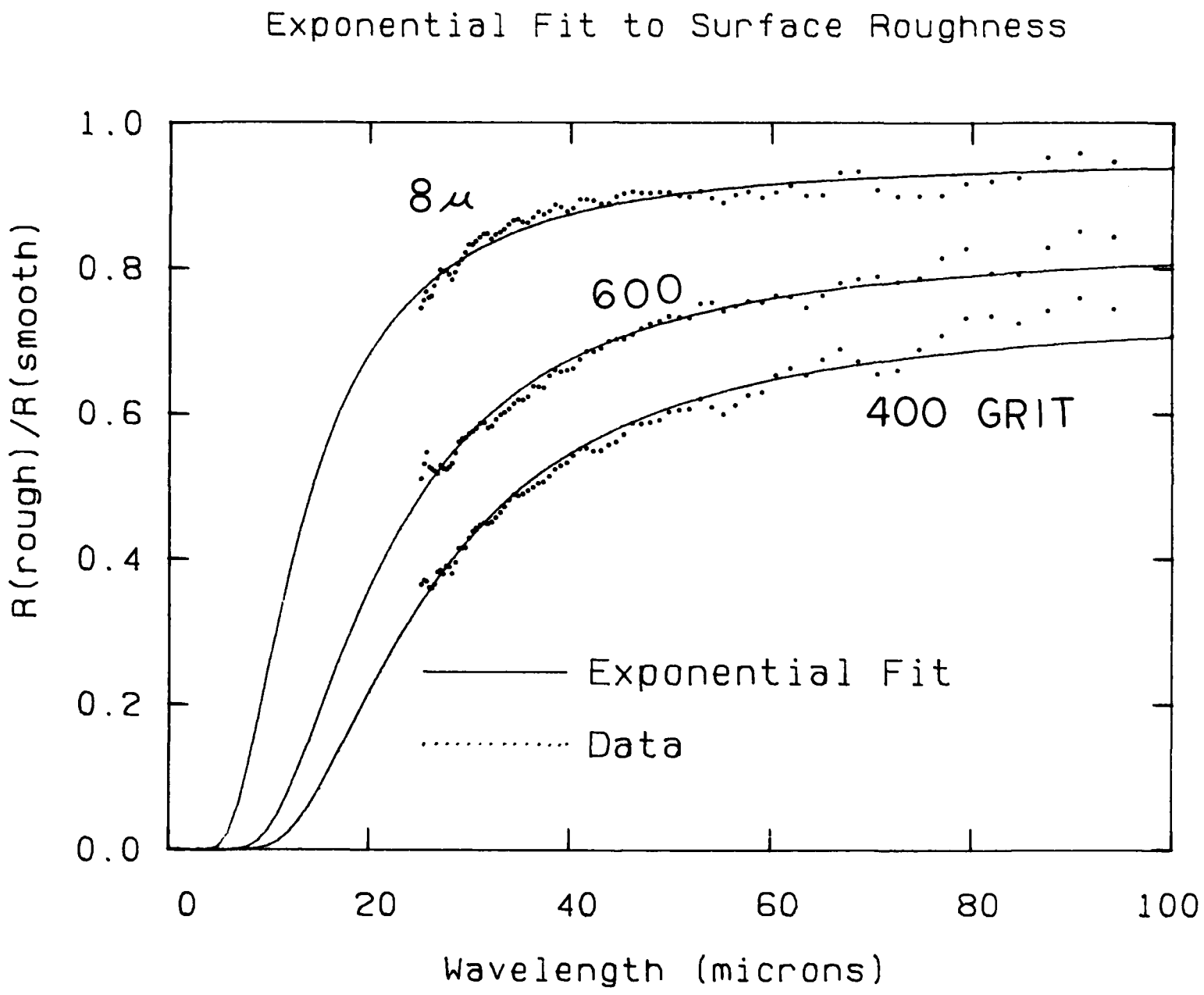

Figure 21. Montmorillonite Surface Roughness with Fit to Equation (17).

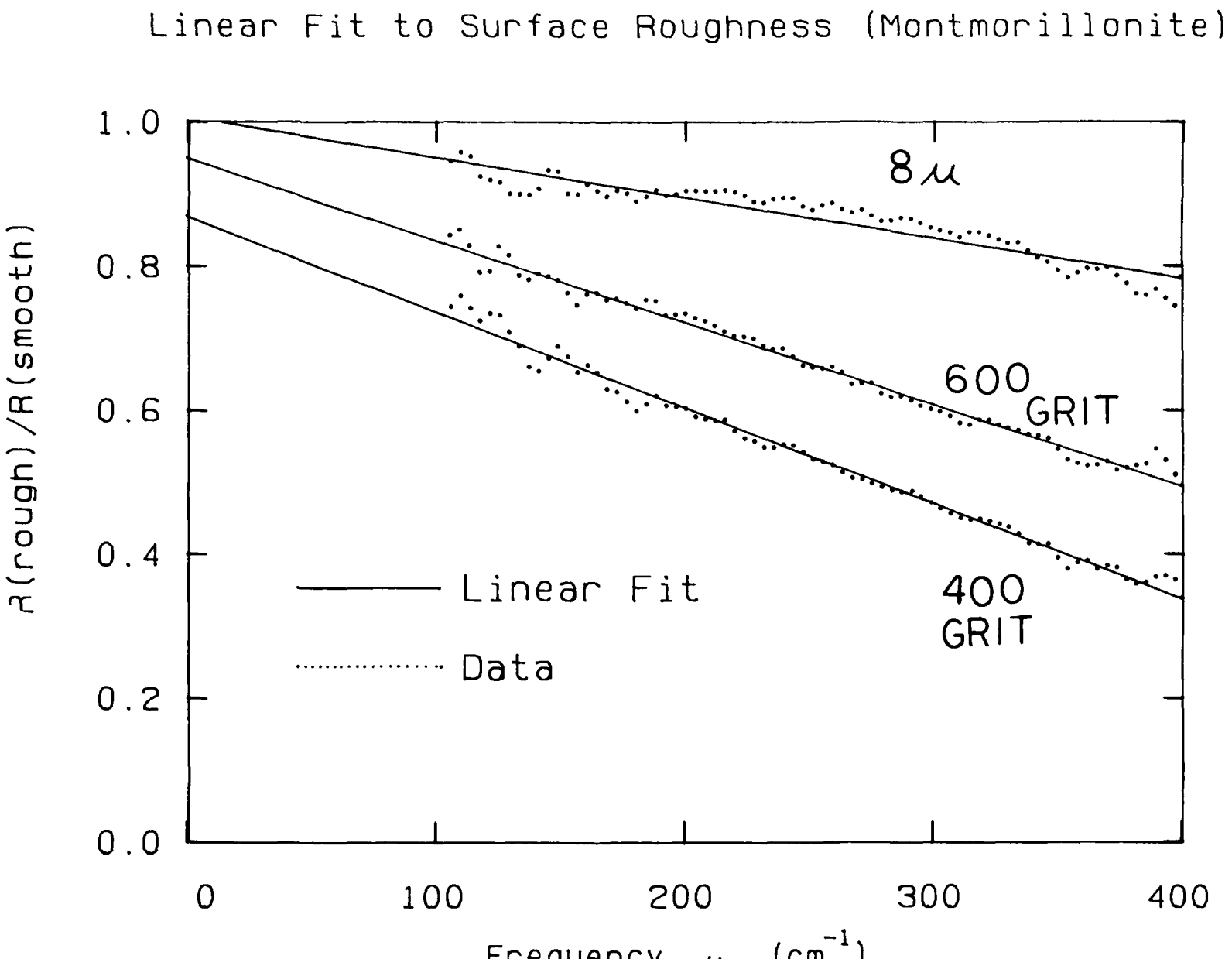

Figure 22. Montmorillonite surface roughness fitted to linear function of wavenumber.

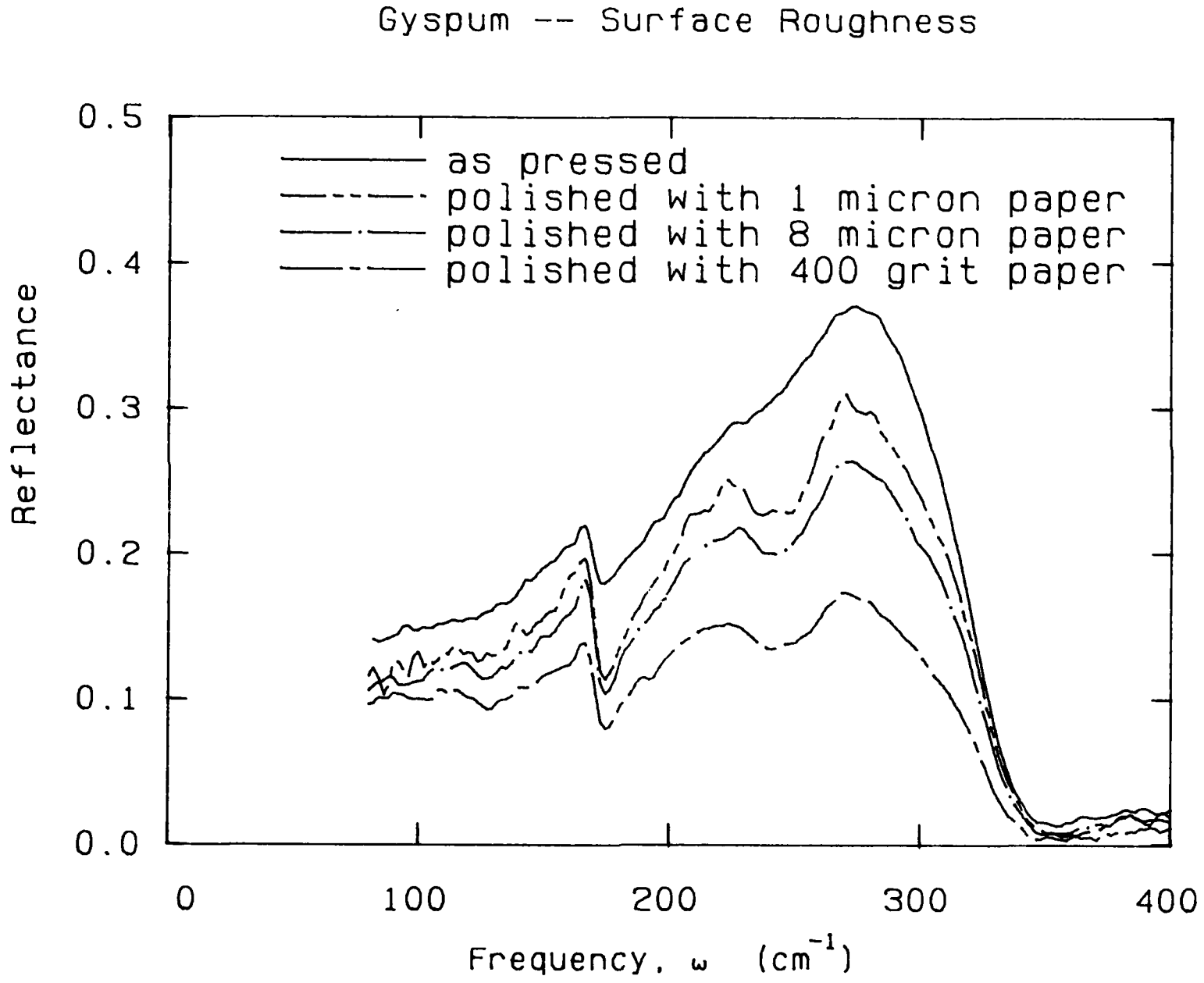

Figure 23. Gypsum with various grit polishes from 1 micron to #400 grit.

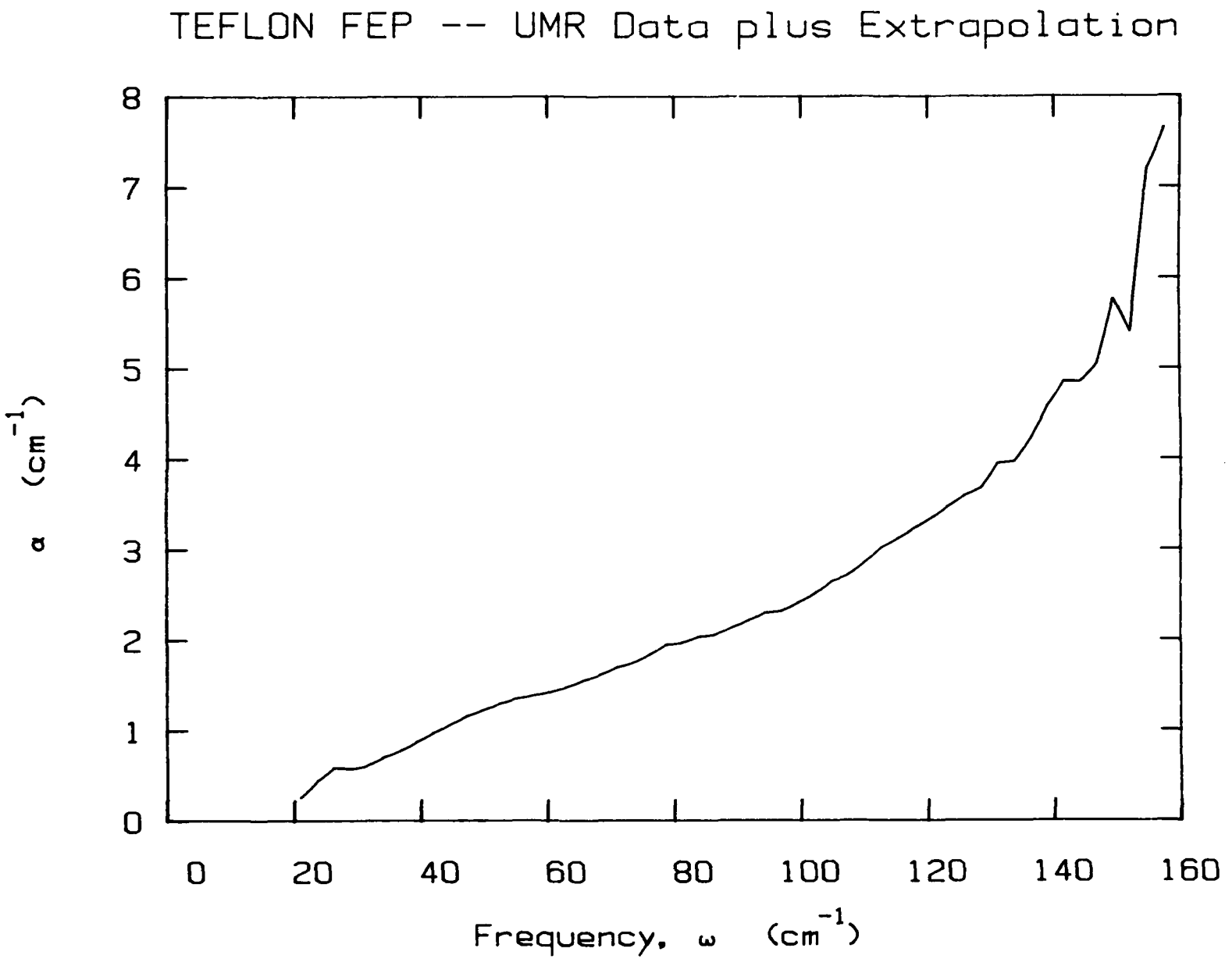

Figure 24. Absorption coefficient of teflon FEP in the far IR and submm.

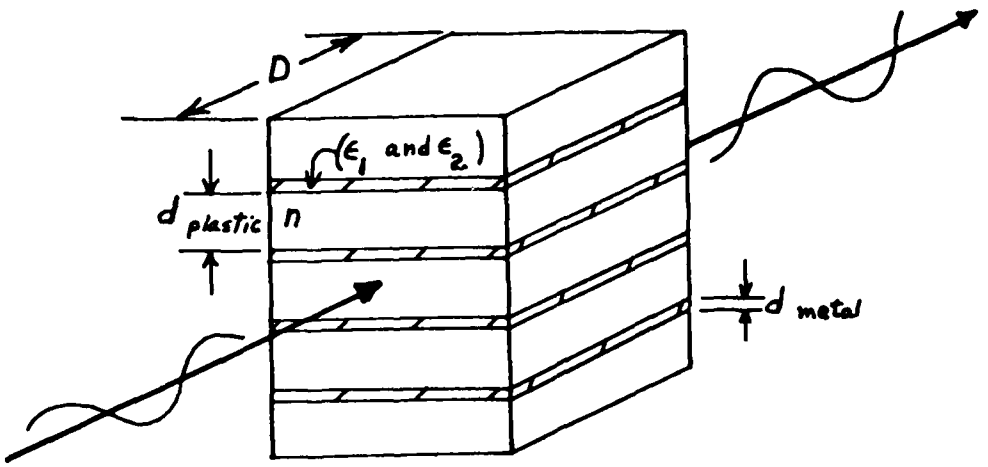

CRUDE DIAGRAM OF THE SAMPLE STACK
USING PLANE-PARALLEL WAVEGUIDE PROCEDURES.

Figure 25. Diagram of the plane-parallel waveguides. d is the $d_{plastic}$ in the figure.

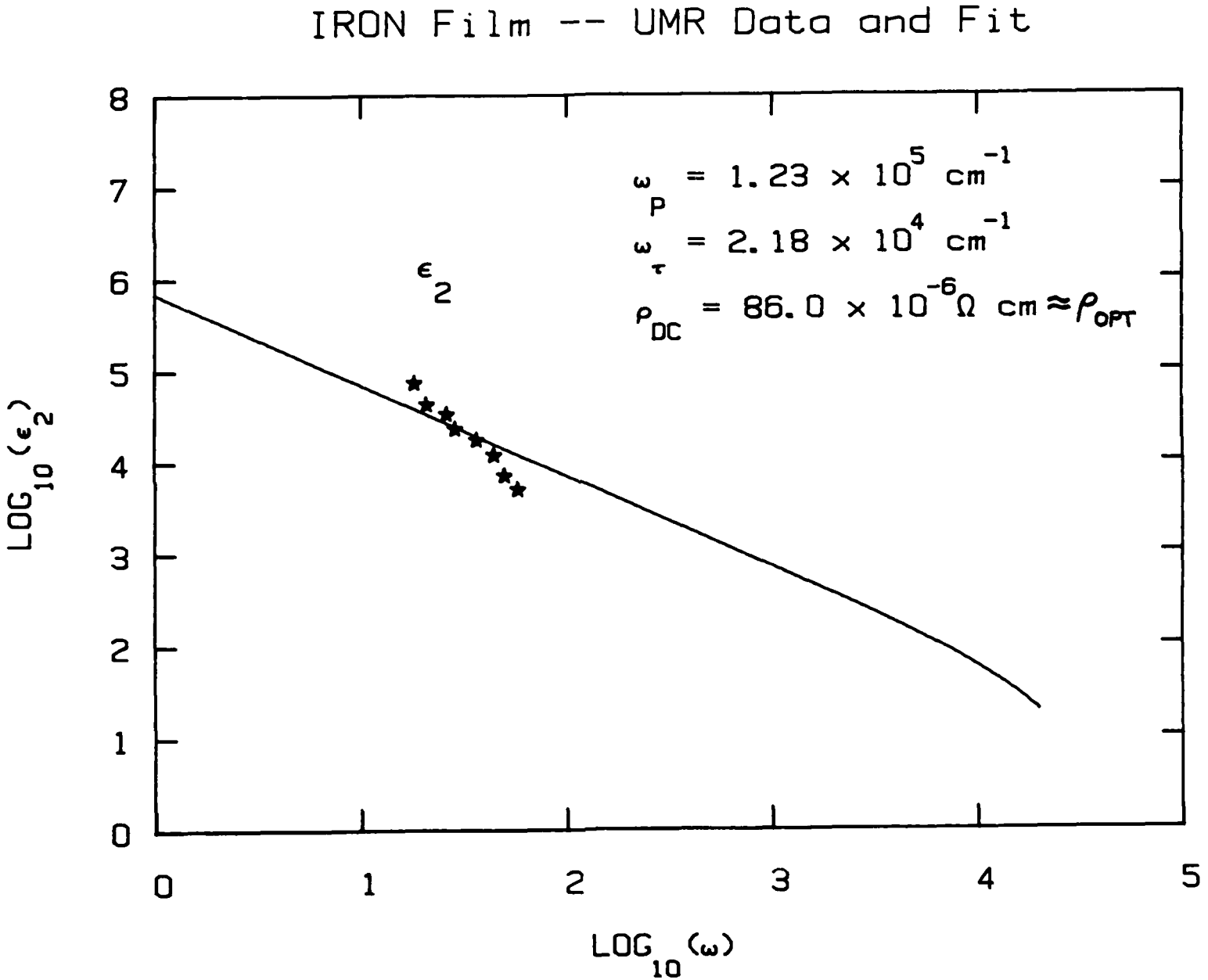

Figure 26. E_2 vs ω for 200nm thick Fe evaporated films on teflon FEP films 25 μm thick and stacked for the plane-parallel waveguide technique.

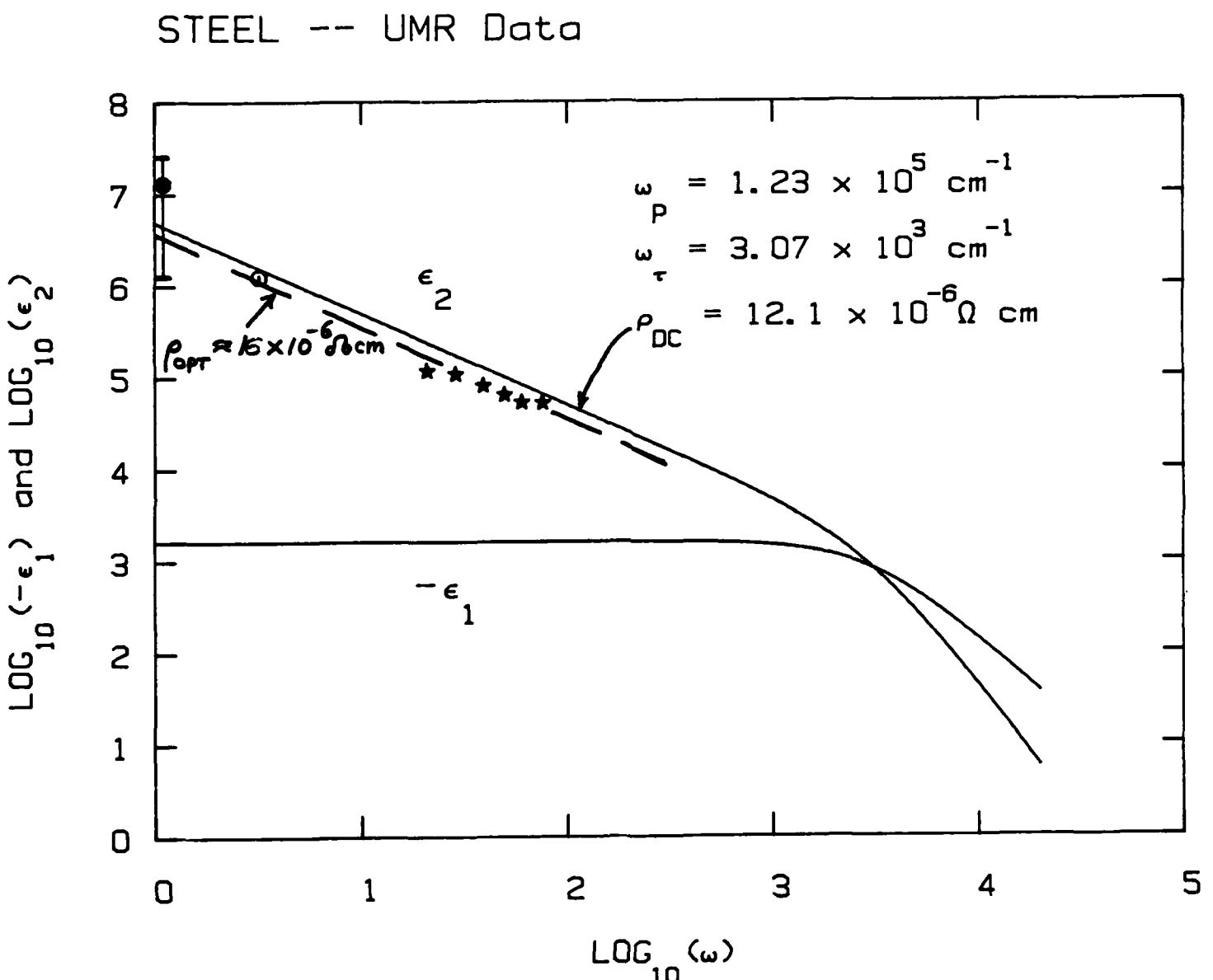

Figure 27. E_2 data (dashed line) for the steel shim stock described in Table 3. Solid hexogon and center dotted hexagon data taken using two solid state diode sources, the stars were taken on the RIIC-FTS. The solid lines were obtained by using the measured $\rho_{dc}=12\text{x}10^{-6}$ ohm-cm and handbook parameters to estimate ω_p and ω_I and hence $-\varepsilon_1$ and ε_2 and $\rho_{dc}=12\text{x}10^{-6}$ ohm-cm. $\rho_{opt}=16\text{x}10^{-6}$ ohm-cm comes from an eyeball fit of the data using Eq. (20).

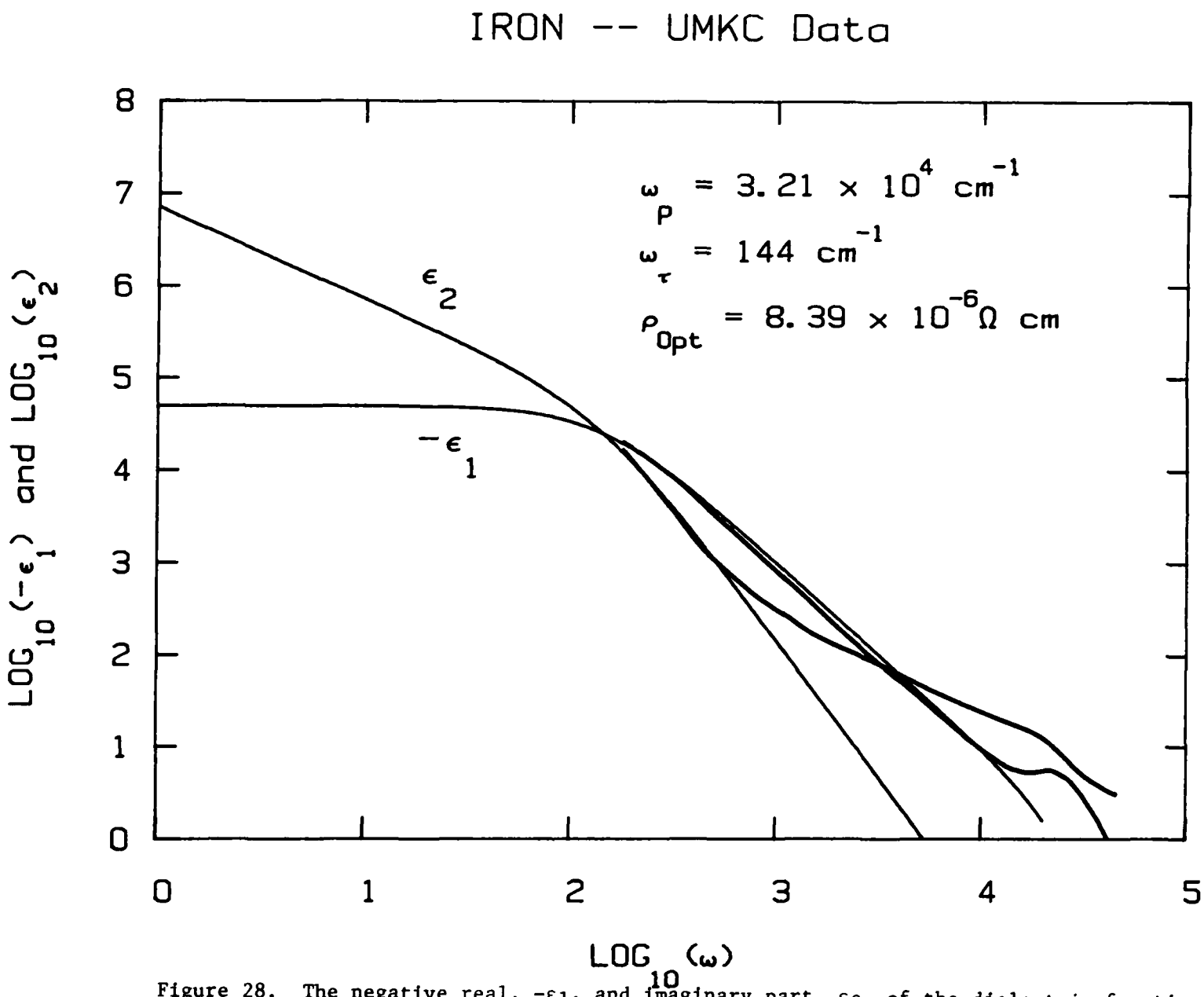

Figure 28. The negative real, $-\varepsilon_1$, and imaginary part, ε_2, of the dielectric function of iron. The fit to the data is from the Drude model with the parameters on the graph.

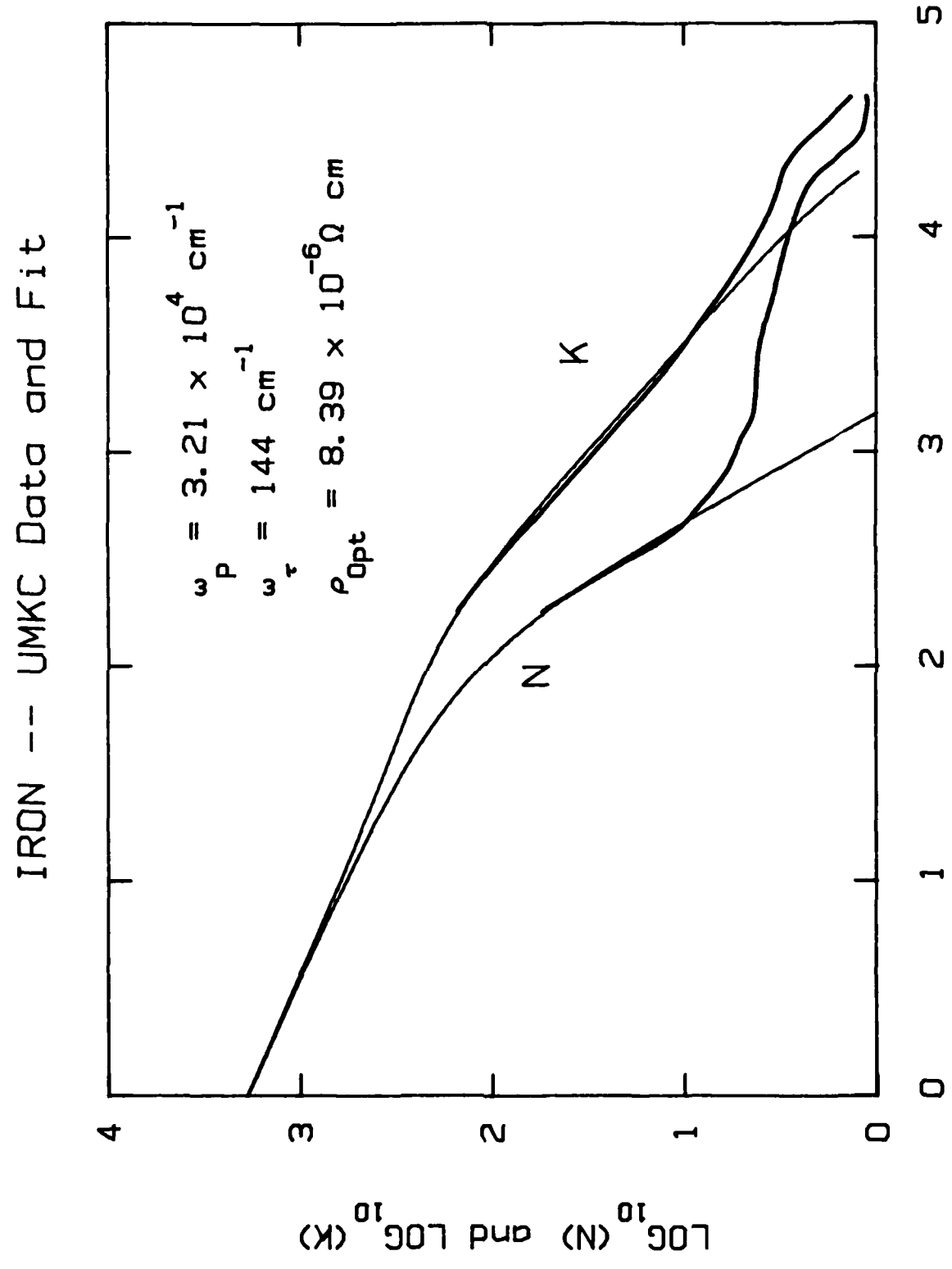

Figure 29. Same as Fig. 28 except this plot is for $n_c^2=(n+ik)^2=\epsilon_1+i\epsilon_2$).

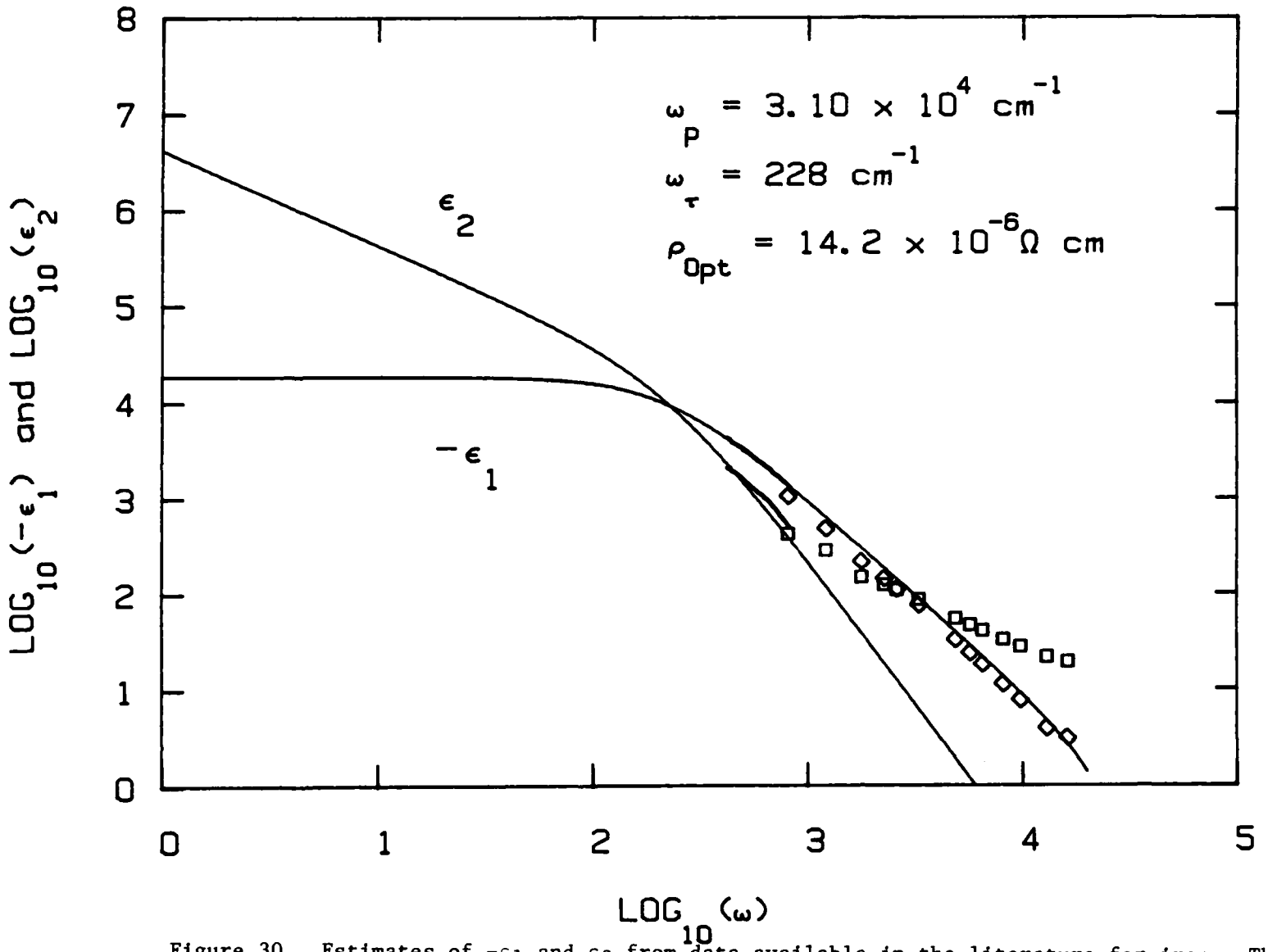

Figure 30. Estimates of $-\varepsilon_1$ and ε_2 from data available in the literature for iron. The heavy line data is from Ref. 13 and the squares and diamonds data are from Ref. 14. The solid lines are our Drude model fits to the data.

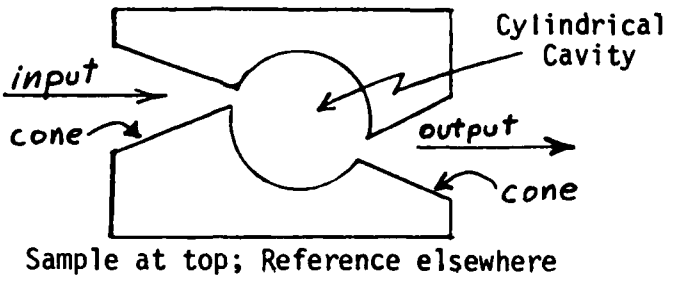

Figure 31. Diagram of the non-resonant cylindrical cavity used in the submm and mm wavelengths.

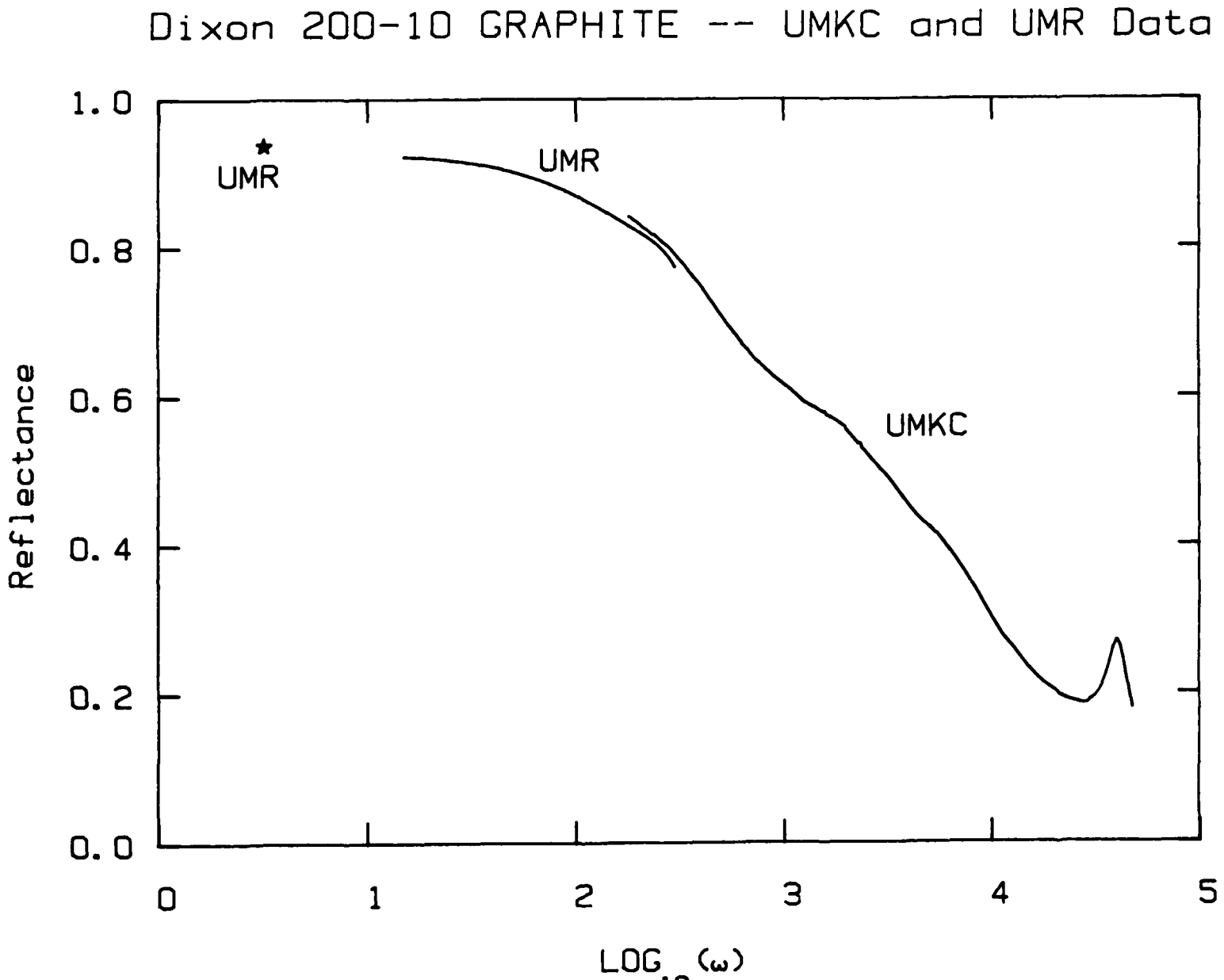

Figure 32. Reflectance of Dixon 200-10 graphite. The star represents UMR datum using a solid state source. The curve data labelled UMR was obtained using a RIIC-FTS and our UMR asymmetric Michelson FTS. The high frequency data was obtained on the same sample at UMKC.

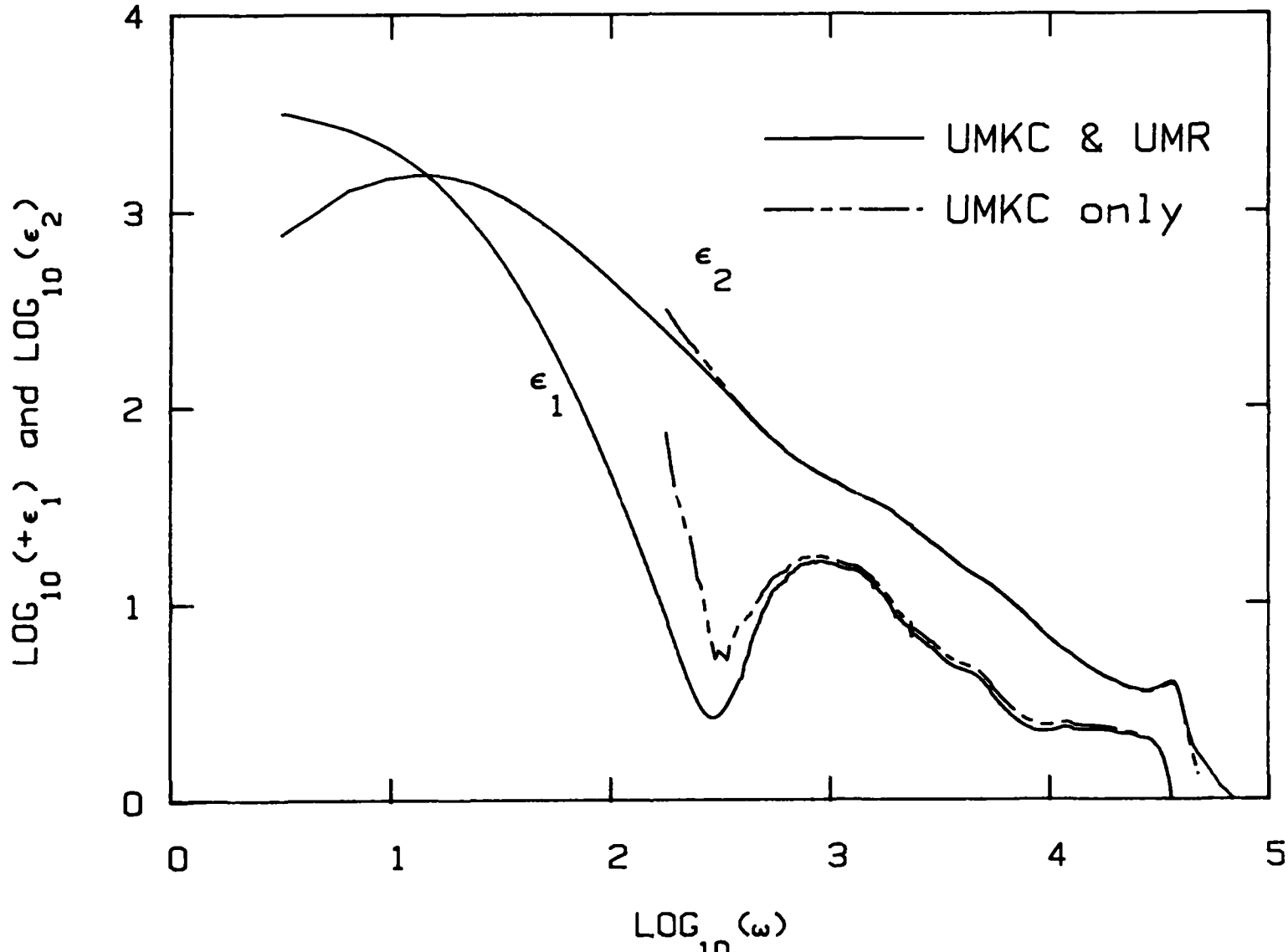

Figure 33. Dielectric functions $E=\varepsilon_1+i\varepsilon_2$ of a single Dixon 200-10 graphite sample. Data obtained from a Kramers-Kronig analysis of all the available data.

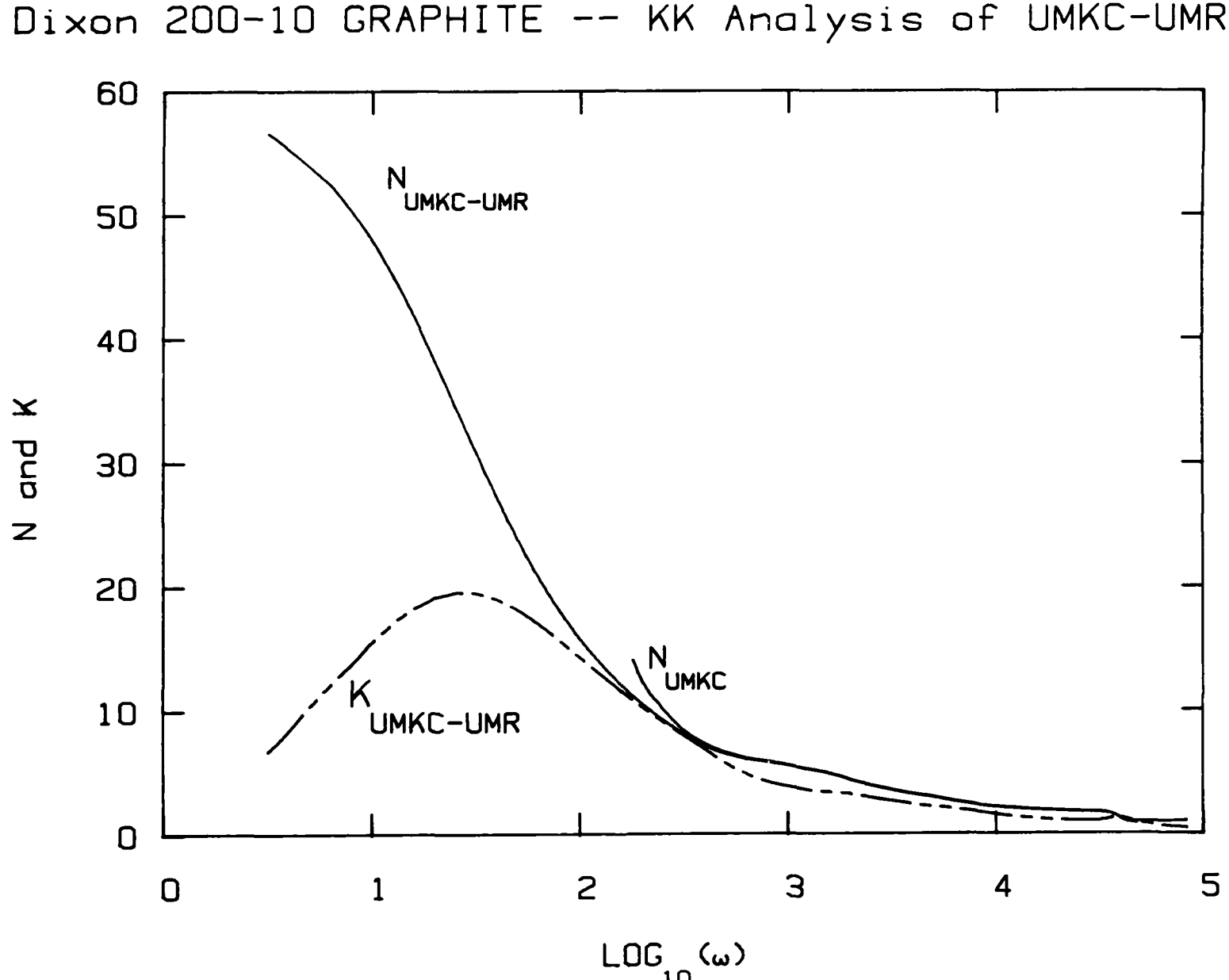

Figure 34. Optical constants n and k of a single Dixon 200-10 graphite sample studied at UMKC and UMR. Kramers-Kronig analysis was used with all sets of data. Same sample as in Fig. 33.

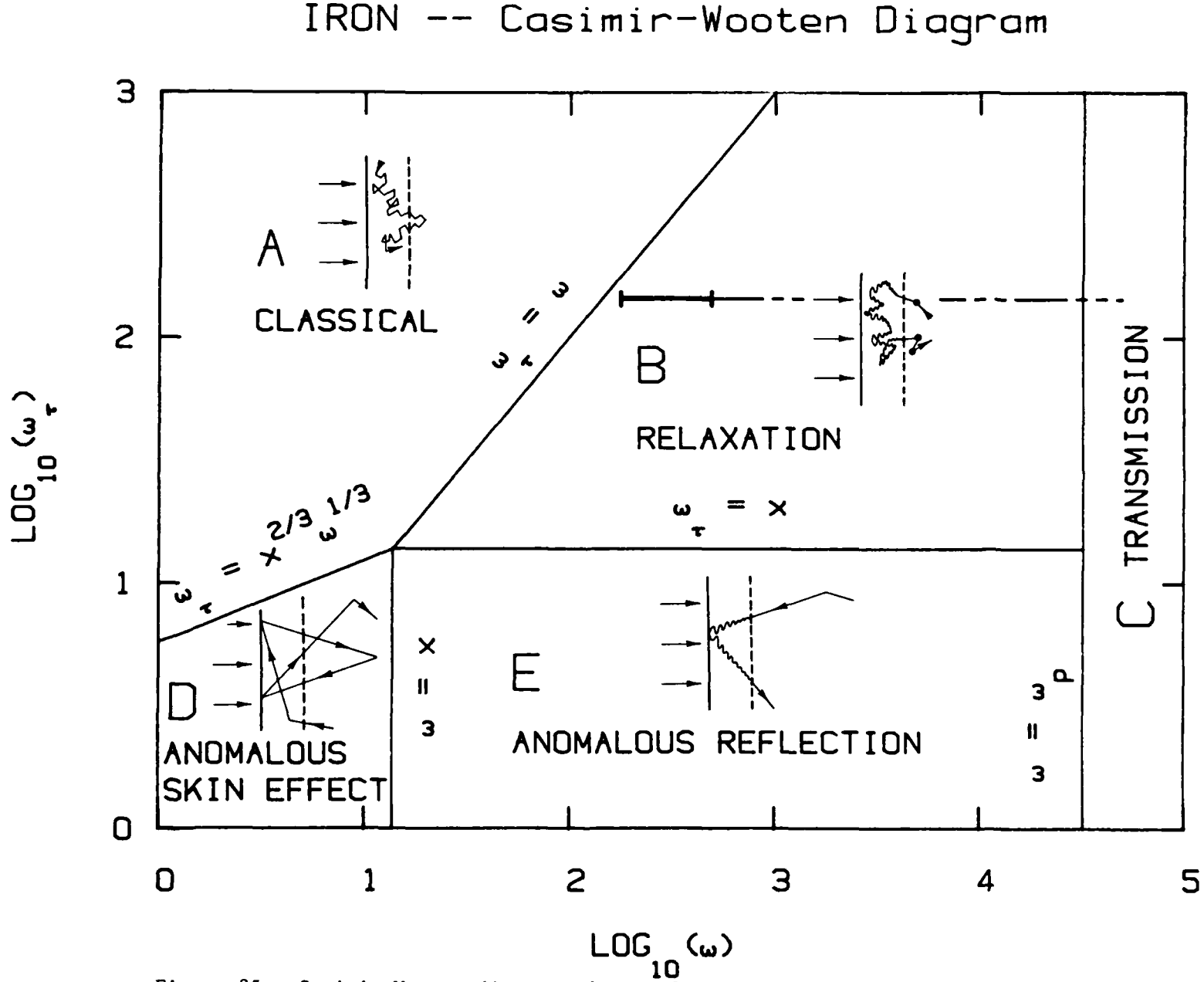

Figure 35. Casimir-Wooten diagram of iron for ω_τ vs ω exhibiting the regions of differing optical behavior. Using $\omega_p = 3.21 \times 10^4$ cm^{-1} implies x=13.8 cm^{-1} for Querry's iron data. See Ref. 23 for more details.

DISTRIBUTION LIST 1

Names	Copies
Commander	
US Army Chemical Research	
and Development Center	
ATTN: SMCCR-DDA	1
SMCCR-DDE	1
SMCCR-DDD	1
SMCCR-ET	1
SMCCR-HV	1
SMCCR-MU	1
SMCCR-MUA	1
SMCCR-MUP	1
SMCCR-MUS	1
SMCCR-MUS-A	1
SMCCR-NB	1
SMCCR-OPF	1
SMCCR-OPP	10
SMCCR-OPR	1
SMCCR-PMI	1
SMCCR-RS (Dr. N. L. Jarvis)	1
SMCCR-RS (Dr. E. J. Poziomek)	1
SMCCR-RSC	1
SMCCR-RSL	1
SMCCR-RSP	1
SMCCR-RSP-A (M. Miller)	1
SMCCR-RST	1
SMCCR-SF	1
SMCCR-SPM	1
SMCCR-SPS-IL	2
SMCCR-SPS-IR	2
SMCCR-ST	1
SMCCR-RSP-B (M. Milham) + Record Cy	5
Aberdeen Proving Ground, MD 21010-5423	
Commandant	
US Army Ordnance Missile and	
Munitions Center and School	
ATTN: ATSK-CM	1
ATSK-EI (Mr. Cranford)	1
ATSK-TME	1
Redstone Arsenal, AL 35897-6700	
Commander	
US Army Missile Command	
Redstone Scientific Information Center	
ATTN: AMSMI-RPR (Documents)	2
Redstone Arsenal, AL 35898-5241	
Commander	
US Army Missile Command	
ATTN: AMSMI-ROC (Dr. B. Fowler)	1
Redstone Arsenal, AL 35898-5242	
Commander	
US Army Missile Command	
ATTN: AMSMI-RGT (Mr. M. Maddix)	1
AMSMI-RKL (Dr. W. Wharton)	1
AMSMI-YDL, Bldg 4505	1
AMSMI-YLP (Mr. N. C. Kattos)	1
Redstone Arsenal, AL 35898-5500	
Commander	
Anniston Army Depot	
ATTN: SDSAN-DAS	1
Anniston, AL 36201-5040	
Commandant	
US Army Chemical School	
ATTN: ATZN-CM	1
ATZN-CM-CC	1
ATZN-CM-CS (Deputy MLSO)	1
ATZN-CM-MLB	1
Cbt Dev Smoke (CPT Gray)	1
Fort McClellan, AL 36205-5020	
Commander	
US Army Electronic Proving Ground	
ATTN: STEEP-MM-IS (FIO Officer)	1
Fort Huachuca, AZ 85613-7110	
McDonnell Douglas Astronautics Company	
ATTN: Mr. J. Adams, III (A3-232, 11-2)	1
5301 Bolsa Avenue	
Huntington Beach, CA 92647	
Commander	
Naval Weapons Center	
ATTN: Code 3893 (Dr. C. E. Dinerman)	1
Code 3893 (Dr. L. A. Mathews)	1
Code 3918 (Dr. F. T. Wu)	1
China Lake, CA 93555	
Commander	
US Army Science and Technology Center	
Far East Office	
ATTN: Medical/Chemical Officer	2
APO San Francisco 96328-5000	
Commander	
North American Air Defense Command	
ATTN: J31CN	1
Cheyenne Mountain Complex	
Peterson AFB, CO 80914-5601	

Director
Office Environmental and Life Sciences
Office of Under Secretary of Defense (R&E)
ATTN: Mr. Thomas R. Dashiell 1
The Pentagon
Washington, DC 20301-3080

Director
Defense Intelligence Agency
ATTN: DT-5A (Mr. C. Clark) 1
Washington, DC 20301-6111

HQDA
ATTN: DAMO-NCC 1
WASH DC 20310-0430

HQ, ODCSOPS
ATTN: DAMO-FDD 1
WASH DC 20310-0460

HQDA
ATTN: DAMA-ARR (Dr. Verderame) 1
WASH DC 20310-0632

HQDA
ATTN: DAMA-CSS-C 1
WASH DC 20310-0643

HQDA
ATTN: DAMI-FIT-S&T 1
The Pentagon
WASH DC 20310-1087

HQDA (DAEN-RDM/Dr. R. B. Gomez) 1
WASH DC 20314

Commander
Air Force Office of Scientific Research
ATTN: NE (MAJ J. W. Hager) 1
Bolling AFB, DC 20332-6448

Commander
Naval Air Systems Command
ATTN: Code AIR-320R (Dr. H. Rosenwasser) 1
Code AIR-53634F (D. C. Caldwell) 1
Washington, DC 20361

Commander
Naval Research Laboratory
ATTN: Code 2526 (Library) 1
Code 4110 (Dr. L. H. Ruhnke) 1
Code 6182 (Dr. R. Taylor) 1
Code 6530-2 (Mr. G. Stamm) 1
Code 6532 (Mr. Curcio) 1
Code 6532 (Dr. G. Trusty) 1
Code 8326 (Dr. J. Fitzgerald) 1
4555 Overlook Avenue, SW
Washington, DC 20375-5000

Commandant
HQ, US Marine Corps
ATTN: Code LMW-50 1
Washington, DC 20380-0001

Toxicology Information Center, JH 652
National Research Council 1
2101 Constitution Avenue, NW
Washington, DC 20418

Federal Emergency Management Agency
Civil Defense Division (Room 625)
ATTN: NP-CP-CD (Mr. David Freund) 1
500 C Street, SW
Washington, DC 20472

OSU Field Office 1
PO Box 1925
Eglin AFB, FL 32542-1925

Commander
Air Force Armament Laboratory
ATTN: DLJW (Mr. L. Nelson) 1
Eglin AFB, FL 32542-6008

Commander
Air Force Systems Command
ATTN: AD/YQ 1
Eglin AFB, FL 32542-6008

Commander
Tactical Air Warfare Center
ATTN: THLO (LTC Kotouch) 1
Eglin AFB, FL 32542-6008

Director
Office of Biosafety
Centers for Disease Control
ATTN: Mrs. M. Brocato 1
(FOR: Dr. F. S. Lisella)
1600 Clifton Road
Atlanta, GA 30333

Commander
US Army Infantry Center
ATTN: NBC Branch, Directorate of Plans
and Training (Bldg 2294) 1
Fort Benning, GA 31905-5273

Commandant
US Army Infantry School
ATTN: ATSH-CD-MLS-F (Mr. D. Dowie) 1
Fort Benning, GA 31905-5400

Commandant
US Army Infantry School
ATTN: ATSH-B, NBC Branch 1
Fort Benning, GA 31905-5410

Commander
US Army Armament, Munitions and
Chemical Command
ATTN: AMSMC-ASN 1
AMSMC-IRD-T 1
AMSMC-SFS 1
SMCAR-ESP-L 1
Rock Island, IL 61299-6000

Director
US Army Materiel Command Field
Safety Activity
ATTN: AMXOS-SE (Mr. Yutmeyer) 1
Charlestown, IN 47111-9669

Commander
Naval Weapons Support Center
ATTN: Code 50C (Dr. B. E. Douda) 1
Code 502 (R. Farren) 1
Code 5062 (C. LohKamp) 1
Crane, IN 47522-5050

Commander
US Army Combined Arms Center
Development Activity
ATTN: ATZL-CAM-M 1
Fort Leavenworth, KS 66027-5300

Commander
US Army Armor Center and Fort Knox
ATTN: ATZK-CD-MS 1
ATZK-DPT-N (NBC School) 1
Fort Knox, KY 40121-5000

Commander
217th Chemical Detachment
ATTN: AFVL-CD 1
Fort Knox, KY 40121-5418

Commander
5th Infantry Division (Mech)
ATTN: AFZX-CL 1
Fort Polk, LA 71459

Science Applications International
Corporation
ATTN: Dr. F. G. Gebhardt 1
3 Preston Court
Bedford, MA 01730-2382

Creative Optics, Incorporated
ATTN: Dr. J. F. Ebersole 1
32 Wildwood Drive
Bedford, MA 01730-2418

Commander
Natick Research and Development Center
ATTN: STRNC-O 1
STRNC-OI 1
Natick, MA 01760-5015

Commander
Natick Research and Development Center
ATTN: STRNC-ICC 1
STRNC-IP 1
Kansas Street
Natick, MA 01760-5019

Commander
Natick Research and Development Center
ATTN: STRNC-YE 1
Kansas Street
Natick, MA 01760-5020

Commander
US Army Materials and Mechanics
Research Center
ATTN: AMXMR-MDF (Dr. S. Isserow) 2
Watertown, MA 02172-0001

Commander
Naval Intelligence Support Center
ATTN: Code 434 (Mr. H. F. St. Aubin) 1
4301 Suitland Road
Suitland, MD 20390

Commander
US Army Intelligence and Security Command
ATTN: IAFM-SFD-III 1
Fort Meade, MD 20755-5000

Commander
US Army Electronics Research and Development Command
ATTN: AMCPM-FD (Mr. E. Dudley) 1
Adelphi, MD 20783-1145

Commander
Harry Diamond Laboratories
ATTN: DELHD-RT-CB (Dr. Sztankay) 1
2800 Powder Mill Road
Adelphi, MD 20783-1197

Director
US Army Concepts Analysis Agency
ATTN: CSCA-RQL (Dr. Helmbold) 1
8120 Woodmont Avenue
Bethesda, MD 20814-2797

Project Manager
Smoke/Obscurants
ATTN: AMCPM-SMK-E (A. Van de Wal) 1
AMCPM-SMK-M 1
AMCPM-SMK-T 1
Aberdeen Proving Ground, MD 21005-5001

Commander
US Army Test and Evaluation Command
ATTN: AMSTE-CM-F 1
AMSTE-CT-T 1
Aberdeen Proving Ground, MD 21005-5055

Director
US Army Ballistic Research Laboratory
ATTN: AMXBR-OD-ST (Tech Reports) 1
Aberdeen Proving Ground, MD 21005-5066

Director
US Army Materiel Systems Analysis Activity
ATTN: AMXSY-CR (Mr. J. O'Bryon) 1
AMXSY-GC (Mr. F. Campbell) 1
AMXSY-MP (Mr. H. Cohen) 1
Aberdeen Proving Ground, MD 21005-5071

Commander
US Army Environmental Hygiene Agency
ATTN: HSHB-O/Editorial Office 1
Aberdeen Proving Ground, MD 21010-5422

Commander
US Army Armament, Munitions and Chemical Command
ATTN: AMSMC-HO (A) (Mr. J. K. Smart) 1
AMSMC-QAC-M (A) 1
AMSMC-QAE (A) 1
Aberdeen Proving Ground, MD 21010-5423

Commander
US Army Technical Escort Unit
ATTN: SMCTE-AD 1
Aberdeen Proving Ground, MD 21010-5423

Commander
US Army Medical Research Institute of Chemical Defense
ATTN: SGRD-UV-L 1
Aberdeen Proving Ground, MD 21010-5425

Commander
US Army Medical Bioengineering Research and Development Laboratory
ATTN: SGRB-UBG (Mr. Eaton) 1
SGRB-UBG-AL, Bldg 568 1
Fort Detrick, Frederick, MD 21701-5010

Commander
US Army Medical Research and Development Command
ATTN: SGRD-RMS 1
Fort Detrick, Frederick, MD 21701

Director
US Army Research Office
ATTN: AMXRO-CB (Dr. R. Ghirardelli) 1
AMXRO-GS 1
PO Box 12211
Research Triangle Park, NC 27709-2211

Commander
US Army Cold Regions Research and Engineering Laboratory
ATTN: CRREL-RG (Mr. G. Aitken) 1
Hanover, NH 03755-1290

Commander
US Army Armament Research and
Development Center
ATTN: SMCAR-LCE-C (Dr. H. Matsugama) 1
SMCAR-LCE-P (Dr. S. Morrow) 1
SMCAR-LCU-CE 1
SMCAR-SCA-E 1
SMCAR-SCF-SD 1
SMCAR-SCS 1
SMCAR-ISS 2
Dover, NJ 07801-5001

Project Manager
Cannon Artillery Weapons Systems
ATTN: AMCPM-CAWS-A 1
Dover, NJ 07801-5001

Director
Los Alamos National Laboratory
ATTN: T-DOT, MS P371 (S. Gerstl) 1
Los Alamos, NM 87545

Commander/Director
US Army Atmospheric Sciences Laboratory
ATTN: DELAS-AE (Dr. F. Niles) 1
DELAS-AE-E (Dr. D. Snider) 1
DELAS-AR (Dr. E. H. Holt) 1
DELAS-AR-A (Dr. M. Heaps) 1
DELAS-AR-A (Dr. R. Pinnick) 1
DELAS-AS (Dr. C. Bruce) 1
DELAS-EO-MO (Dr. R. Sutherland) 1
White Sands Missile Range, NM 88002-5501

Director
US Army TRADOC Systems Analysis Activity
ATTN: ATOR-TSL 1
ATOR-TDB (L. Dominguez) 1
White Sands Missile Range, NM 88002-5502

Director
Office of Missile Electronic Warfare
ATTN: DELEW-M-TAC (Ms. J. L. Arthur) 1
White Sands Missile Range, NM 88002-5513

Commander
US Army Scientific and Technical
Information Team, Europe
ATTN: AMXMI-E-CO 1
Box 48
APO New York 09079-4734

Commander
US Military Academy
Department of Physics
ATTN: Maj Decker 1
West Point, NY 10996-1790

Battelle, Columbus Laboratories
ATTN: TACTEC 5
505 King Avenue
Columbus, OH 43201-2693

Science Applications International
Corporation
ATTN: Dr. R. E. Turner 1
1010 Woodman Drive, Suite 200
Dayton, OH 45432

Commander
Air Force Aerospace Medical Research
Laboratory
ATTN: TS 1
Wright-Patterson AFB, OH 45433-6503

Commander
Foreign Technology Division
ATTN: TQTR 1
Wright-Patterson AFB, OH 45433-6508

Director
Survivability/Vulnerability Information
Analysis Center
AFWAL/FIES/SURVIAC 1
Wright-Patterson AFB, OH 45433-6553

Commandant
US Army Field Artillery School
ATTN: ATSF-GA 1
Fort Sill, OK 73503-5600

Commandant
US Army Academy of Health Sciences
ATTN: HSHA-CDH (Dr. R. H. Mosebar) 1
HSHA-CDS (CPT Eng) 2
HSHA-IPM 2
Stimson Library (Documents), 1
Bldg 2840
Fort Sam Houston, TX 78234-6100

Commander
Aerospace Medical Division
ATTN: AMD/RDSM (Lt Col D. Marshall) 1
AMD/RDTK (Lt Col J. Milligan) 1
Brooks AFB, TX 78235-5000

Commander
US Army Dugway Proving Ground
ATTN: STEDP-SD (Dr. L. Salomon) 1
Dugway, UT 84022-5010

Commander
US Army Dugway Proving Ground
ATTN: STEDP-SD-TA-F (Technical Library) 1
Dugway, UT 84022-6630

Director
US Army Night Vision and Electro-Optics Laboratory
ATTN: DELNV-D (Dr. Buser) 1
DELNV-V (L. Obert) 1
Fort Belvoir, VA 22060-5677

Commander
Marine Corps Development and Education Command
ATTN: Code D091, SPWT Section 1
Quantico, VA 22134-5080

Commander
US Army Nuclear and Chemical Agency
ATTN: MONA-CM 1
7500 Backlick Road, Bldg 2073
Springfield, VA 22150-3198

Administrator
Defense Technical Information Center
ATTN: DTIC-DDAC 12
Cameron Station, Building 5
Alexandria, VA 22304-6145

Director
Institute for Defense Analysis
ATTN: Mr. C. H. Leatherbury 1
1801 N. Beauregard Street
Alexandria, VA 22311

Commander
US Army Materiel Command
ATTN: AMCCN 1
AMCMT-M 1
AMCSF-C 1
5001 Eisenhower Avenue
Alexandria, VA 22333-0001

Commander
Naval Surface Weapons Center
ATTN: Code E4311 1
Code F56 (Mr. D. Marker) 1
Dahlgren, VA 22448

Commander
US Army Foreign Science and Technology Center
ATTN: AMXST-CW-2 (F. Poleski) 1
220 Seventh Street, NE
Charlottesville, VA 22901-5396

Director
Applied Technology Laboratories
ATTN: SAVDL-ATL-ASV 1
SAVDL-ATL-ASW 1
Fort Eustis, VA 23604-5577

Commander
US Army Training and Doctrine Command
ATTN: ATCD-N 1
Fort Monroe, VA 23651-5000

Commander
US Army Logistics Center
ATTN: ATCL-MGF 1
Fort Lee, VA 23801-5000